UNIVERSITÀ DEGLI STUDI DI PALERMO

Dipartimento di Scienze della Terra e del Mare (DiSTeM)

DOTTORATO DI RICERCA

Geochimica (GEO/08)

XXIV Ciclo

Ph.D. Thesis

Ocean Acidification studies in the Baia di Levante (Vulcano island, Italy).

Advantages and disadvantages of the "in situ" approach.

Coordinatore/Tutor

Ch.mo Prof. Francesco Parello

Dottorando

Fulvio Boatta

Co-Tutors:

Ch.mo Prof. Marco Milazzo

Dr. Walter D'alessandro

Anno accademico 2013-2014

Index.

"*'Oh I know' exclaimed Alice, 'who had not attended to this last remarks, it's a vegetable. It doesn't look like one, but it is'.*

'I quite agree with you, said the Duchess; and the moral of that is' – Be what you would seem to be – or if you'd like it put more simply – 'Never imagine yourself not to be otherwise than what it might appear to others that what you were or might have been was not otherwise than what you had been would have appeared to them to be otherwise.'"

(Cit. Lewis Carroll)

Abstract.

Years of scientific research have shown that acidification of oceans (OA) is an undisputed fact. Why is it so important to increase knowledge about OA? Because many animals and plants in the ocean have calcium carbonate skeletons or shells, and a decreasing in pH can affect their population health state and the marine-ecosystem structure. Another point of view about OA which must to be considered is that it may alter the behavior of sediment-bound metals, modifying their bioavailability and thus toxicity. The toxic free-ion concentration of metals such as copper may increase by as much as 115% in coastal waters in the next 100 years due to reduced pH. Since increasing atmospheric CO_2 over the next 200 years will cause a pH decrease in ocean water, and consequently change the organic and inorganic speciation of metals in surface ocean waters, and it will effect on their interaction with marine species.

Most of the intense submersed hydrothermal seeps are located near the isthmus of the Baia di Levante along the beach (38°25'01.44"N, 14°57'36.29"E), where dispersed underwater leaks cover a 130 × 35m shallow water area (<1m depth). Here we aim at studying the geochemical characteristics of seawater in the Baia di Levante area. We studied the most prominent geochemical parameters across the whole bay and focused on the spatio-temporal variability of pH/CO_2 along a stretch of coast in the northeastern part of the bay in the Vulcanello area. Eh and pH were greatly affected by the main vents. Eh values range from -152 to 170 mV in April and from -23 to 171 mV in September 2011 and from -39.7 to 181.3 in May 2012, while pH values range between 5.70 and 8.05 in April and from 6.05 to 8.03 in September 2011 and from 5.85 to 8.03 in May 2012. These is the reason why a pH and Eh gradient (from bubbles to offshore) affect seawater chemistry and biota in the Bay.

About 3.6 tonnes of CO_2 bubble into Baia di Levante per day which strongly influences the seawater chemistry of the area. The pH displayed a clear gradient from 5.65 at the main gas vents increasing to 8.1 and may represent suitable sites for ocean acidification studies. The ternary diagram of CH4-(N_2+O_2)-CO_2 confirms the atmospheric contribution to dissolved gases and shows variable ratios between CH_4 and CO_2. Dissolved gases samples were analysed with gas chromatography.

Calcite and aragonite saturation in the bay is achieved only in the northern part where pH values exceed respectively 7.5 and 7.6. According to projections, 7.8 is the predicted average global sea surface pH value for the year 2100, and it is considered an ecological tipping point at which most subtidal calcifiers disappear in the Mediterranean.

Vulcano's seawater composition in terms of the major elements is close to that of Mediterranean surface waters even if salinity is few higher than oceans and greater variability is recorded for dissolved Fe concentrations and trace metals distribution along the bay. Major elements were analyzed with IC (Ionic Chromatography). Calculated enrichment factors (EF) for trace metals in general show that in general we can considered V as not so enriched, Ni, Al, Cu, Fe and Zn as medium enriched and Mn as very enriched, furthermore, EF show that, except for Cu, trace metals are enriched in Baia di Levante probably because of the hydrothermal input. Average seawater concentration for each metals are; 5.1 µg/l for Al, 0.8 µg/l for V, 11.4 µg/l for Mn, 3.7 µg/l for Fe, 0.3 µg/l for Ni, 0.5 µg/l for Cu, 2.3 µg/l for Zn and 5.2^{-3} µg/l for La. Seawater samples were pre-concentrated with chelex-100 resin and analyzed with ICP-MS.

A transplant mussel experiment in acidic condition (natural seawater respectivly) was conducted and, after one month exposure mussel (Mytilus gallorpovincialis) had accumulated Fe, Zn, Cu and V. Soft body mussel metals concentration are 0.7 µg/g for Ni, 2.7 µg/g for V, 4.5 µg/g for Cu, 7.2 µg/g for Mn, 23 µg/g for Al, 78.6 µg/g for Zn and 336.4 µg/g for Fe. Mussels are confirmed to be good bioaccumulator of heavy metals, although, their study in situ in the context larger of OA studies is complicated despite the fact have a lot of vantages. Geochemical approach is fundamental in this field, and biota accumulation should always be matched with geochemical survey in their habitat in order to better understand the bio-accumulation dynamics.

Chapter 1 – Ocean Acidification (OA).

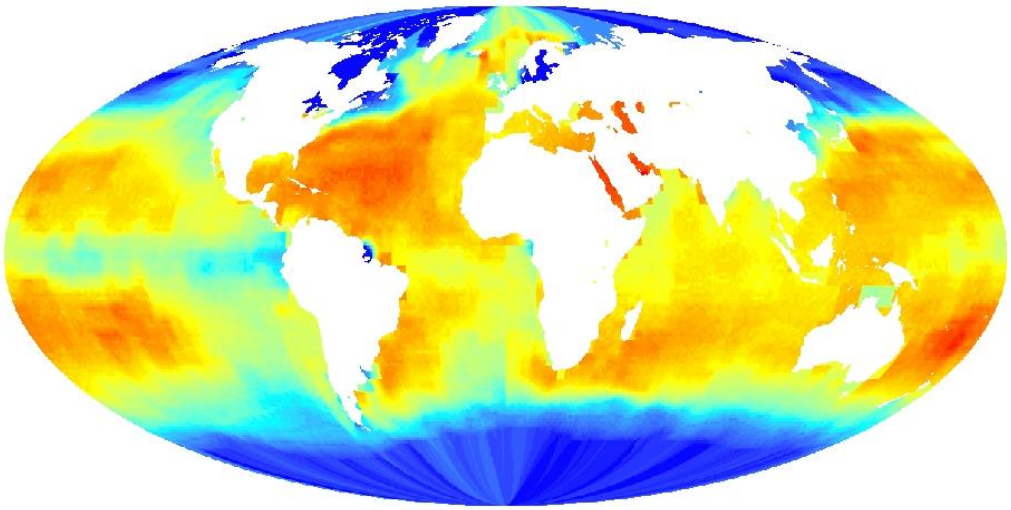

1.1. Acidification of Oceans (O.A.).

Years of scientific research have shown that acidification of oceans (OA) is an undisputed fact (Riebesell et al., 2010). Marine habitats are changing at an unprecedented rate in terms of sea surface temperature, sea ice cover, salinity, alkalinity, pH and ocean circulation (Bulling et al., 2010; Rogers & Laffoley, 2011; Hönisch et al., 2012). Increased emissions of carbon dioxide (CO_2) as a result of anthropogenic activities are predicted to cause rising atmospheric and oceanic temperatures with direct implications for the ecology of terrestrial and marine ecosystems (Sabine et al., 2004; Turley et al., 2010). The world's oceans are a major sink for anthropogenic CO_2 and the effects of increased CO_2 dissolution in seawater on fundamental acid-base equilibrium are well understood (Gattuso & Hansson, 2011). The ocean presently takes up one fourth of the anthropogenic carbon CO_2 emitted in to the atmosphere (Riebesell et al., 2010). As this CO_2 dissolves in the surface ocean, it reacts with seawater to form carbonic acid, increasing ocean acidity and shifting the partitioning of inorganic carbon species towards increased CO_2 and dissolved inorganic carbon, and decreased concentration of carbonate ion.

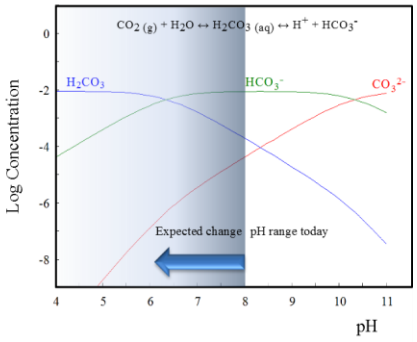

Fig. 1 - Log Concentration carbonates species vs pH.

Since the beginning of the industrial revolution, 250 years ago, the seawater pH has decreased by 30%. Anthropogenic CO_2 released into the atmosphere in the past two centuries has been taken up by the ocean (Sabine et al., 2004) and the current annual rate of global oceanic uptake is estimated to be 2.2 $*10^9$ metric tons C (Mikaloff Fletcher et al., 2006).

The global annual average concentration in 2011 was 390.9 ppm, that is 40 per cent higher than pre-industrial levels. With the current rate of increase it is estimated that the global annual average concentration will exceed 400 ppm by 2015 or 2016 (United Nations Environment Programme, http://www.unep.org/newscentre/default.aspx?DocumentID=2716&ArticleID=9503).

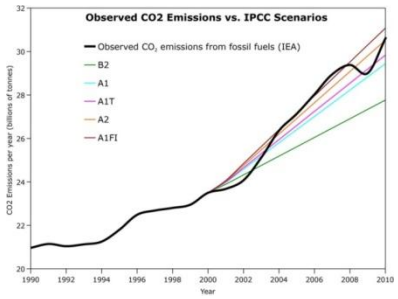

*Fig. 2 - *IEA observed CO_2 emission vs IPCC scenarios (A1F1 = low growth, A1T = moderate growth; B2 = High growth).*

In aquatic systems CO_2 gas dissolves, hydrates and dissociates to form weak carbonic acid, which is the main driver of natural weathering reactions (Drever, 1997). As the ocean surface absorbs CO_2, pH is lowered according to the following reaction:

$$CO_{2\,(g)} + H_2O \leftrightarrow H_2CO_{3\,(aq)} \leftrightarrow H^+ + HCO_3^-$$

$$Ca^{2+} + HCO_3^- \leftrightarrow CaCO_{3\,(aq)} + H^+$$

The result of the CO_2 increase is that surface seawater, although still being an alkaline solution, becomes more acidic (Doney et al., 2009). Due to CO_2 uptake since the year 1750, the surface pH has already decreased by 0.1 units, which corresponds to a 30% increase in the concentration of H^+ ions (Sabine et al. 2004). Projections of global CO_2 emissions lead to a prediction of an additional decrease in ocean pH of 0.1–0.35 units by the end of this century (IPCC, 2007 – Fig.2 and 3). With the continued emission of CO_2 from burning of fossil fuels, changing land use, and cement production the partial pressure of CO_2 is expected to reach 2000 ppm in about 150 years, and consequently a decrease in the seawater surface from 8.1 to 7.4 is expected (Caldeira et al., 2003). The current increase in ocean acidity is hundred times faster than any previous natural change that has occurred over the last many millions of years. In the case of unabated CO_2 emissions the level of ocean acidity will increase to three times the preindustrial level by the end of this century. Recovery from this large and rapid perturbation will require tens of thousands of years.

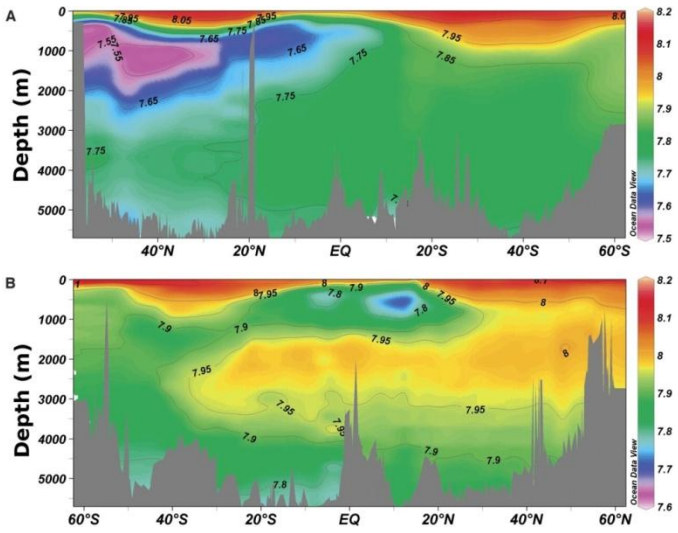

Fig. 3 - Image from Millero et al., 2010; shows a pH maps in the section of Ocean Pacific - A - and Atlantic - B - bathymetry is shown in grey. The north-south transit in the Atlantic is along 30° W and in the Pacific along 150° W.

Why is so important to increase knowledge about OA? Because of the fact that many of the animals and plants in the ocean have calcium carbonate skeletons or shells. The decrease in carbonate ion concentration has spurred many papers which explain on how it affects the

production of calcium carbonate ($CaCO_3$) by calcifying organisms (Orr et al., 2005; Gattuso et al., 1998; Langdon et al., 2003). Some of these are at the base of the food chain (such as for instance plankton), other are very important for humans' diet as mussels, besides, other species are considered as "habitat formers" because they are builders of coral reef, which are the nursery for catchable fish species. The ocean not only provide us with food (half of Earth productivity is given by the ocean) but it supports us in many other ways; for instance, in the air we breathe, the percentage of oxygen depends more from photosynthetic organism which live in the ocean than in the terrestrial ecosystems. Furthermore the oceans bring us social, esthetic and health benefits. Another example which can show how OA can affect our economy is represented by the oyster industry, in 2005 scientists had estimated that there has been a decline of $111 million/annum affecting this industry in the US Pacific coast. The acidified sea water rising from deep could be enough corrosive to kill the oyster larvae (Riebessel et al., 2010).

OA is not only progressively decreasing the ability of many organism to build their shells, but it will also affect ecosystems' structure and function. OA could be responsible of a chain reaction of impact through the marine food web, beginning with larvae that are the most vulnerable stage in an organisms life. Most of ocean regions will become inhospitable to coral reefs thus affecting food security, tourism and biodiversity. There is evidence that OA can also affect the sense of direction of many marine pelagic organisms, for instance, cetaceous' ability to orientate them self is based on the sound waves velocity which could be affected by the hydrogen ion concentration, thus the variation of the pH may also affect these marine ecosystems' keystone species (Riebesell et al., 2010).

As acidity and sea temperature increase, the ocean's ability to adsorb atmospheric CO_2 will be reduced, thus exacerbating the rate of climate change.

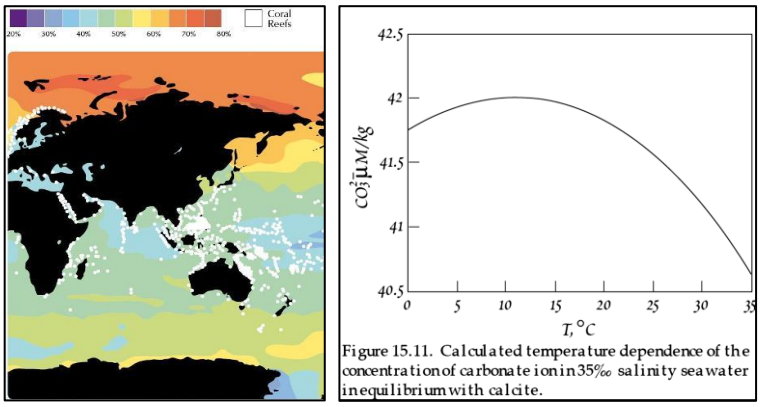

Fig. 4 - Left; Expected pH increase in 2010, (EPOCA, 2011). Right; solubility of calcite with temperature (White - Geochemistry).

The impact of OA will vary in intensity in time and space, in fact, polar region undergoing the greatest relative changes, because the temperature is lower than in equatorial region, the seawater ability to adsorb CO_2 is bigger, furthermore, in polar regions solubility of calcite is lower due to the lower temperature than equatorial regions (Fig. 4).

Besides, CO_2-induced changes in physicochemical attributes of the oceans cannot be considered isolated from other man-induced modification of the hydrosphere. Pollution, for example, is a continuing threat to the marine environment (Rogers & Laffoley, 2011). It has become apparent that climate change and CO_2 emissions may have indirect effects on marine ecosystems, and may also interact with concurrent stressors or other natural phenomena. Climate change may increase the susceptibility of marine species to disease and marine communities to invasion by exotic species, or alter the bioavailability and toxicity of contaminants. This latter indirect effect of climate change has been the focus of much recent research, with several excellent syntheses available (Macdonald et al., 2005; Noyes et al., 2009).

Our understanding of how increased ocean acidity may affect marine ecosystems is at present very limited, basically, there are three kinds of approaches to study OA:

a) *microcosms*,
b) *mesocosms*,
c) *in situ perturbation experiments* (which consist in natural venting sites, spatial/temporal gradients in ocean pH, manipulative in situ $p(CO_2)$ perturbations).

Microcosms are essentially small containers where, under controlled pH and temperature conditions, single species of microorganism are grown in order to assess the physiological stress caused by acidification.

Mesocosms are big container where a known number of species are grown in pH and temperature controlled conditions, in order to assess the interaction between each other species and between the species with the environment in the different pH conditions.

The most complicated approach is ***in situ***, but it can provide more information about the resilience capacity of the ecosystem and how it can influence the studied specie which is affected by the acidification.

Fig. 5 - Micro-Mesocosm and In situ perturbation experiment (from left to right).

In order to study the acidification phenomena in ecosystem it is useful to choose a natural acidified sea water such as in a volcanic vents system, because of the fact that in a such ecosystem there is a natural pH gradient better match for the complex interactions typical in nature.

For instance a study of Hall-Spencer et al., 2008, showed how the typical rocky shore communities with abundant calcareous organisms shifted to communities lacking scleractinian corals with significant reductions in sea urchin and coralline algal abundance in the island of Ischia (Italy), along gradients from pH (8.1–8.2) to lowered pH (mean 7.8–7.9, minimum 7.4–7.5. This fact clearly highlight that pH can heavily influence the composition of communities in a marine ecosystem. According to this study sea-grass production was highest in an area at mean pH 7.6 (1,827 µatm p_{CO2}) where coralline algal biomass was significantly reduced and gastropod shells were dissolving due to periods of carbonate sub-saturation. The species populating the vent sites comprise a suite of organisms that are resilient to naturally high concentrations of p_{CO2} and indicate that ocean acidification may benefit highly invasive non-native algal species.

Short-term laboratory experiments indicate that many calcareous organisms may be unable to build their skeletons as oceans acidify over the next 100 years. This may combine with other stresses, such as global warming, to drive tropical coral reefs towards functional collapse.

Natural CO_2 flux to the atmosphere from volcanic vents and high heat flow areas amounts to less than 0.5% of anthropogenic emissions in the global carbon budget, but can alter locally the ocean chemistry.

Marine CO_2 vents are abundant in the Mediterranean, especially around Italy and Greece where they sometimes eject volcanic fluids containing up to 1–2% hydrogen sulphide (Dando et al., 1999). Some marine CO_2 vents are at ambient seawater temperature and lack toxic sulphur compounds; such vents can prevail for years to millennia and may be used as natural experiments to advance our understanding of ocean acidification at the ecosystem level.

Vent systems however, are not perfect predictors of future ocean ecology owing to temporal variability in pH, spatial proximity of populations unaffected by acidification and the unknown effects of other global changes in parameters such as temperature, currents and sea level.
Nevertheless, such vents acidify sea water on sufficiently large spatial and temporal scales to integrate ecosystem processes such as production, competition and predation. Lush stands of sea-grass and brown algae can thrive along natural pH gradients where aragonitic and then calcitic calcareous organisms are lost owing to skeletal dissolution.
This confirms experimental and modeling predictions that differential responses of benthic species to decreased pH can lead to substantial changes in community structure.
It is unknown whether there will be sufficient refuge or enough time for these groups to adapt to survive the predicted rapid rate of ocean acidification.
The biological responses of organisms to OA are relatively difficult to predict and experimental studies have produced a range of results. Until recently, OA research mainly considered the effect of declining pH and perturbed carbonate chemistry on a range of physiological processes, initially focusing on the calcification process of marine invertebrates such as crustaceans, echinoderms, coccolithophores and corals. For instance, shell formation in a variety of calcifying species may be affected by OA and this could have global effects for carbonate production in the ocean (Lebrato et al., 2010). More recently, other pH-dependent processes such as acid-base regulation, metabolism and reproduction have also been studied (e.g. Spicer et al., 2011; Stumpp et al., 2012). Meta-analyses have shown that taxa vary in their sensitivity to OA, and that some organisms may be more resilient than commonly predicted due to compensatory biological processes and small-scale spatial and temporal variability in ocean pH (Hendriks et al., 2010).
More recently attention has shifted to the potential impact of OA on energetic partitioning between different physiological processes (Wood et al., 2008; Pascal et al., 2010). Increasing evidence suggests that exposure to OA can lead to metabolic depression (Miles et al., 2007), reduced growth (Michaelidis et al., 2005) and reduced energy reserves (Langenbuch & Pörtner, 2002, 2003), particularly in species with poor ion regulation (Whiteley, 2011). Thus, even species that show no direct effects of OA on calcification may exhibit physiological and behavioural trade-offs (Findlay et al., 2011).

1.2. Acidification and metals in seawater.

Another point of view about OA, which must to be considered, is that it may alter the behavior of sediment-bound metals, modifying their bioavailability and thus toxicity (Roberts et al., 2012).

In order to provide this hypothesis, a group of scientists (Roberts et al., 2012) had done an experimental test with the amphipod *Corophium volutator*. Amphipods were exposed to two test sediments, one with relatively high metals concentrations (Σmetals 239 mg kg^{-1}) and a reference sediment with lower contamination (Σmetals 82 mg kg^{-1}) under conditions that mimic current and projected conditions of OA (390–1140 µatm pCO_2). Survival and DNA damage was measured in the amphipods as indicator of environmental stress in relation with acidification conditions and heavy metals availability, whereas the flux of labile metals was also measured in the sediment and water column. Results shown that there was a 2.7-fold increase in DNA damage in amphipods exposed to the contaminated sediment at 750 µatm pCO_2, while increased DNA damage in organisms exposed to the reference sediment, were found only at 1140 µatm pCO_2.

Metals are one of the most common types of coastal contaminant and are found in high concentrations in the waters and sediments of many coastal and estuarine systems (Bryan & Langston, 1992). Ocean Acidification is expected to alter the bioavailability of water-borne metals (Millero et al., 2009). The toxic free-ion concentration of metals such as copper (Cu) may increase by as much as 115% in coastal waters in the next 100 years due to reduced pH (Pascal et al., 2010; Richards et al., 2011), whereas the free-ion concentration of other metals including cadmium (Cd) may decrease or be unaffected (Lacoue- Labarthe et al., 2009, 2011, 2012; Pascal et al., 2010). One might therefore predict greater metal toxicity in organisms with exposure under higher pCO_2. This hypothesis is supported by the observed influence of increased pCO_2 on the bioaccumulation of trace metals in the eggs and embryos of the squid *Loligo vulgari* (Lacoue- Labarthe et al., 2011, 2012) and eggs of the cuttlefish *Sepia officinalis* (Lacoue-Labarthe et al., 2009).

While these studies have measured bioaccumulation, the only current study to investigate the influence of OA on metal toxicities showed increased toxicity of Cu, but not Cd, to *Amphiascoides atopus* (a crustaceans copepod) under conditions of elevated pCO_2 (Pascal et al., 2010). This early study is suggestive of interactions between aqueous metals and OA. Even less is currently known about how OA may influence the behavior of metals bound to sediments (Royal Society, 2005; Millero et al., 2009). A recent report examined the role of elevated CO_2 in controlling fluxes of labile metals from contaminated sediments (Ardelan et al., 2009). However, this experiment focused on the failure of CO_2 storage sites and therefore considered pCO_2 concentrations far in excess of those predicted to occur through OA from atmospheric carbon sources. The implications of such altered metal fluxes for the health of sediment-dwelling biota have not been considered to date.

A study of Roberts et al., 2012, about the relationship between OA and metal contaminated sediments, highlights how there is a negative relationship between seawater pH and metals such as dissolved Ni and Fe. They have calculated for different metal contaminated sediments, at different pCO_2, the different fluxes for each metal (including Ni, Fe, Cu and Zn). There was no effect of sediments or pCO_2 on dissolved Mn fluxes to the sediment water interface. There was a significantly greater flux of Fe to the sediment water interface from the reference sediment under the higher pCO_2. Fluxes of Cu to the overlying water were greater from the reference sediments than from the contaminated sediments. However, at the sediment water interface fluxes from the contaminated sediments were greater for Cu and Zn. Fluxes of Fe and Zn to overlying water were unaffected by the pCO_2 treatments and did not differ between the test sediments.

Elevated pCO_2 also influenced the flux of metals from sediment bound to labile states. Ni in particular dissociated more rapidly from the test sediments at the highest pCO_2 of 1140 µatm, relative to rates measured at the background pCO_2 of 390 µatm (fluxes were intermediate at 750 latm). A similar pattern was detected for Zn, It is possible that metals within the contaminated sediment were strongly bound to fine particles and within organic complexes and were therefore less liable to dissociation than metals in the sandier reference sediment.

Most divalent metals form strong complexes with organic ligands and fine particulates, and the stability of these complexes differs between metals (Millero et al., 2009). In contrast, free-ion concentrations of metals such as Cd that form pH-independent bonds may be relatively unaffected (Pascal et al., 2010).

Roberts et al., 2012 in their paper propose that the interaction between OA and toxicity is the result of additive effects of the two stressors rather than synergistic effects. Sediment properties such as carbon content and grain size are likely to influence the interaction between sediment-bound metals and pH, and characteristics of species such as their life history, behaviors and feeding modes will influence their susceptibility to the combined stressors. Additional experimental evidence on these responses is clearly needed to broaden our understanding of the wider implications of OA.

Since increasing atmospheric CO_2 over the next 200 years will cause a pH decrease of ocean water, it will change the organic and inorganic carbonates speciation. The decrease of OH^- and CO_3^{2-} ions can affect the solubility, adsorption, toxicity, and rates of redox processes of metals in seawater.

However few studies have considerate also the effect that the lower pH will have on the speciation of metals in natural waters (Turner et al., 1981; Byrne et al., 1988; Byrne, 2002). Both OH^- and CO_3^{2-} form strong complexes with divalent and trivalent metals in ocean water (Baes et

al., 1976; Bryne et al., 1997, 1998; Millero et al., 1992, 1995). Since these anions are expected to decrease in surface waters by 82% and 77% respectively, it will change also the speciation of a number of metals ions in sea water (Bryne et al., 2002; Millero et al., 2001).

The pH will also affect adsorption of metals to organic material (Frank et al., 2009). In organic matter the surfaces sites will become less available to adsorb metals as a consequence of a pH decrease (Crist et al., 1988; Wilde et al., 2006). Furthermore, most of metals are more soluble in acidic waters so their concentrations are expected to change as well (Frank et al., 2009).

Trace metals in seawater can be classified in five groups (according to the dominant inorganic ligand that complexes them) (Bryne et al., 1988):

1. *Hydrolyzed* (OH^-); Al (III), Fe (III), In (III), Th (IV), U (IV).
2. *Carbonate* (CO_3^{2-}); Cu (II), UO^{2+}, Rare Earths, Y (III).
3. *Chloride* (Cl^-); Ag (I), Au (I), Cu (I), Hg (II).
4. *Free*; Mn (II), Fe (II), Co (II).
5. *Transition/Mixed*; Pb (II), Y (III), Sc (III), Ac (III).

Metals that form strong complexes with hydroxide and carbonate will undergo significant changes in speciation as the pH of seawater decrease, metals that form strong complexes with chloride will see little if any change in speciation because decreasing the pH will not change the chloride concentration. These metals include Cu^+, Cd^{2+} and Hg^{2+}.

The decrease in pH is not expected to strongly influence metals that are predominantly in the free form. The metals Co^{+2}, Zn^{2+}, and Mn^{2+} will only increase by a few percent (Frank et al., 2009).

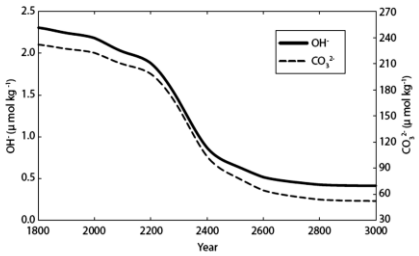

Figure 2. The decrease in the concentrations of OH^- and CO_3^{2-} ions in seawater due to ocean acidification (calculated using the Millero et al., 2006, carbonate constants).

Fig. 6 - Graphic from Millero et al., 2006.

The effect of pH on the speciation will not be strongly affected because the changes are largely related to changes in the OH^- and CO_3^{2-} ions (Millero et al., 2009).

The inorganic speciation of metals in seawater is a function of pH and time (estimated from Caldeira and Wickett, 2003). Because the pH is expected to decrease to 7.7 by 2100, the most rapid change will occur over the latter half of this century.

Divalent Metals such as iron and copper, and although less also nickel, tends to form carbonates complexes. The largest percentage increase for carbonate-dominated metals is for Cu^{2+} (about 30%) (Steeman-Nielsen and Wium-Anderson, 1970; Sunda and Ferguson, 1983) (Fig. 7 and 8).

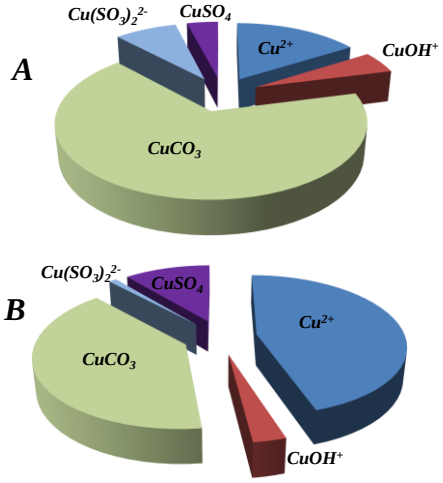

Fig. 7 – A actual copper chemical speciation in seawater; B expected chemical seawater copper speciation, from Millero et al., 2010.*

**image from Millero et al 2010 (DOI: 10.2113/gselements.6.5.299). Inorganic speciation of Cu(II) in seawater at pH 8.1 (A) and at pH 7.4 (B). The changes in going from 8.1 to 7.4 for the various species are as follows: Cu^{2+}: 16 to 45%; $CuOH^+$: 5 to 2.8%: $CuCO_3$: 65 to 40%; $Cu(CO_3)_2^{-2}$: 8 to 1%; $CuSO_4$:4 to 11%.*

Most trivalent metals like Fe(III), Al(III), and As(III) are more soluble in acidic solutions than normal seawater pH (Liu and Millero, 2002, Martin, 1990). For such metals as pH decreases as solubility increases in different percentages. A decrease in pH from 8.1 to 7.4 will increase the solubility of Fe(III) by about 40%, which could have a large impact on biogeochemical cycles because iron is an important micronutrient. Metals such as aluminum tends to form hydroxides complexes. The largest change will be to the $Al(OH)_3$ complex, which will increase by 36% (Brand, 1991, Millero et al., 2006).

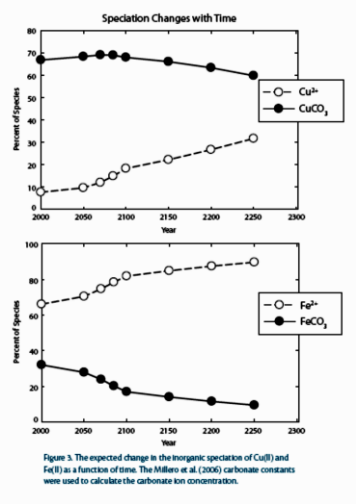

Fig. 8 - Image from Millero et al., 2006.

The effect of ocean acidification on different metals may also affect the competition of various metals for surface sites (Bruland et al., 1991). Future measurements are needed to examine the effect of ocean acidification on biogeochemical processes in the ocean.

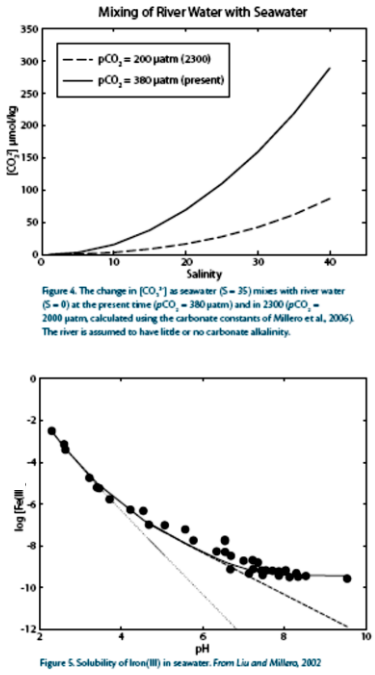

Fig. 9 - Images from Millero et al., 2006.

The inorganic speciation of many divalent metals in seawater only affects a small fraction of the total metal. Significant fractions of the total concentrations (most > 99%) of metals such as iron, cobalt, copper, zinc, and lead are in the form of metal-organic complexes (van den Berg, 1984; Hering et al., 1987; Sunda and Hanson, 1987; Coale and Bruland, 1988; Donat and van den Berg, 1992). This observation is important, particularly for assessing the bioavailability of

metals in the surface ocean. The role of metals in biological processes is quite significant. In the surface ocean, the biochemically significant metals for microorganisms are manganese, iron, nickel, cobalt, copper, zinc, and cadmium (Morel et al., 2003). These trace metals are needed for the growth and survival of photosynthetic organisms. Low concentrations of these metals, primarily iron, have been linked to the paucity of primary producers observed in areas of the ocean with otherwise high nutrient concentrations (Martin and Fitzwater, 1988; Landry et al., 1998). Copper, cadmium, and lead have all been shown to be toxic at higher concentrations in the marine environment than seawater normal background (Casas and Crecelius, 1994; Paytan et al., 2009). Ambient trace metal concentrations in the open ocean are low, and as a result, marine organisms have evolved efficient mechanisms, many of which are yet to be characterized, of concentrating these metals for their needs (Morel et al., 2003). Thus, small increases in concentration of normally scarce metals often result in toxic effects to organisms unaccustomed to the higher concentrations (Sunda and Huntsman, 1992). This has been observed with the free form of Cu(II) at concentrations as low as 10-12 nM, which are reported to be toxic to marine phytoplankton (Brand et al., 1986).

A number of researchers have shown that many biologically significant metals form strong complexes with organic ligands in seawater, including: Cu(II), Fe(III), Co(II), Zn(II), Cd(II), Pb(II), Ni(II) (Millero et al., 2009) (Fig. 10).

Table 2. Conditional stability constants for metals in seawater (Millero, 2001b)

Metal	[M]	[L]	log Kc
Cu(II)	1–10 nM	2–60 nM	8.5
Zn(II)	0.1–2 nM	1.2 nM	12
Cd(II)	2–800 pM	100 pM	12
Pb(II)	17–49 pM	200–500 pM	11
Ni(II)	1.7–4.3 nM	2–4 nM	17–19
Co(II)	10–103 pM	9–83 pM	11–16
Fe(III)	0.2–8 nM	0.4–13 nM	19–23

Fig. 10 - From Millero et al., 2009.

Whether the labile fraction of the inorganic metal complexes is available in nutrient form or contributes to a toxic response is difficult to determine and is not consistent for all organisms (Croot et al., 1999). Using the stability constants (Kc) for the formation of organic complexes, it is possible to examine the competition of the inorganic and organic complexes to assess the fractionation of a metal. A number of scientists (given above, Fig. 11) have studied the formation of Cu(II) organic complexes.

Table 3. Literature data for Cu(II) complexation with L_1 and estimated values of the free $[Cu(II)]_e$ at pH 8.1 and 7.4

Location	$[Cu]_T$ (nM)	$[L]_T$ (nM)	log Kc	pH 8.1* $[Cu]_e$ (pM)	pH 7.4* $[Cu]_e$ (pM)	Reference
NE Pacific	0.59	1.6	11.8	1.1	1.7	Coale and Bruland (1988)
Biscayne Bay	2.7	5.1	12.0	1.1	2.4	Moffett and Zika (1987)
Montauk Point	5.9	20	11.7	0.84	1.3	Hering et al. (1987)
Narragansett Bay	21	35.	12.3	0.70	1.9	Sunda and Hanson (1987)
Indian Ocean	1.7	3.1	12.6	0.42	1.2	Donat and van den Berg (1992)
North Sea	3.2	16.	12.4	0.10	0.14	Donat and van den Berg (1992)
South Atlantic	2.3	11	12.2	0.17	0.24	van den Berg (1984)
Balaguier Bay	14.8	138	9.9	15.1*	20.9*	Louis et al. (2009)

* Estimated values using pKa = 8.6 (Louis et al., 2009) for L_1.
* When a value of log Kc of 12 is used to compute $[Cu]_e$, the pH 8.1 and 7.4 values are 0.12 and 0.17 nM, respectively.

Fig. 11 – From Millero et al., 2009.

The effect of pH on the speciation of metal organic complexes, in the marine environment, is not as well characterized as the inorganic ligands due to the non-homogenous composition and unknown structures of the organic ligands (Dittmar and Paeng, 2009; Sleighter and Hatcher, 2007). Scientists find that marine organic material has similar properties to the better-characterized metal complexing organics in freshwater systems (Millero et al., 2009). It is clear that the marine dissolved organic material can complex metals in function of pH, because of the presence of phenolic and carboxylic functional groups (Millero et al., 2009). Cu(II) is linked with organic matter through an organic ligand (on the surface of organic matter) and for a pH decreasing, the concentration of this ligand decreases by 25%. That's increase the dissolved copper (Louis et al., 2009, Fig. 12). Millero et al., 2001, say that, in upwelling areas, where pH is frequently lower due to ocean acidification, metal organic complexing studies may be useful. These studies show that Fe(III) forms strong complexes with organic ligands in seawater, and for lower pH values, increase the solubility of Fe(III) in seawater (Liu and Millero. 2002).

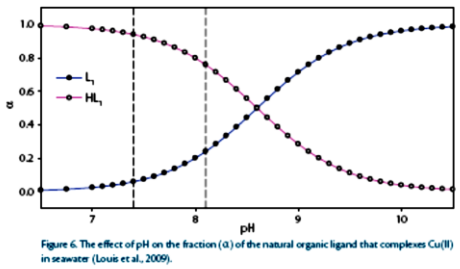

Figure 6. The effect of pH on the fraction (α) of the natural organic ligand that complexes Cu(II) in seawater (Louis et al., 2009).

Fig. 12 – From Millero et al., 2010.

Chemical reaction rates are also affected by pH changes (Millero, 2001b), including the oxidation and reduction of metals (Cu(I), Cu(II), Fe(II), Fe(III), Cr(III), Cr(IV)), and of sulfur compounds.

The kinetic rate constant for the reduction of Cu(II) to Cu(I) is a function of pH because the reaction is slower at high concentrations of the carbonate ion (Fig.13). As the ocean becomes

more acidic, reduction of Cu(II) will increase, as the ionic form of Cu(II) is reduced faster than the Cu(II) in either the $CuCO_3$ o or $Cu(OH)^+$ species (Millero et al., 1991; Millero, 2001a).

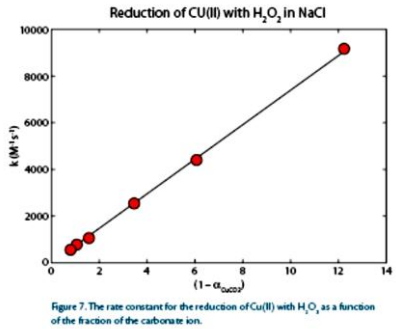

Fig. 13 - From Millero et al., 2001.

Photochemical processes in [illegible] surface waters produce a number of free radicals that can change the oxidation state of a number of metals. The free radical O_2^- is produced by the adsorption of organic chromophores (Zika et al., 1985):

$$Org + h\nu = Org^+ + e^-$$
$$e^- + O_2 = O_2^-$$
$$O_2^- + HO_2$$

Increasing evidence also shows the production of HO_2 by a wide range of microorganisms (Rose et al., 2008). Millero et al., 1987, has estimated the overall rate constant for the disproportionation of the superoxide molecule as a function of pH. Assuming a constant value for $[HO_2^-]T$, the half-life of the superoxide decreases by 20% at pH = 7.4. A decrease in concentration of the superoxide molecule would affect the redox equilibrium of biologically important trace metals, as it is important in the reduction of organically complexed Fe(III) (Rose and Waite, 2005) and redox reactions of organic and inorganically complexed Cu(II) and Cu(I) (Zafiriou et al., 1998; Voelker et al., 2000).

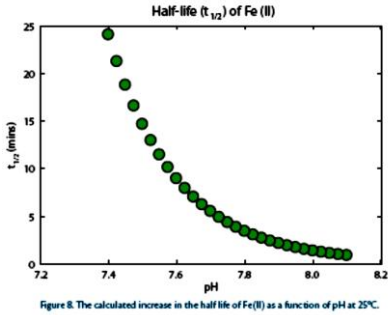

Fig. 14 - From Millero et al., 2010.

Some other studies about Fe availability, on the contrast, shows that for some planktonic species it decreases with decreasing pH. For in stance a study about the relationship between acidification and iron bioavailability (Shi et al., 2010) shows that the bioavailability of dissolved Fe is affected by the ocean acidification, in fact, in acidic microcosms containing various Fe compounds, decreased the Fe uptake rate of diatoms and coccolithophores. A slower Fe uptake by a model diatom with decreasing pH is also seen in experiments with Atlantic surface water (Shi et al., 2010) (Fig. 15).

Iron (Fe) is the biologically important element whose chemistry is most sensitive to pH. The bulk of Fe(III) in the ocean is known to be chelated by organic compounds, and the fraction that is not chelated is present as hydrolyzed species, $Fe(OH)_x^{(3-x)+}$, with the neutral tri-hydroxy species, $Fe(OH)_3$, being very insoluble (Millero et al., 2009). As ocean waters acidify, decreasing the hydroxide ion concentration, Fe's speciation and solubility will be altered. A decrease in pH by 0.3 unit should slightly increase iron's solubility in seawater. The hydroxide ion and organic chelators compete for binding Fe(III) so that a decrease in pH should affect the extent of organic chelation of Fe and hence its availability to ambient organisms. At the same time that a decrease in pH may affect the availability of Fe to phytoplankton, an increase in PCO_2 may change their Fe requirements.

For example, increasing the extracellular concentration of CO_2 should decrease the need to operate a carbon-concentrating mechanism (CCM) for CO_2 fixation and hence may allow an economy in the Fe involved in the photosynthetic or respiratory processes that provide energy for the CCM. Through changes in Fe availability and requirements, ocean acidification may affect primary production and the ecology of phytoplankton. Those experiment shows how physiology of species can change in acidic conditions.

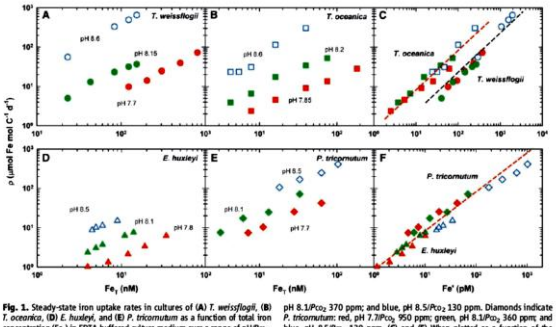

Fig. 1. Steady-state iron uptake rates in cultures of (**A**) *T. weissflogii*, (**B**) *T. oceanica*, (**D**) *E. huxleyi*, and (**E**) *P. tricornutum* as a function of total iron concentration (Fe_T) in EDTA-buffered culture medium over a range of pH/Pco_2. Circles indicate *T. weissflogii*: red, pH 7.7/Pco_2 950 ppm; green, pH 8.15/Pco_2 320 ppm; and blue, pH 8.6/Pco_2 90 ppm. Squares indicate *T. oceanica*: red, pH 7.85/Pco_2 680 ppm; green, pH 8.2/Pco_2 290 ppm; and blue, pH 8.6/Pco_2 100 ppm. Triangles indicate *E. huxleyi*: red, pH 7.8/Pco_2 770 ppm; green, pH 8.1/Pco_2 370 ppm; and blue, pH 8.5/Pco_2 130 ppm. Diamonds indicate *P. tricornutum*: red, pH 7.7/Pco_2 950 ppm; green, pH 8.1/Pco_2 360 ppm; and blue, pH 8.5/Pco_2 130 ppm. (**C** and **F**) When plotted as a function of the unchelated iron concentration, Fe', uptake rates coalesce for each organism following a one-to-one line. The red dashed line in (**C**) is identical to the one shown in (**F**). Results of each organism are from a single experiment. Additional experiments yielded results that follow the same lines shown in (**C**) and (**F**).

Fig. 15 - Immage from Shi et al., 2010.

1.3. Vulcano: a natural laboratory for OA studies.

Several submersed CO_2 vent systems are present in deep (>100m) near shore (<100m) and shallow waters (<5m) sites in the Aeolian archipelago (North-eastern Sicily, Italy, Fig. 16), consisting of seven volcanic islands and numerous seamounts. It is regarded as a typical volcanic arc generated by subduction processes in the Southern Tyrrhenian seafloor (Carapezza et al., 2011). There are two active non-submarine volcanoes in the Stromboli and Vulcano Islands, while volcanic activity of steaming fumaroles and submerged seeps are on most of the islands.

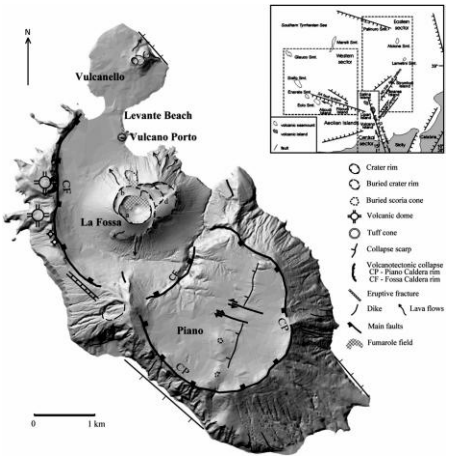

Fig. 16 - Image from Carapezza et al., 2011; 207(2011) 130-144.

The southernmost volcanic island of Vulcano (38°25'08.52"N, 14°57'39.13"E) has a maximum elevation of 500 m asl, but it extends below the sea level for additional 1000 m. It host the most recently active centre in the Gran Cratere at the top of the Fossa cone (last eruption 1888-1890) and several minor volcanic centers (Keller, 1980). Most of the intense submersed seeps are located near the isthmus of the Baia di Levante along the beach (38°25'01.44"N, 14°57'36.29"E), where dispersed underwater leaks cover a 130 × 35m shallow area (<1m depth).

Volcanic activity on Vulcano island started in the upper Pliocene (Frazzetta, 1984) with the first subaereal activity dated at 120 ka building up a trachybasaltic – trachyandesitic stratocone (South Vulcano) in the southern sector of the island (Keller, 1980). This edifice was truncated by a caldera formed by several collapse events. During the last 10 ka volcanic activity produced a cone, named La Fossa Crater, 391 m high above sea level, where the last volcanic activity took place between 1888 and 1890 (Silvestri and Mercalli 1891).

Since the 1888–90 eruption, La Fossa has been in a quiescent state, with episodic occurrences of "crises", characterized by increases in temperature (T) and gas output of the crater fumaroles, expansion of the fumarolic field and chemical and isotopic changes (e.g. increase of CO_2, He, N_2, $^3He/^4He$) indicating an increasing output of magmatic gas (Sicardi, 1941; Barberi et al.,

1991; Chiodini et al., 1993; Nuccio and Paonita, 2001). Only minor ground uplift (Bonforte and Guglielmino, 2008) and a characteristic shallow seismicity accompany these crises, which sometimes occur after significant regional earthquakes (Montalto, 1994a; Aubert and Alparone, 2000). Both shallow seismicity and minor uplift of the fumarolic zone of La Fossa cone are likely related to gas and steam pressure increase in shallow fractures within a geothermal system (Montalto, 1994b; Gambino and Guglielmino, 2008; Alparone et al., 2010).

These manifestations are located over an elongated area that is the surface expression of an active regional fault (Frazzetta et al 1983). After the last eruption of Vulcano island some authors reported wide fluctuations in the hydrothermal activity and consequent changes in the gas composition (de Fiore, 1920; Sicardi 1941). The presence of a geothermal aquifer at shallow depth has been proved by geothermal exploration wells drilled between 1951 and 1957 in the Baia di Levante area (Sommaruga, 1984). The gas emissions coming from the geothermal aquifer has been interpreted as the result of a mixing between magmatic and hydrothermal fluids feeding the crater fumaroles afterwards modified by secondary low temperature subsurface processes (Chiodini et al. 1991a, 1995). In a more recent work, Capaccioni et al. 2001 analyzed the low temperature emissions at Baia di levante beach; on the base of chemical and thermodynamical calculations, suggesting the presence of three distinct groups of CO_2 rich gas emissions at different distances from the La Fossa Crater. The gas emissions close to the Faraglione area being characterized by CO_2 contents between 97% and 98% vol, and H_2S content ranging from 2.2% close to the Faraglione to less than 0.005 % near the northern part of Baia di Levante beach (Capaccioni et al., 2001). Moreover they stated that the relative large variability in the Baia di Levante gas discharge can be attributed to either different interaction between iron sulphades and weakly acid waters.

Furthermore, studies on Levante's Bay sediments of Vizzini et al., 2013, highlight how the Bay of Levante can be considered to be affected by low trace metals contamination with moderate potential for adverse biological effects, especially in the area between about 150 and 350 m from the primary vent.

Their results support the complex spatial dynamics of trace elements in the studied area, which are constrained by both direct input from the vent and/or biogeochemical processes affecting element precipitation at the sediment-seawater interface. Consequently, great caution should be used when relating biological changes along pH gradients to the unifactorial effect of pH only, as interactions with concurrent, multiple stressors, including trace element enrichments, may occur. This finding has implications for the use of CO_2 vents as analogues in ocean acidification research. They should be considered more appropriately as analogues for low pH environments

with non-negligible trace element contamination which, in a scenario of continuous increase in anthropogenic pollution, may be very common. Baia di Levante's sediments are composed mainly of sand, in fact, the main granulometric fraction of sediments is from 77.6 to 99.9% composed by sand; organic matter content is in the range 0.33-3.92% (Vizzini et al., 2013). Trace element concentrations in sediments ranged between 13.86-78.28 mg kg^{-1} for Zn, 17.75-48.34 mg kg^{-1} for Ni, 26.49-76.15 mg kg^{-1} for Cu, 75.06-339.11 mg kg^{-1} for V, and 89.34-945.26 mg kg^{-1} for Mn, Fe concentrations varied from 14,910 to 40,494 mg kg^{-1}. In brief in the sediments of the Levante Bay, Cu and Ni concentrations were close to effects-range-low (ERL) and threshold effects level (TEL - Vizzini et al., 2013).

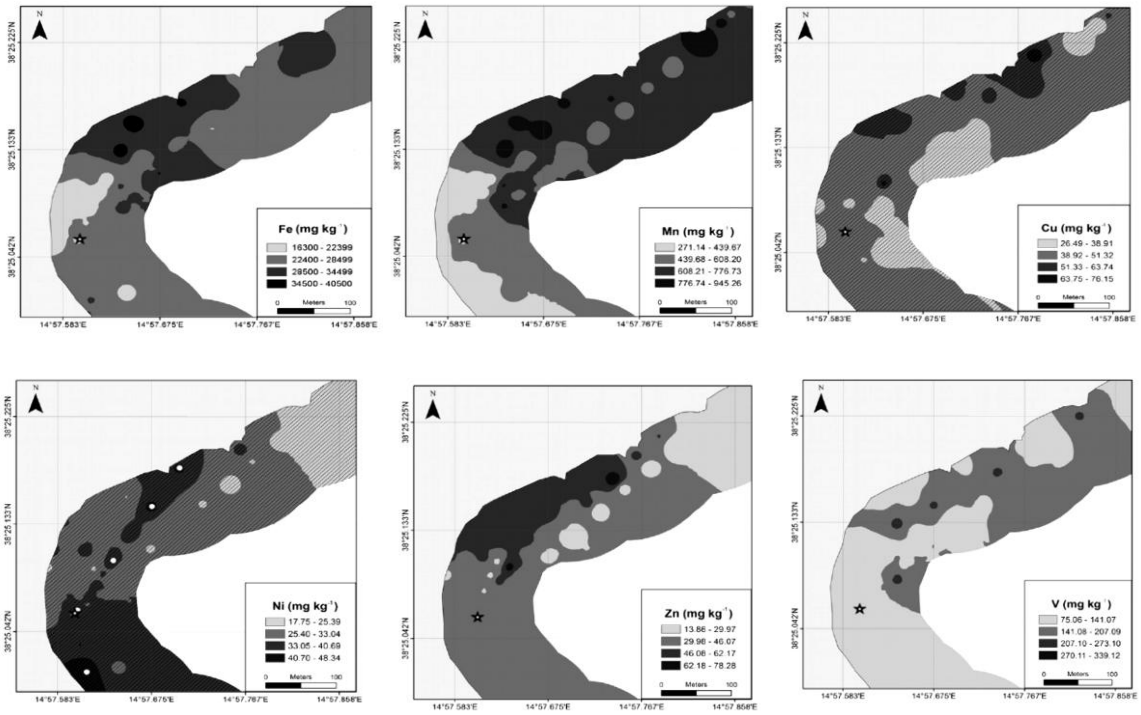

Fig. 17 - Image from Vizzini et al., 2013; metals concentration in sediments of "Baia di Levante" (Vulcano, Italy).

Chapter 2 - Seawater chemistry.

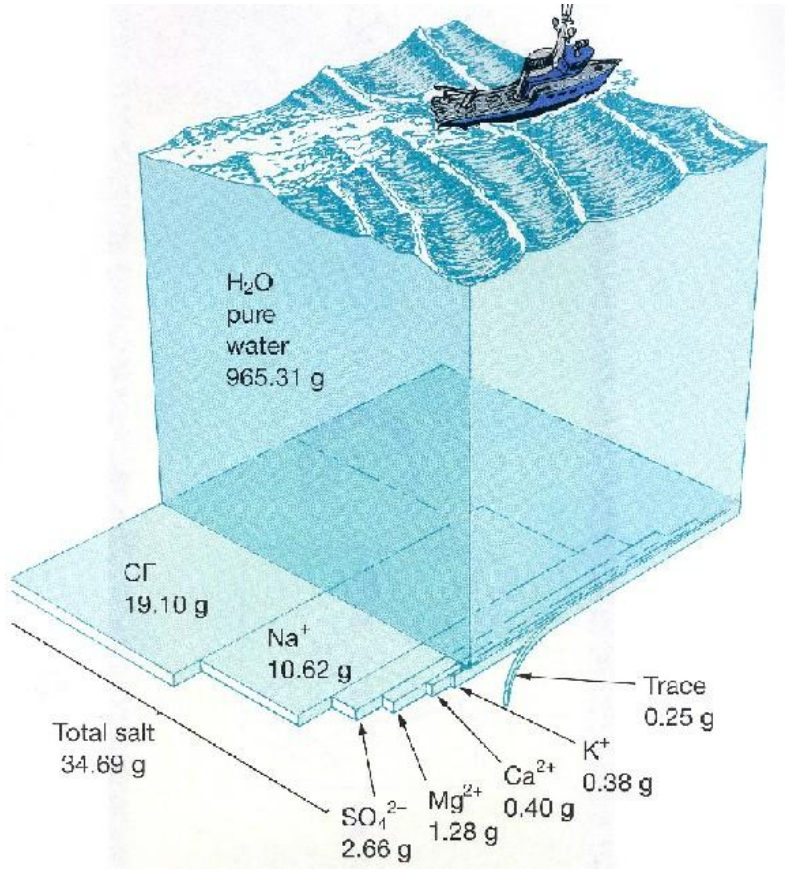

2.1. Introduction.

"*Most of the salts in the oceans are derived from weathering of the continents and delivered to the oceans by rivers. Some components of seawater are derived from hydrothermal metamorphism of the oceanic crust. […] Other components in seawater, most notably the principal anions as well as water itself, are derived from neither weathering nor hydrothermal reactions. These so-called "excess volatiles" are derived from volcanic degassing*". (White, 2003).

2.2. Chemical-physical parameters.

Chemical-physical parameters are fundamental in order to study a seawater sample, because of they can influence the thermodynamic of reactions and speciation in such complicated solution. The main chemical physical parameters that we should considered are: pH, temperature, Eh and density.

2.2.1. pH and alkalinity.

The pH of most natural waters is buffered by the carbonate system and this is certainly true for seawater. Compared to other natural waters, seawater has a relatively constant pH, with a mean of about 8, but the variations in dissolved CO_2 produce pH variations of about ±0.3 (White, 2003). This variation is largely due to biological activity: removal of dissolved CO_2 by photosynthesis increases pH, while release of CO_2 by respiration decreases it. The reason for this is easy to understand looking at the reaction that synthetizes the process:

$$6CO_2 + 6H_2O \leftrightarrow C_6H_{12}O_6 + 6O_2$$

At the pH of seawater, bicarbonate is the predominant carbonate species and we can describe the dissolution of CO_2 as:

$$CO_2 + H_2O \leftrightarrow H^+ + HCO_3^-$$

Since photosynthesis extracts CO_2 from water, the reaction is driven to the left, consuming H^+. Respiration produces CO_2, driving this reaction to the right, producing H^+. This is the main reason why the pH of the ocean decreases with depth. The pH is also affected by precipitation and dissolution of calcium carbonate. Since bicarbonate is the most abundant carbonate species, the precipitation reaction is effectively:

$$Ca^{2+} + HCO_3^- \leftrightarrow H^+ + CaCO_3$$

Precipitation of calcium carbonate decreases pH while dissolution increases it. Thus production of biogenic carbonate in surface water and its dissolution in deep water acts to reduce the vertical pH variations produced by photosynthesis and respiration.

Another important parameter used to describe ocean chemistry, is alkalinity, defined as the sum of the concentration (in equivalents) of bases that are titrable with a strong acid. It is a measure of acid-neutralizing capacity of a solution. An operational definition of total alkalinity for seawater is:

$$Alk = [HCO_3^-] + 2[CO_3^{2-}] + [B(OH)_4^-] + [H_2PO_4^-] + 2[HPO_4^{2-}] + [NO_3^-] + [OH^-] - [H+]$$

Alk is not conservative because of evaporation and dilution can affect it; indeed, these processes are the principal cause of variation in alkalinity (which is strongly correlated with salinity).

2.2.2. Temperature.

Temperature, along with salinity, determines the density of seawater. Since density differences drive much of the flow of ocean water, these are key oceanographic parameters. Temperature in the oceans can be reported as, *potential* or *in situ* temperature, but the "in situ" is the most commonly used. Potential temperature, is the temperature the water would have if brought to the surface. In situ temperature is the actual temperature of a parcel of water at depth.

2.2.3. Density.

The density of seawater is 2 to 3 percent greater than that of pure water. Average seawater, with a salinity of 35‰ and a temperature of 20°C, has a density of 1.0247 g/cc. Seawater density is controlled by temperature and salinity, so this circulation is also called the *thermohaline circulation.* The concentrations of dissolved elements vary both vertically and horizontally in the ocean and it is influenced by circulation. In a brief focus on Mediterranean Basin seawater, we can say that the circulation is influenced by exchanges between different water masses (close to the Gibraltar strait), thermo-haline streams, fresh and salt water inputs and winds (Robinson et al. 2001).

2.3. Major, minor and trace elements.

The most abundant elements in seawater are those on the "wings" of the Periodic Table (Fig. 18), the alkalis, the alkaline earths, and the halogens.

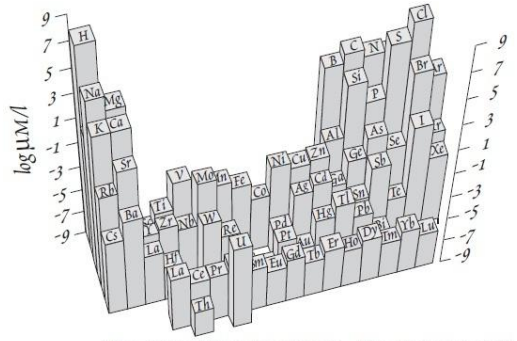

The composition of seawater. The most abundant elements are those on the sides of the periodic table. Elements in the interior tend to be less abundant.

(Image from W.M. White - Geochemistry)

Fig. 18 - Image from White - Geochemistry.

Major elements are considered "hard" ions that have inert gas electronic structures; they have relatively small electrostatic energy and large radius (low Z/r ratio), so that in solution they are present mainly as free ions rather than complexes.

Other elements (in the interior of periodic table in Fig.18) have higher Z/r ratios, and form bonds of a more covalent character, and are strongly hydrolyzed. The latter tendency leads to their rapid removal by adsorption on particle surfaces

In a seawater solution we can distinguish major elements which are considered conservative and also minor and trace elements. The conservative elements share the property of being always found in constant proportions to one another and to salinity in the open sea, even though salinity varies. All the major ions in seawater, except for bicarbonate, are included in this group.

Some minor and trace elements are also present in constant proportions; Vanadium is nearly conservative, with a total variability of only about ±15 (White – Geochemistry).

Salinity can be considered as the total dissolved solids in seawater. It is usually defined as "*the weight in grams of the dissolved inorganic matter in one kilogram of water after all the bromide and iodide have been replaced by the equivalent amount of chloride and all carbonate converted to oxide"*. Salinity is determined by measuring electrical conductivity. Another useful definition is *chlorinity*, which is "*the halide concentration in grams per kilogram measured by titration with silver and calculated as if all the halide were chloride"* (total halides are actually 0.043% greater than chlorinity). Chlorinity can also be measured by conductivity. As we shall see, Cl is always present in seawater in constant proportion to the total salt, and therefore there is a direct relationship between chlorinity and salinity. By definition:

$$S‰ = 1.80655\ Cl‰$$

"Standard seawater", which is close to average seawater, has a salinity of 35.000 parts per thousand (ppt or ‰) and a chlorinity of 19.374 ‰. Open ocean water rarely has salinity greater than 38‰ or less than 33‰. Mediterranean waters are in general supersaturated respect to Aragonite and Calcite (Schneider et al., 2007) from the bottom to the surface. Basin's Total alkalinity (TA) and Total dissolved inorganic carbon (TC) concentrations are higher than the oceans average values: ~2600 $\mu molkg^{-1}$ and ~2400 $\mu molkg^{-1}$, versus ~2400 $\mu molkg^{-1}$ and ~2200 $\mu molkg^{-1}$ (Schneider et al., 2007).

About minor and trace elements, it is important to highlight how they are essential for life. B, and Mo are widely or universally required and F, Br and Sr are required by some species. However, these elements are sufficiently abundant in seawater that biological activity produces no variation in their concentration in the ocean. For this reason, these elements are sometimes referred to as bio-unlimited. In addition to these elements, Mn, Fe, Cu, and Zn are widely or universally required and the elements V, Cr, Ni, Se, and I are required by some species.

With respect to the decomposition of organic matter there are two kinds of elements bio-geo-chemical behaviors: elements that are rapidly released known as **labile elements**, and elements

which are released more slowly, such as Si, known as **refractory**. Labile nutrients include nitrate, Mn, Cd, and Ni. Once it was thought that this different geochemical behavior was due to the fact that all refractory elements were incorporated in hard tissues and labile in soft tissue. However, Collier and Edmond (1984) demonstrated that several refractory elements are present only in soft tissues of plankton, but nevertheless undergo only slow release. These elements include Cu, Zn, and Fe.

Most elements are present in seawater at concentrations far below their equilibrium solubility. On the contrary, Ca is present in surface water at concentrations above solubility. The composition of seawater is not only controlled by thermodynamic solubility (only the concentrations of the inert gases are controlled by equilibrium solubility), in fact, the composition of seawater is controlled also by the rates at which dissolved matter is added to and removed from seawater. Rivers represent the principal "*source*" of dissolved solids in seawater and sediments represent the principal "*sink*" but there are, however, a variety of other sources and sinks (Fig. 19).

For any given element, one of these sources or sinks might be dominant, and some or most of the sources might be negligible, essentially depending on the ***residence time***. Residence time, is defined as the ratio of the mass of an element in the ocean divided by the flux to the ocean.

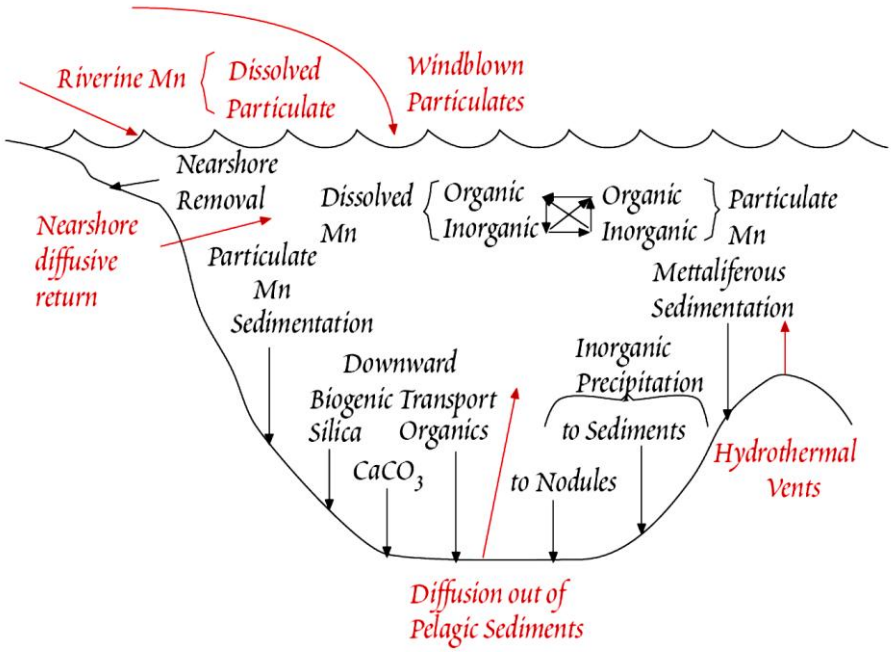

Figure 15.23. Marine geochemistry of Mn, illustrating the range of possible sources and sinks, as well as internal processing, of dissolved material in seawater.

Fig. 19 - Image from White-Geochemistry, 2003.

The residence times are not well known for all elements. Nevertheless, residence times of elements in seawater clearly vary greatly: from 150 Ma for Cl to a few tens of years for Fe.

As known one of the most important source of elements for seawater are rivers. As seawater mixes with river water, the resulting increase in ionic strength and change in pH and solute composition induces the flocculation of riverine colloids which dramatically affects trace metal chemistry.

Aerosols have several sources: sea spray, mineral dust derived from soils and desert sands, volcanic eruptions, condensation reactions in the atmosphere, the biosphere (including fires), and anthropogenic activity such as combustion of fossil fuels, mining and mineral processing, agriculture, and the production and consumption of various chemicals.

Interestingly, sea spray does not have the same composition as seawater. Sea spray is enriched in trace metals and other substances. This reflects the enrichment of these elements found in the surface micro layer at the ocean-atmosphere interface. Within the micro layer, metals are adsorbed or complexed by organic substances that form a thin film on the sea surface.

The material flux from the atmosphere to the ocean may occur through *dry deposition*, which includes both settling of particles from the atmosphere and gas adsorption, and *wet deposition*. Wet deposition includes all matter, both particulate and gaseous, first scavenged from the atmosphere by precipitation (i.e., rain and snow) before being delivered to the oceans.

2.4. Dissolved gases.

The concentrations of dissolved gases in the oceans are maintained primarily by exchange with the atmosphere. Such as for dissolved elements also gases may be divided into conservative and non-conservative ones.

The noble gases and nitrogen constitute the conservative gases. Since they are all minor constituents of seawater, we can use Henry's Law to describe the equilibrium solubility of atmospheric gases in the ocean:

$$C = kP$$

where C is the concentration in seawater, k is the Henry's Law constant and P is the partial pressure of the gas in the atmosphere. Due to the temperature dependence of gas solubility (they are more soluble at lower temperature), the conservative gases are not uniformly distributed in the ocean. Gas solubility is also strongly dependent on salinity and pressure. For example, at 20°C the solubility of oxygen is 20% lower in seawater with a salinity of 35‰ than in pure water. The gas solubility increase directly with pressure. However, pressure increases rapidly with depth in the ocean, by 1 atm for every 10 meters depth, and that is why oceans' deep water

are considered a CO_2 sink. O_2 and CO_2 are the principal non-conservative gases, because of photosynthesis and respiration:

$$6CO_2 + 6H_2O \leftrightarrow C_6H_{12}O_6 + 6O_2$$

Regarding oceanic carbon dioxide, most CO_2 dissolved in water is present as carbonate or bicarbonate ions (HCO_3^- and CO_3^{2-}). CO_2 cannot be treated strictly as a dissolved gas, as there are sinks and sources of CO_2 other than the atmosphere. For example, much of the dissolved CO_2 is delivered to the ocean by rivers as bicarbonate ion. In general about CO_2 distribution, surface water is often supersaturated with respect to the atmosphere in equatorial regions (because of photosynthesis) as upwelling brings CO_2-rich deeper water to the surface and warming decreases it solubility. The greatest degree of under saturation occurs in polar regions, where photosynthesis decreases CO_2 and cooling increases it solubility.

Biological activity is responsible for vertical variations of CO_2 in the ocean. Photosynthesis converts CO_2 to organic matter in the surface water. The total amount of dissolved CO_2 converted to carbonate is small compared to that converted to organic carbon. However, a much larger fraction of biogenic carbonate sinks out of the photic zone, so that the downward flux of carbon in carbonate represents about 20% of the total downward flux of carbon. A larger fraction of carbonate produced is also buried, so that the flux of carbon out the ocean is due primarily to carbonate sedimentation rather than organic matter sedimentation. The transport of CO_2 from surface to deep water as organic matter and biogenic carbonate is called *the biological pump* (White, 2003). For these reasons, biologist thinks that variations of ocean temperature and pH, may greatly affect the CO_2 balance of surface waters, because the biota will be dramatically influenced.

2.5. Previous studies on Vulcano.

2.5.1. Gases.

Main volcanic emissions include harmful gas species, such as CO_2, SO_2, H_2S, HF and HCl (Hansell et al., 2006). In addition, acid rains from steam condensation, and emission of Rn, Hg and many other metals and trace elements (Fulignati et al., 2006) may be hazardous for people living or working on volcanoes (Aramaki et al., 1994).

Gas (mainly CO_2) can be diffusively emitted from the soil and submarine vents (Chiodini et al., 1996, 1998; Carapezza et al., 2003; Carapezza and Granieri, 2004). It is long known that large diffuse CO_2 emissions occur around and on La Fossa cone (Badalamenti et al., 1988, 1991a, 1991b; Carapezza, 1994; Carapezza et al., 1994; Chiodini et al., 1996; Carapezza and Granieri, 2004) and important variations in the rate

of CO_2 diffuse degassing have been reported to be associated with changes in the level of fumarolic activity (Granieri et al., 2006).

The area of Baia di Levante with abundant CO_2 emissions varied with time but the most important and continuous degassing occurs in the southern part, between the Faraglione and the thermal pool. Variations of up to one order of magnitude were recorded in the CO_2 soil flux, from 96 to 940 g/m^{2}day with an average of 412 g/m^{2}day in the Isthmus area (Carapezza et al., 2011).

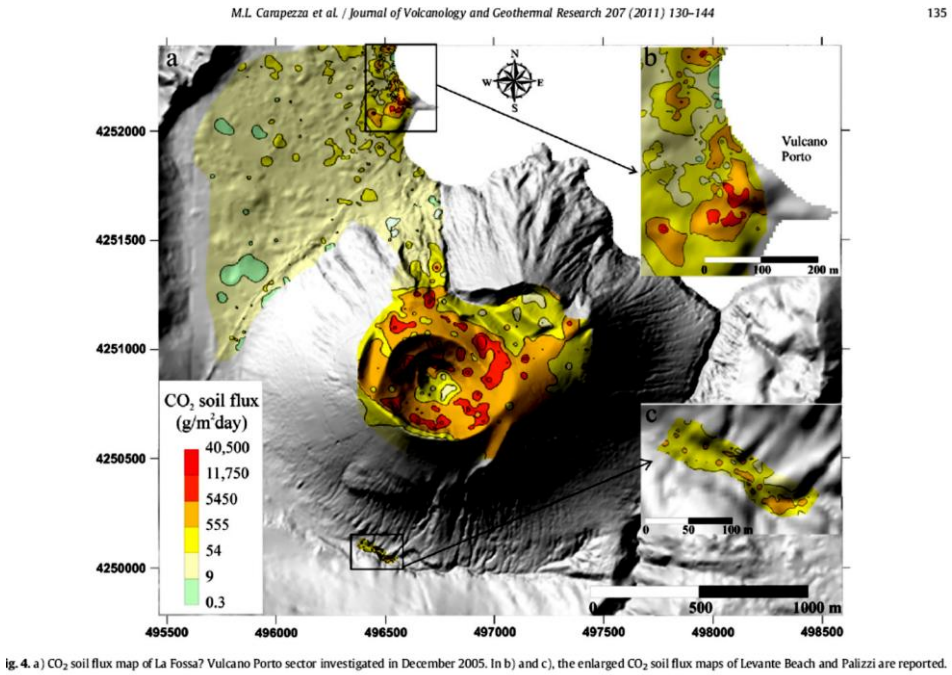

ig. 4. a) CO_2 soil flux map of La Fossa? Vulcano Porto sector investigated in December 2005. In b) and c), the enlarged CO_2 soil flux maps of Levante Beach and Palizzi are reported.

Figura 20 - From Carapezza et al., 2011.

In all Baia di Levante, the gas emissions were visible as bubble trains rising in the water. Other small fumaroles were located at the base of Faraglione (Fig. 20). The gas composition of these fumaroles is well known and CO_2 and H_2S concentrations range from 95 to 97.72% and from 1.57 to 2.47% respectively, with an average ratio of 47.8 (Chiodini et al., 1991, 1995; Capaccioni et al., 2001) (Fig. 21). Similar values were found in our 2007 and 2009 field analyses (Carapezza et al., 2011).

Estimation CO_2 and H_2S viscous fluxes from Levante beach subaqueous fumaroles. (Carapezza et al., 2011)		
	CO_2 flux kg/day	H_2S flux kg/day
Sea 2007	370.55	5.41
Thermal pool 2009	52.9	0.91
Sea 2009	1053.7	15.4
Beach pond 2009	1114.9	16.44

Fig. 21 – Estimated gasses fluxes from Levante Beach (Vulcano), Carapezza et al., 2011.

Furthermore, a study of Capaccioni et al., 2001 show that in Levante's beach gas sample were characterized by CO_2 contents up to 84.9%, hydrogen sulphide content was from 2.5 to 0.0005%. Sadwick et al., 1996 show that some samples of seawater of the bay contained from 273 to 153 µM/kg H_2S, which should be considered as lower limits on the H_2S fumaroles fluids (Fig. 22 and 23).

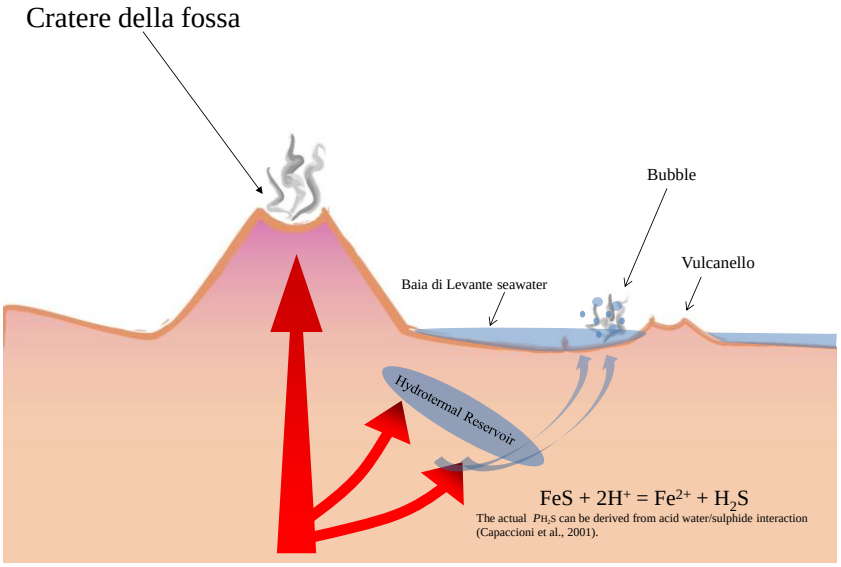

Fig. 22 – Model of the hydrothermal reservoir in Levante's Bay (Vulcano).

Table 1
Chemical composition of the gases in Levante Bay area.

Site	Date	CO_2 (%)	N_2 (%)	O_2 (%)	CH_4 (ppm)	H_2 (ppm)	H_2S (ppm)	References
Isthmus	1989	96.0	3.3	0.2	460	1300	18,000	Italiano et al. (1984)
Sea shore	1990	98.5	1.6	<0.05	1025	17	9000	Italiano et al. (1984)
FM	May 1995	96.7	0.6	0.0001	760	4600	21,600	Capaccioni et al. (2001)
Vu1	May 1996	98.1	1.0	0.0001	1020	7.2	8000	Capaccioni et al. (2001)
Vu2	May 1997	97.8	1.0	0.0001	710	774	10,200	Capaccioni et al. (2001)
Vu3	May 1998	76.2	23.2	0.0001	1710	10.8	50	Capaccioni et al. (2001)
FM	November 1995	97.7	0.8	0.0002	550	6600	15,100	Capaccioni et al. (2001)
Vu1	November 1996	98.2	1.0	0.22	1440	5.6	6100	Capaccioni et al. (2001)
Vu2	November 1997	97.8	1.0	0.06	960	568	10,500	Capaccioni et al. (2001)
Vu3	November 1998	84.6	15.2	1.8	1710	5.4	<50	Capaccioni et al. (2001)
Grip	2001	98.6	1.4	n.r.	1500	2374	n.r.	Amend et al. (2003)
Acque Calde 2	2001	98.8	0.9	n.r.	1290	19,800	n.r.	Amend et al. (2003)
Campo Frizzante I	2003	99.1	0.8	n.r.	1320	570	n.r.	Rogers et al. (2007)
Campo Frizzante II	2003	99.0	0.9	n.r.	1360	<5	n.r.	Rogers et al. (2007)
I-1	2010	98.6	0.9	0.08	1400	1410	n.r.	Inguaggiato et al. (2012)
I-5	2010	97.6	0.8	0.07	1300	1390	n.r.	Inguaggiato et al. (2012)
I-15	2010	96.9	1.2	0.16	1400	1520	n.r.	Inguaggiato et al. (2012)
I-26	2010	97.5	1.1	0.13	1300	1380	n.r.	Inguaggiato et al. (2012)
I-37	2010	98.3	1.0	0.12	1400	1450	n.r.	Inguaggiato et al. (2012)
Vent (free gas)	April 2011	98.0	1.5	0.21	1700	<5	400	This study
Vent (dissolved gas)	April 2011	13.0	64.5	0.17	430	<5	n.a.	This study

n.r. = not reported; n.a. = not analysed.

Fig. 23 - Comparison between previously studies on volcanic gasses and the present study, image from Boatta et al., 2013.

2.5.2. Trace elements.

There are considerable evidences that volcanic emissions significantly contribute to the natural cycling of trace elements in the uppermost geochemical spheres, many authors attributed the presence of these metals to the reaction of acidic solutions with the wallrock (Aiuppa et al., 1999). Sortino and Bichler (1997) have emphasized the role of halogens in transporting volatile metals such as As and Sb. Deep sea hydrothermal vents are considered "chemical reactors" for the formation of both organic and inorganic compounds and their transformation through abiotic and biotic processes (Luther, 2004), and are a significant source of metals to the ocean.

Minerals identified in Vulcano include: Cannizzarite ($Pb_{46}Bi_{54}S_{217}$), Galenobismuthite ($PbBi_2S_4$), Cotunite ($PbCl_2$), Sphalerite (ZnS), Pyrite (FeS_2), Lillianite ($Pb_3Bi_2S_6$) and Greenockite (CdS). Dongarrà and Varrica (1998) have shown the presence of heavy metals (Pb, Sb, As, Cu, Zn and Au) of volcanic origin in air particulates at Vulcano Island. Many studies (Martini, 1980; Carapezza et al., 1983; Dongarrà et al. 1988; Capasso et al., 1991, 1992, 1999; Panichi and Noto, 1992; Bolognesi and D'Amore, 1993) have pointed out that the shallow groundwaters of Vulcano Porto, a plain bordering the north-western flank of the now-active La Fossa volcanic edifice, strongly interact with rising volcanic–hydrothermal fluids. Aiuppa et al., 1999 shown that trace elements exhibit a wide range of concentrations, as a result of the large variability in the chemical–physical conditions. Largely, trace elements data confirm the range of

concentrations observed in previous studies (Cellini Legittimo et al., 1980; Brondi and Dall'Aglio, 1991). Compared with his results, the average metal concentrations for Fe, Mn, Cd, Zn, Cu and Pb reported by Cellini Legittimo et al. (1980) are considerably higher, possibly due to an enhanced interaction of rising gases with the aquifer at that time.

Recent research suggests that an unknown fraction of this flux escapes from precipitation/flocculation reactions partly due to stabilisation by organic ligands (Sander and Koschinsky, 2011; Toner et al., 2009; Bennett et al., 2008), and due to nanoparticles reported to be kinetically stable (Yucel et al., 2011). Thermal water discharges from the Istmo-Porto di Levante beach further complicate the water chemistry of the bay (Aiuppa et al., 2000) by their input of elevated conductivity, high Na and Cl content, very low pH and Eh and high content of volatile metals, due to acid gas condensation (Aiuppa et al., 2000). Such underwater volcanic emissions create a natural pH gradient that provide excellent sites to study the environmental behaviour (i.e. stability, mobility, and persistence) of metal-rich and organic nano particles (NPs) from various volcanic fluids and/or gas (Kadar et al., 2012). Seawater of Baia di Levante are enriched in Mn, Fe, Cr, Cu, and Zn. Comparison between un-filtered and 0.1 μm filtered seawater concentrations showed that most elements that were enriched relative to control sea water were predominantly present as NPs (nano particles), organic and/or inorganic complexes of free ions in the 100 nm fraction, with the exception of Fe, Pb, Ag and Cu (Kadar et al., 2012). However, the filter-passing fraction of Fe was much larger (80%) at the bubble site with pH 5 and intense gas emission. At such high concentrations (e.g. in the order of μM), Fe in seawater is usually found predominantly associated with large particles that are retained by 0.45 μm filters (Kardar et al, 2012). The large percentages of Mn and Zn in the 100 nm filtrates are in accord with their inorganic speciation being dominated by free divalent ions or chloride complexes, forming only weak complexes with organic ligands and Fe-oxyhydroxide surfaces (Long and Angino, 1977; Byrne, 2002). The formation of natural NPs at cold CO_2 seeps showing an enrichment in trace metals (e.g. Fe>Mn, Cr>Pb>Cu>Ba) as compared to control samples with pH 8; most of these elements are in the 100 nm indicanting the persistence of nano-clusters in the seawater surrounding CO_2 seeps (Kardar et al, 2012).

Chapter 3 - Mussels bio-monitoring.

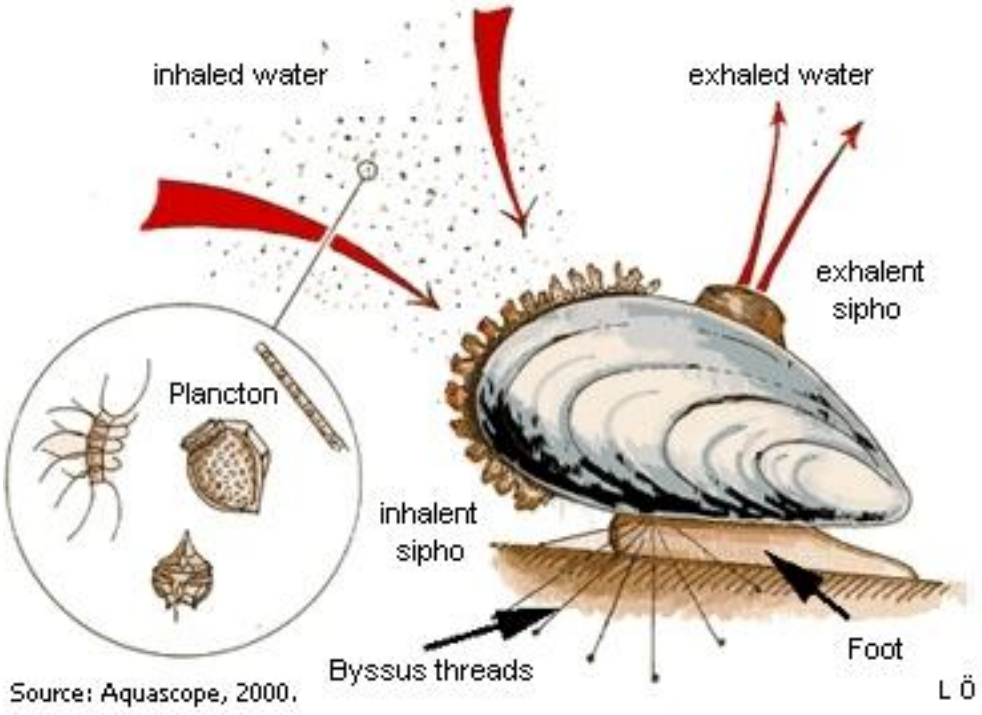

3.1. Environmental Monitoring.

Environmental monitoring is the technique which describes the bio-geo-chemical processes which we need to investigate and monitor in order to evaluate the health state and quality of the environment. Environmental monitoring is used to assess the environmental impact of human activities that pose a risk of harmful effects on the natural environment.

In environmental monitoring there are two main approaches: *chemical approach* and *biological approach*.

Chemical approach consist in collecting data on the chemistry of the bio-geo-spheres (Atmosphere, Hydrosphere, Pedosphere and Biosphere); it is used in order to understand the quality and quantity of the different kind of pollutants and their fate in the ecosystem in a short period of time.

In order to evaluate the ecosystem's functionality and health state in a long period of time, is useful also to use the *biological approach*, which consists in the study of some kind of animal or plants species which can represent the environmental quality state. Since hundreds of species in an ecosystem cannot all be monitored, it is essential to develop a suite of *bioindicators or biomonitor* that can be used to assess status and trends within that ecosystem and across regions. Such specie is called biomonitor of the environment, because observing its health state it is

possible to understand also the ecosystem's health state. A good biomonitor is a species which is sensible to a disturbance (such as a special kind of pollutant or environmental physical perturbation etc.) and can show the presence of a such disturbance through changes in his population, bio-geographical distribution, physiology and behavior. Another useful tool in the bio-monitoring field is the "*bioaccumulator*", which is a special kind of specie (animal or plant) which can resist to the accumulation of a massive concentration of pollutants (which are present in his habitat) without die or fall ill. A good bioaccumulator must have a cosmopolitan distribution (because it allows to compare monitoring studies in different part of the Earth), it must be easy to collect and to recognize, it must have a long enough biological cycle in order to accumulate the pollutant in appreciating quantity, and it must be a sedentary specie, because this gives the security that through the analysis of his tissue the concentration of the pollutant is proportional to the concentration of the same in his environment. In a good accumulator the body concentration of pollutants is several orders of magnitudes higher than and always proportional to the environmental concentration one. Such behavior facilitates the assessment and estimation of the environmental concentration of the investigated pollutant. A disadvantage in the use of bioaccumulator is that researcher often needs to use a large number of organisms, because of the individual variability. Only the use of a big number of individuals decreases errors. The ideal number of the population depends from the used specie. For a mussel biomonitoring study a good population should be composed from about 100-150 individuals (ICRAM manuals for mussels monitoring, 2003).

3.2. Mussels bio-monitoring programs.

Bivalve mollusks, as filter-feeding organisms, are able to concentrate in their soft tissues various contaminants from ambient water due to the bioaccumulation process; foreign substances can be incorporated into shells during growth or through the passive adsorption on their surfaces from the extrapallial fluid and the water column (Zuykov et al.2013).

Fig. 24 – Mussel collection for consumer.

Some pollutants from aquatic systems are known to accumulate in aquatic organisms and to *biomagnify* through the food chain, being a real health risk for consumers (Licata et al., 2004).

Bioaccumulation of various metals has been demonstrated in the literature for a number of

species of bivalves. The utilization of shells and byssal threads of bivalves as sentinels for metal pollution monitoring in marine waters can offer several advantages over that of soft tissues but it requires a longer monitoring period, because accumulation in soft body is faster than in the shell. Both soft tissues and shells of bivalves are good bioindicators of environmental metal contamination, although, they provide independent data on metal concentrations .

Marine organisms have been recognized as useful tool for monitoring of the environment in which they live, because of their ability to accumulate chemical elements in their tissues proportionally to their bioavailability (Visnja et al., 2005, Kadar et al., 2006a and 2006b). It is shown that the bioaccumulation is applicable to most of the bivalent metals and organic compounds (O'Connor, 2002). Mussels are suitable because they are sedentary organisms and filtrate large amounts of water accumulating the substances from the environment (both soluble and particulate form), have suitable dimensions for easy identification and collection, are readily accessible by hand picking or by dredging in the intertidal zones (Seeds, 1992), and are cosmopolitan species. Mussels are excellent bio-indicators of the trace metals in their environment, in fact, the environmental trace metals concentration is always in relation with the soft tissue trace metals concentration. Mussels are considered good bioindicators especially for lead, zinc and cadmium.

In the United States of America, the National Status and Trends Program, run by the National Oceanic and Atmospheric Administrations (NOAA) is an extensive Biomonitoring program (O'Connor and Ehler, 1991), a key element of which is "Mussel Watch", started in the 1970s (O'Connor, 1996, 2002). It offers the most comprehensive measure of coastal marine metal pollution in the United States (Sarver et al., 2004). Similar program have been instituted independently in some states, as well as other countries, such as France (Cossa et al., 2002), India (Senthilnathan et al., 1999), Russia (Tkalin et al., 1998), South Africa (Albertus et al., 2002) and Taiwan (Hung et al., 2001). The most used specie in Mediterranean basin is *Mytilus galloprovincialis*, because of it is a wide spread specie in all basin of the area (Visnja et al., 2006).

Another important aspect of the issue, worthy of special consideration, is surely the potential human health risk:

1. mussels and similar species are a part of human diet, they can be used as model,
2. this species can resist to acidification phenomena and heavy metal pollution in the ecosystem where they live,
3. the heavy metal pollution is tightly linked with anthropogenic activities, therefore, mussel's breeding areas are interested by pollution events.

In case of pH decrease an increase of metals in the water column and a consequent bioavailability could be possible (Millero et al., 2009) leading to an increase of some metals in soft part of mussel's bodies.

There is a difference between wild and transplanted mussels population (Fig. 25), in fact, transplanted raft mussels feed mostly on phytoplankton, which is usually abundant and high in organic content and consequently, they grow faster than wild mussels (Labarta et al., 1997). As they are permanently submerged, they do not enter into anaerobic metabolism like the wild mussels do when they emerge, therefore, keeping their valves closed (Saavedra et al., 2004).

Fig. 25 - Wild mussels (left) and trasplanted raft mussels (right).

Problems identified with the use of bivalves as bioindicators have included the effects of biotic factors such as age, size, sex, feeding activity and reproductive state, and abiotic effects such as organic carbon levels, temperature, pH, dissolved oxygen levels and hydrology, on the uptake of toxicants (Edler and Collins, 1991; Boening, 1999).

A factor which can influence the accumulation capability of the mussel is **size**, mostly because it is usually related to age, food acquisition capability and weight. Some studies report metal levels increasing with size of the mussel (Tewari et al., 2000; Wiesner et al., 2001) but it depend from metals because some metals (such as copper) decrease with shell size.

Season can also influence the accumulation rate in mussel, as some authors say, metals such as Cd, Zn and Cu concentrations decreased in mussels throughout the season with a transient increase during the summer. In general lipid-soluble metals are accumulated in gonads and digestive gland, insoluble metals fraction are accumulated in gills. The fact that soluble metals fraction accumulate in gonads can explain why in summer the accumulation rate increase, just because of the fact that breeding period is cause of an hypertrophy of gonads (Pellerin et al., 2009, Hawkins & Bayne, 1985). Other studies say that metal levels are higher in winter (Avelar

et al., 2000; Unsal, 2001; Odzak, 2002) or at the end of winter (Kaimoussi et al., 2000), and in older animals (Odzack, 2002).

Another factor which can influence the accumulation rate and quality is the **habitat**, many authors say that mussels which are living in submarine vents area, has a particular enrichment for peculiar trace elements such as Fe, Mn, Co, Cu, Cd, Zn, Pb and Hg as compared to ordinary seawater (Kadar et al., 2006a and 2006b).

In hydrothermal vent sites the key factor controlling the rate of bioaccumulation and thus bioavailability of a trace element in aquatic organisms is chemical speciation (Sarradin et al., 1999; Desbruyeres et al., 2001; Kàdàr et al., 2005; Birge et al., 2000).

Fig. 26 - Volcanic Vents of Ischia.

Since in a submarine vents area pH is lower than standard seawater, it was clear that mussel can resist to the dissolution (in negative SI aragonite) because of the periostracum presence which protect the shell. In fact, microscope showed (Fig. 27) severely dissolved shells where the periostracum was damaged (in dead samples exposed in acidic condition - A), moderate damage in live samples were periostracum was not too damaged despite the acidic condition (B) and the periostracum in normal conditions (live samples at normal pH - C) (Rodolfo-Metalpa et al., 2011).

Mussel exposed in acidic condition (respect natural seawater) can accumulate more trace elements such as Cu (because of the speciation) than normal pH, and can resist quite well to the shells' dissolution, this fact may represent an important aspect in the assessment of the future impact of OA in humans health because of the consumption of these species.

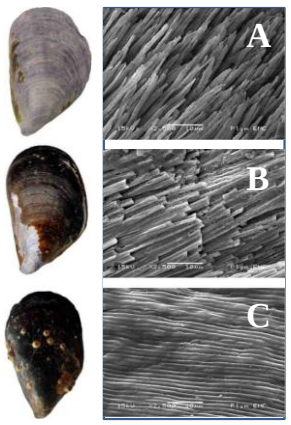

Fig. 27 - A dead samples in acidified condition;

B live samples in acidified condition;

C live sample in normal condition (Rodolfo-Metalpa et al., 2011).

Chapter 4 - Materials and Methods.

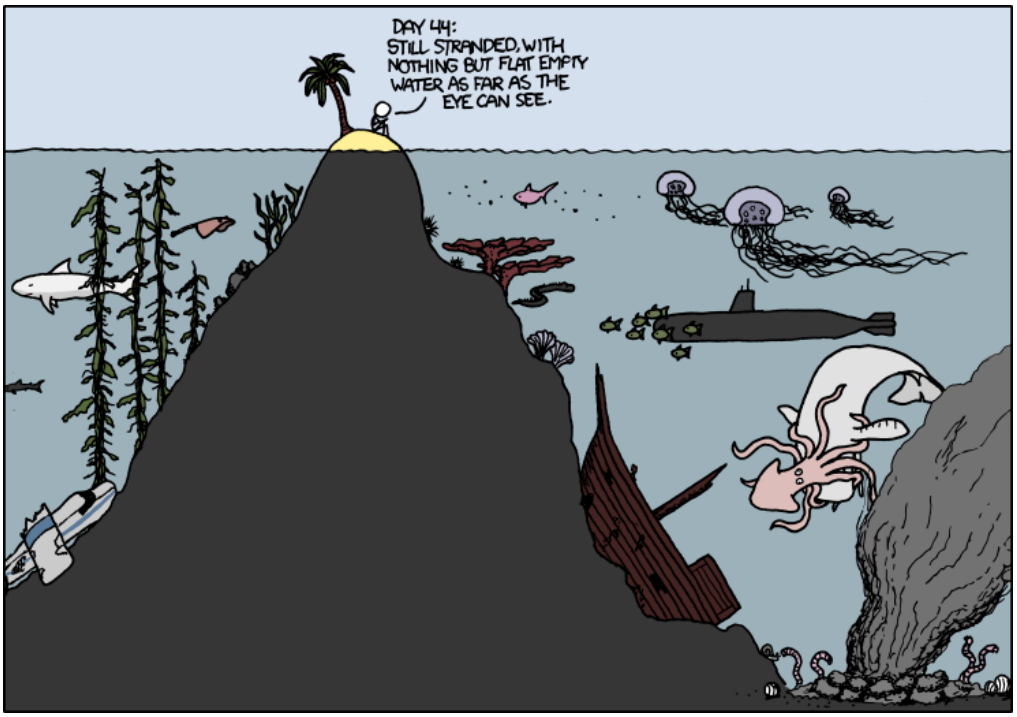

4.1. Study site description.

The Levante bay area, located on the eastern side of the isthmus of Vulcano island (Fig. 28), is characterized by the presence of gas vents both on land and underwater. Thanks to the presence of submarine vents a constant gradient of pH is moving from most acidic condition (5.6 on the bubble – the red star) to the normal pH condition (8.2 on R1).

The bay could be considered a semi-closed geochemical system, where seawater on the closest part to the coastline is the result of mixing processes between hydrothermal fluid and seawater. The outer part of the bay can be considered as background seawater with the same chemistry and chemical-physical parameters of the Mediterranean Sea.

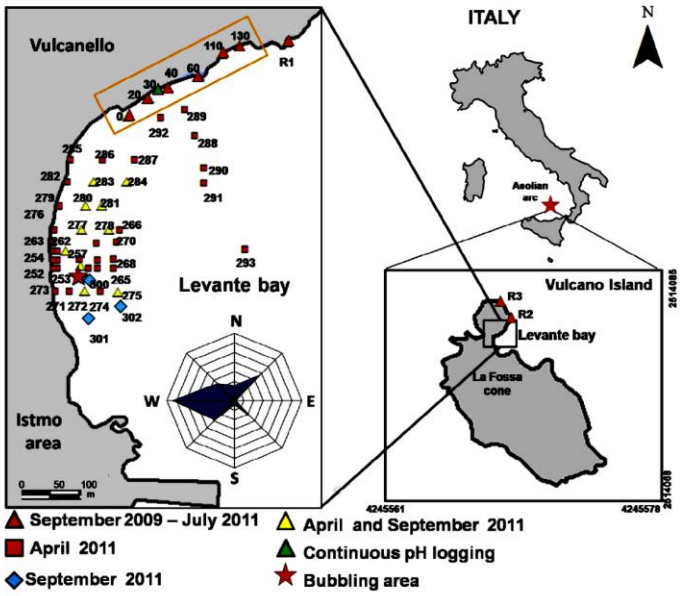

Fig. 28 - Baia di Levante (Vulcano), sampling network for chemical-physical parameters, chemistry and gasses. Red triangle is September 2009 and July 2011; Red square is the April 2011 sampling; Blue rumble is September 2011 sampling; Yellow triangle both; Red star is the bubble (maximum venting gas emission).

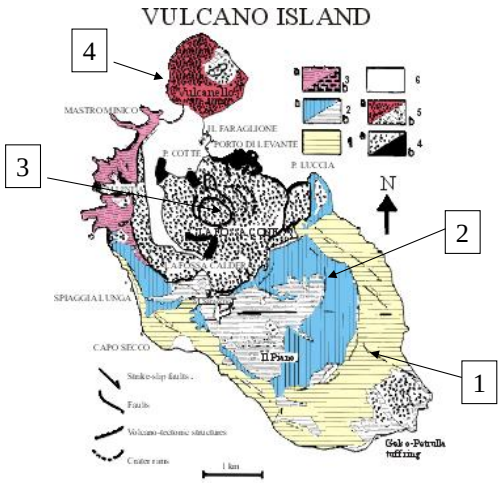

Fig. 29 - Geologic chart of Vulcano.

1-Vulcano Primordiale, 120-100 Ka.

2-Caldera del Piano, 107-99.5 Ka.

3-Cratere della Fossa, 6000 ya.

The main physical-chemical parameters (T, pH, Eh, electric conductivity) were measured at more than 70 geo-referenced sites (Appendix I) and 40 samples were collected for chemical analyses (Appendix II) at representative points.

From geological point of view, we can recognize in the actual structure of the Island at least four activity centers (Fig. 29): 1) the older unit, Vulcano primordial o del Piano, 120-100 Ka. 2) Caldera del Piano 107 – 99 ka. 3) After the collapse of the volcanic edifice of Lentia started (<14 ka) the new edifice cratere della Fossa active at least from 6000 years. 4) The most recent event Vulcanello, 183 B.C. The last eruption of this eruptive center took place in the XVI century. Baia di Levante is still the most active part of the Island.

In the sea surrounding the Aeolian Islands the prevailing winds are from N, E and SE in 2011 and N, S, W and NW in 2012 and average speed is 1-2 m/s (Fig. 30; data available from SIAS: Servizio Agro-metereologico Siciliano).

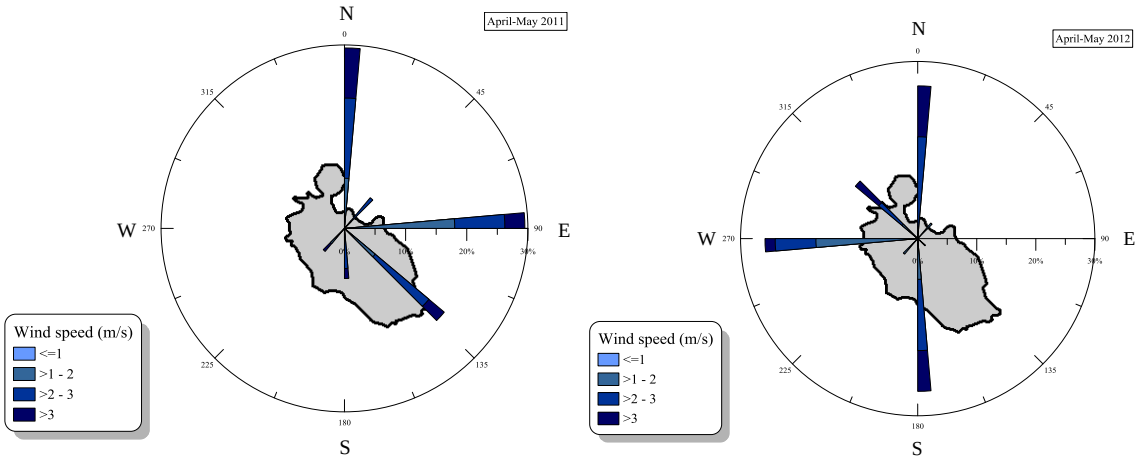

Fig. 30 - Data's Wind Chart available from the SIAS (Sicilian forecast service); data are obtained from the nearest station located in the island of Salina at 10 m from soil level in the months of April and May for both years.

In the sampling days winds were from SE (average speed 1.2 m/s) in 2011 and from N (average speed 0.9 m/s) in 2012.

4.2. Chemical-physical parameters.

Standard chemical analyses (major, minor and trace elements) were performed on subsamples of the same water sample allowing comparability of the results. Analyses were conducted at the INGV, Palermo, Italy.

A grid of sampling points was used to map the seawater chemistry of Levante Bay in April and September 2011 and May 2012 (Fig. 28). Most of the samples were positioned around the

underwater vents and along the beach of the Istmo area. Although almost simultaneous, the sampling for chemical analyses and the measurement of physic-chemical parameters, probably do not warrant the perfect comparability due to the fact that the sampled system has to be considered highly dynamic.

In April and September 2011 and May 2012, the main physical-chemical parameters (temperature, pH, Eh and electrical conductivity) were measured using a 556 MPS YSI (Yellow Springs, USA, Fig. 34) probe at 70 sites (Fig. 31). Temperature, pH and Eh measurements were within ±0.1 °C; ±0.05 pH units, and ±1 mV respectively, while conductivity data were ±2%. The pH-meter was calibrated using TRIS/HCl and 2-aminopyridine/HCl buffer solutions (DOE, 1994). As for other volcanic vents systems (Fabricius et al., 2011; Kerrison et al., 2011) we recorded pH fluctuations along the shallow CO_2 gradient in the northern shore of the bay (triangles in Fig.48, Chapter 5), with measurements were repeated on several visits from September 2009 to July 2011 under different weather conditions and at various hours of the day. For each site along the north shore, average pH values were calculated from hydrogen ion concentrations before re-converting back to pH values, using the collected dataset.

Fig. 31 - Sensor of the 556 MPS YSI logger.

To assess pH variability, we used an in situ modified *Honeywell Durafet pH sensor* to record pH and temperature hourly (Fig. 32). The sensor was deployed at 1 m depth at site 30 (where our monitoring data had an average pH of 7.7 units) from April 26th to May 30th, 2010 The sensor was removed for 1.5 days to avoid damage during a storm. Discrete water samples were collected for Total Alkalinity (TA) within 0.25 m of the pH sensor during the initial deployment and the retrieval of the sensor. Additional water samples for TA analyses were collected at each site along the north shore from September 2009 to July 2011. One hundred ml of water sample were passed through 0.2 µ pore size filters, poisoned with 0.05 ml of 50% saturated mercuric chloride ($HgCl_2$) to stop biological activity, and then stored in the dark at 4 °C. Three replicate sub-samples were analyzed at 25 °C using a titration system. The pH was measured at 0.02 ml increments of 0.1 N HCl. Total alkalinity was calculated from the Gran function applied to pH variations from 4.2 to 3.0, as µmol kg^{-1} from the slope of the curve HCl volume versus pH. Titrations of TA standards provided by A.G. Dickson (batch 99 and 102) were within 0.6 µmol

kg^{-1} of the nominal value. Parameters of the carbonate system (pCO_2, CO_2, CO_3 , HCO_3) and saturation state of calcite and aragonite were also calculated from pH, TA, temperature and salinity using the *free-access CO_2 SYStat* package (Pierrot et al., 2006). Dissociation constants of H_2CO_3 and HCO_3^- were derived from Roy et al. (1993). Data are reported as mean and standard deviation throughout the manuscript. Temperature and pH were logged every 30 min during the exposure in one replicate tank from each treatment.

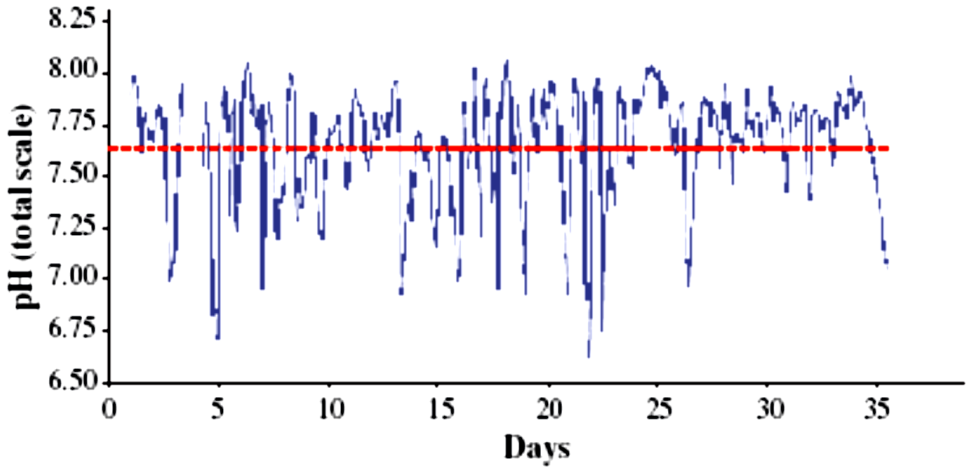

Fig. 32 - Time series of hourly seawater pH values measured by a Honeywell Durafet pH sensor in a low pH site along the north shore (site 30, see Fig. 31). The time series was recorded from April 26th to May 30th, 2010. The dashed red line indicates the average pH value (n = 807).

4.3. Dissolved gases.

During April 2011, 40 water samples were collected and analyzed for the presence of dissolved gases as well as major and minor elements. These samples were also used to determine the influence of heated water emissions. Water samples for chemical analyses were collected and stored in prewashed HDPE bottles. A gas sample was collected at the most actively bubbling site with an inverted funnel and a glass sampler with two gas-tight stopcocks.

Dissolved gases were determined using the analytical method proposed by Liotta and Martelli (2012) (Fig. 33), which is based on the equilibrium partition of gases between a liquid and a gas phase after introducing a known amount of carrier gas into the sampling vial. Each sample was collected 50 cm below the water surface in order to avoid sampling any surface films (Morley et al., 1997) and to allowCO_2 dissolution through thewater column (Kadar et al 2012).

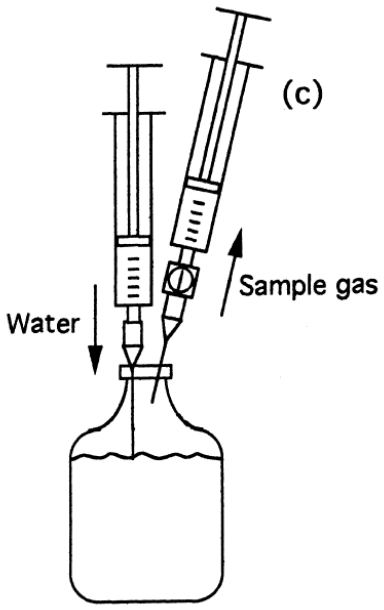

Fig. 33 - Henry law KH=Pi/i Pi partial pressure of species "i" of gas in the vapour phase and i molar fraction in the liquid phase. N.B. The Henry constant is independent from the gas pressure but is strong dependent from temperature and salinity of the solution. The extraction of a dissolved gas is based on his re-equilibraton with a new gas host phase.

This method is based on the equilibrium partition of gases between a liquid and a gaseous phase after the introduction of host gas (Ar). Gas concentrations were measured using the GC Perkin–Elmer Clarus 500 equipped with Carboxen 1000 columns, Hot Wire and Flame Ionization detectors with methanizer and Ar as carrier gas. The gas samples were injected through an automated injection valve with a 1000 µL loop. Calibration was made with certified gas mixtures. Analytical precision (±1σ) was always better than ±5%. The detection limits were about 1 ppm vol. for CH_4, 2 ppm vol. for H_2, 5 ppm vol. for He, 20 ppm vol. for CO_2, 200 ppm vol. for O_2 and 500 ppm vol. for N_2.

Dissolved H_2S measurements were carried out using Draeger tubes (detection limit 0.5 ppm). Absolute seawater pH and pCO_2 was calculated from TA and DIC with CO2SYSver using published dissociation constants (Mehrbach et al., 1973; Dickson & Millero, 1987; Dickson, 1990; Lewis & Wallace, 1998). In addition, water samples from the overlying water column (WC) were taken at the conclusion of the experiment for analysis of organics (PCB and PAH suite) and ammonia.

4.3.1. About reduced sulphur (S^{2-}) species in sea water.

In order to sample S^{2-} we tried to apply a method described from Montegrossi et al., 2006 which was used for natural water discharges. In this method, the determination of reduced S species in natural waters is particularly difficult because of their high geochemical instability and the presence of chemical-physical interferences with commons analytical methods. Montegrossi et al. (2006) proposed a rapid analytical procedure called Cd-IC method. This method consist in the determination of $\sum S^{2-}$ oxidation to SO_4^{2-} after chemical trapping with ammonia-cadmium solution, that allows precipitations of all sort of S reduces species as CdS. In that analytical procedure the $\sum S^{2-}$ are determined by ion-chromatography after oxidation as SO_4^{2-}.

Total reduced S species (the sum of dissolved H_2S, HS^-, S^{2-}, poly-sulphides and metal-sulphide complexes) are present in natural waters in different range of concentrations. Usually natural water which are typically enriched in S species are geothermal and volcanic (Sola et al., 1997; Yin and Xia, 2004; Horwell et al., 2005), furthermore, a part of that compounds are produced by the decomposition of organic matter and by bacterial reduction of SO_4^{2-}. Sulphides in natural waters can be grouped in three categories:

1) total sulphides H_2S, HS^- and S^{2-}, poly-sulphides and acid-soluble metallic sulphides;

2) dissolved – sulphides, which are the compound that remaining after suspended solid removing;

3) un-ionized H_2S. All this compounds can be toxic for humans and aquatic organisms, (Förstner, 1995; Jay et al., 2004).

The analytical determination of total S species in a solution is affected by several problems since sulphides include unstable and reactive anions, which tend to react with each other. For instance, S^{2-} and SO_4^{2-} react to form elemental S, furthermore, also suffer air oxidation. For that reason it is really hard to find the correct sampling method and storage procedures in order to minimize oxidative and degradative processes.

The main problems in making a quantitative determination of the natural waters ΣS^{2-}, is the instability of S-bearing compounds, in fact, oxidation state may change after sample collection trough H_2S exolution and oxidative processes. Another problem derives from matrix interferences. In order to solve these problems, natural water samples have to be mixed in situ with a Cd solution, allowing the complete separation of ΣS^{2-} as a CdS precipitate, avoiding possible interference and inhibiting subsequent reactions. CdS is very stable and samples can be stored for long periods without any significant

compositional changes. The usefulness of Cd as a precipitating metal for ΣS^{2-} is supported by the low K_{ps} value of CdS respect other metals-S K_{ps} value (Fig. 34).

Metal (M)	**K_{ps} (MS)**	**Precipitate**
Cadmium (Cd)	1.4×10^{-29}	CdS
Zinc (Zn)	2×10^{-4}	ZnS
Silver (Ag)	1.1×10^{-49}	AgS
Copper (Cu)	1.3×10^{-36}	CuS
Pond (Sn)	3.2×10^{-28}	SnS
Mercury (Hg)	6.4×10^{-53}	HgS
Arsenic (As)	1.0×10^{-54}	As_2S_3

Fig. 34 - (CRC, 2001) from Montegrossi et al., 2006.

In general the quantitative of CdS precipitate is favoured at relatively high pH and stabilized under slightly reducing conditions; consequently, the Cd precipitate is prepared in ammonia buffer solution, which maintains the pH at about 10, besides, at these conditions, the $Cd(OH)_2$ formation ($K_{ps} = 5.3 \times 10^{-15}$) can occur only after the complete precipitation of CdS.

In order to prepare the ammonia-cadmium solution, 0.5 mol of $Cd(CH_3COO)_2$ must to be dissolved in 225 mL of $30\%_{v/v}$ NH_3 solution and in 1 L of ultra pure Milli-Q water. Although NaOH is also able to stabilize CdS precipitates (Montegrossi et al., 2001), an NH_3 solution is preferred because of it can minimize matrix interferences. In the field, water samples are collected in 15 mL plastic tubes, to which 2 mL of the ammonia-cadmium solution have previously been added. As 1 mL of the precipitating solution contains 0.5 mmol of Cd^{2+}, 2 mL of solution in 10 mL of water sample are able to precipitate up to 100 mmol/L of S^{2-}.

The extract amount of water collected is determined by weighting the sampling plastic tubes before and after water collection. Water samples are centrifuged at 5000 rpm for 30 min. This operation is repeated twice to allow the complete separation of precipitate, deposited on the bottom of the sampling tubes, from the supernatant. Moreover, the precipitate must be rinsed several times with Milli-Q water to avoid possible contamination by residual liquid sample or by SO_4^{2-} adsorption on the precipitate. Successively, the solid CdS is dissolved and oxidized by adding 2 mL of H_2O_2 $30\%_{v/v}$ and then, transferred to to 25 mL tubes.

The full oxidation of CdS via H_2O_2 needs about 3 days (Montegrossi et al., 2001). This allows the transformation of S^{2-}, deriving from dissolution of CdS to SO_3^{2-} and, eventually, to SO_4^{2-}. Thus S^{2-} is determined as SO_4^{2-} by ion-chromatography with a Dionex DX 100 ion-chromatographer equipped with ad Ionpac AS9-HC column and using a 8.5 mmol/L $NaCO_3$ solution as eluent. Under such analytical conditions, the SO_4^{2-} peak has a retention time of ~10.5 min (Fig. 35). The resulting chromatogram has no peak overlaps, since the final solution is composed only of SO_4^{2-}, H_2O_2, Milli-Q water and Cl^- (at very low concentration) that is adsorbed in the CdS precipitate. Finally, S^{2-} contents are calculated by taking into account the sulphide-S^{2-} SO_4^{2-} transformation and the dilution operated on the water sample.

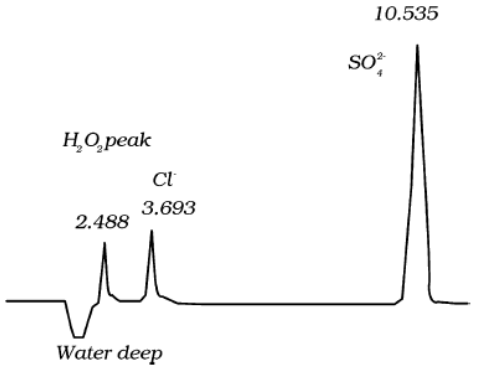

Fig. 1. Chromatogram for the determination of ΣS^{2-} (0.072 mg/L) as SO_4^{2-} after the oxidising procedure with H_2O_2. Numbers refer to the retention time (min).

Fig. 35 – Image from Montegrossi et al., 2006.

This method was applied for the Baia di Levante seawater, in May 2012 and December 2012 two samples campaign were done, data obtained are not reliable because too different from the expected background values, in fact, data obtained for Bubble with the other method, shows that the concentration of H_2S was 400 ppm but with this method was 95 ppm. The Data obtained (Fig. 36) show that, in both case distribution of H_2S is too homogeneous, this suggests that the cadmium ammonia solution is saturated due to the presence of sulfate without catch all the sulphide in solution.

Sample	Date	HS^- (ppm)
0	29/5/2012	60.02
30	5/30/2012	57.68
35	5/29/2012	57.62
40	5/29/2012	56.89
60	5/29/2012	53.32
262	5/29/2012	54.44
277	5/29/2012	56.73
310	5/30/2012	50.69
Bubble	12/15/2012	94.77
257	12/15/2012	96.00
277	12/15/2012	96.71
300	12/15/2012	97.74
283	12/15/2012	100.44
0	12/15/2012	92.35
30	12/15/2012	93.82

Fig. 36 – data on HS– obtained with Montegrossi's method.

For this reason the method should be revised for S^- seawater samples in order to avoid the total saturation of the ammonia-cadmium solution a try to catch all the S^- present in the water, without the influence of the sea salt sulfate, it would be necessary to try again with different proportion of cadmium ammonia solution at different concentrations respect same volume of seawater sample.

4.4. Major, minor and trace elements.

For each sample (Appendix II) we had measured also chemical-physical parameters (T, pH, Alk and Eh). Samples were taken 10−20 cm underneath the surface to avoid oil contamination at the interface. Samples were analyzed in the INGV of Palermo laboratory for the dissolved phases of several trace elements, major ions.

Water samples used for the determination of dissolved major were first filtered using 0.45 μm Millipore MF filter and then collected in 50 ml LD-PE (low-density polyethylene) bottles for major element analyses, acidifying to pH 2 the aliquot destined to cation determination with HCl.

Untreated aliquots of 100 ml were stored for alkalinity determinations, made via titration with HCl (0.1 N). Electric conductivity and pH were measured in the field using Orion instruments equipped with Hamilton electrode (pH). Major ions were determined by ionic chromatography (Dionex ICS 1100) using columns AS14 and CS12 for anions and cations respectively (Fig.37), the dilution factor of each sample is 40 and the standard certificates are used SPSSW1-2 by "*Spectrapure Standards*". Trace metals were sampled in two campaign, one at beginning of May and other at the end of the same month, at 6 and 15 sampling point respectively, each sample were taken in three replicates.

Fig. 37 – Dionex ICS 1100 (image picked in INGV of Palermo).

Seawater trace metals were pre-concentrated with Chelex – 100 technique. Such "ion exchange resins" is very popular between chemists and is composed of a polymer matrix derivatized with functional groups which are available for exchange with the solution's ions.

Pre-concentration and separation of metals were made by column method which is a solid-liquid extraction method, in which, a known volume of solution flow down thanks to gravity through the resin. The dissolved analyte is blocked in the solid phase and then is eluted with an appropriate solution. The columns where filled with Chelex-100 resins and then conditioned with a buffer solution 6 M (pH 6) made with ammonia and acetic acid. 250 ml of sample were conditioned with the buffer (to pH 6) and litmus paper were used to assess pH. Solutions were passed through the columns at constant flux (about 5.6 ml per minute) and then analytes were recovered with 10 ml of HNO_3 (1M). Each sample were made in three replicas and for each analysis set a procedural blank was made (Standard Protocol from Oliveri, 2011 MSc thesis) . Trace elements (REE, Al, Cu, Fe, Mn, Ni, V and Zn) in the obtained solution, were analyzed by inductively coupled plasma mass spectrometry (ICP-MS) using an Agilent 7500ce instrument. The instrument was equipped with a standard peristaltic pump, a Micro Mist concentric nebulizer, a Peltier-cooled spray chamber, the Plasma Forward Power, the Shield Torch System, and a Collision/Reaction Cell system. An autosampler (ASX 520, Cetac Technologies) was employed to introduce the samples into the plasma of the ICP-MS (Fig. 38). Introduction was done with a Micro Mist concentric nebulizer and Scott-type quartz glass spray chamber. Helium was used as the collision gas for Cu, Ni, and Zn analyses. No cell gas was used for the other elements.

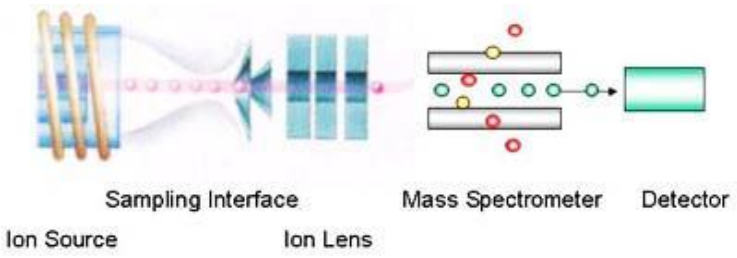

Fig. 38 -ICP-MS scheme.

Calibration solutions of all investigated elements were prepared daily by appropriate dilution of 100 mg l-1 and 1000 mg l-1 stock standard solutions (Merck) with 0.14 mol l-1 high-purity nitric acid. The accuracy of the method was checked analysing certified reference materials of natural waters (Nist 1643e, Environment Canada TM-24.3 and TM-61.2, Spectrapure Standards SW1 and SW2) at regular intervals during sample analysis. The experimental concentrations determined in this study agreed well with these certified values (within ±5%). Matrix induced signal suppressions and instrumental drift were corrected by internal standardization. Indium was used for elements up to mass 138 (Ba138), and rhenium was used for heavier elements. Average procedural blank results are: 0.3 µg/l for Al, 0.005 µg/l for V, 0.01 µg/l for Mn, 0.7 µg/l for Fe, 0.01 µg/l for Ni, 0.02 µg/l for Cu, 1.1 µg/l for Zn and 0.0002 µg/l for La.

Elemental speciation has been calculated with PHREEQC version 2 using *llnl.dat*, which is a computer program for simulating chemical reactions and transport processes in natural or polluted water. The program is based on equilibrium chemistry of aqueous solutions interacting with minerals, gases, solid solutions, exchangers, and sorption surfaces, but also includes the capability to model kinetic reactions with rate equations that are completely user-specified in the form of Basic statements. (Parkhurst & Appelo, 1999). PHREEQC is based on conservation of mass for a chemical principle:

4.4.1.The Advection-Reaction-Dispersion Equation.

Conservation of mass for a chemical that is transported yields the advection-reaction-dispersion ARD equation:

$$\frac{\partial C}{\partial t} = -v\frac{\partial C}{\partial x} + D_L\frac{\partial^2 C}{\partial x^2} - \frac{\partial q}{\partial t}$$

where C is concentration in water (mol/kgw), t is time (s), v is pore water flow velocity (m/s), x is distance (m), DL is the hydrodynamic dispersion coefficient [m^2/s, $D_L = D_e +$

$\alpha_L v$], with *De* the effective diffusion coefficient, and the dispersivity (m), and q is concentration in the solid phase (expressed as mol/kgw in the pores). The term $-v\frac{\partial C}{\partial x}$ represents advective transport, $D_L\frac{\partial^2 C}{\partial x^2}$ represents dispersive transport, and $\frac{\partial q}{\partial t}$ is the change in concentration in the solid phase due to reactions (q in the same units as C). The usual assumption is that v and DL are equal for all solute species, so that C can be the total dissolved concentration for an element, including all redox species.

The transport part of equation is solved with an explicit finite difference scheme that is forward in time, central in space for dispersion, and upwind for advective transport. The chemical interaction term for each element is calculated separately from the transport part for each time step and is the sum of all equilibrium and non-equilibrium reaction rates. The numerical approach follows the basic components of the ARD equation in a split-operator scheme (Press and others, 1992; Yanenko, 1971). With each time step, first advective transport is calculated, then all equilibrium and kinetically controlled chemical reactions, thereafter dispersive transport, which is followed again by calculation of all equilibrium and kinetically controlled chemical reactions. The scheme differs from the majority of other hydrogeochemical transport models (Yeh and Tripathi, 1989) in that kinetic and equilibrium chemical reactions are calculated both after the advection step and after the dispersion step. This reduces numerical dispersion and the need to iterate between chemistry and transport.

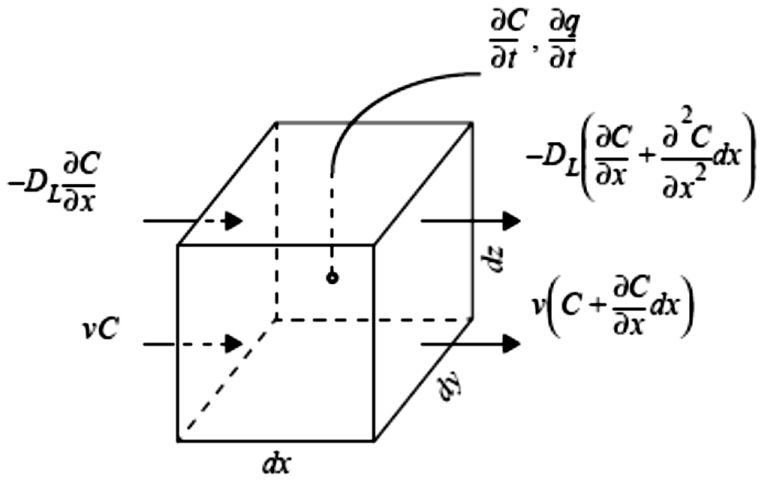

Figure 1.--Terms in the advection-reaction-dispersion equation.

Figu. 39 - Immage from Phreeqc Manual, Advection-reaction-dispersion equation which is based on conservation of mass principle.

4.5. Mussels transplant.

We chose the *Mytilus gallorpovincialis* because it is considered a good bio-accumulator, besides, that specie is widely consumed, being therefore is also important to assess possible human health's impact. We choose commercially obtained individuals to estimate the accumulation rate for some metals in their soft body after one month exposition in an acidified seawater.

Fig. 40 – Taranto's fishing centre (Mussel farm) of Taranto, red dot in chart is the mussel farm centre, image from Internet.

We made the transplant experiment in the summer because, according to some literature data, accumulation is faster in summer than winter and weather is more stable (better condition for sampling trace metals and evaluate speciation dynamics). Mussels were taken from the "fishing center of Taranto", located near the Taranto's harbor (Fig. 40), then they were settle for three days in the sorting center of Palermo located in Mondello (Addaura) before being implanted in the Vulcano acidified area.

A population of 120 individuals of blue mussel were selected (according to literature data on the individual size, Fig. 45 Chaper 5) and prepared to be transplanted in the Baia di Levante according to ICRAM manual (2001-2003) protocol (Fig. 41). Blue mussels were exposed for 28 days (since May to June 2012) at an average pH of 7.7.

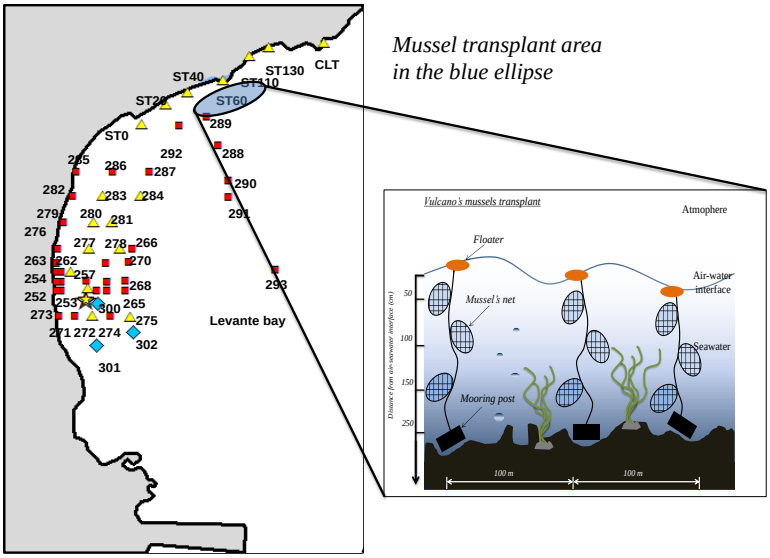

Fig. 41 - Mussel transplant position (Istmo of Vulcano).

With a stochastic criterion, before exposition, blanks were taken from the population and frozen at -20 °C until analyses, then, the transplanted mussels were divided in three groups located in three different sampling points, arranged along the pH gradient (7.3 – 8.03) 100 meters close to each other (Fig. 42).

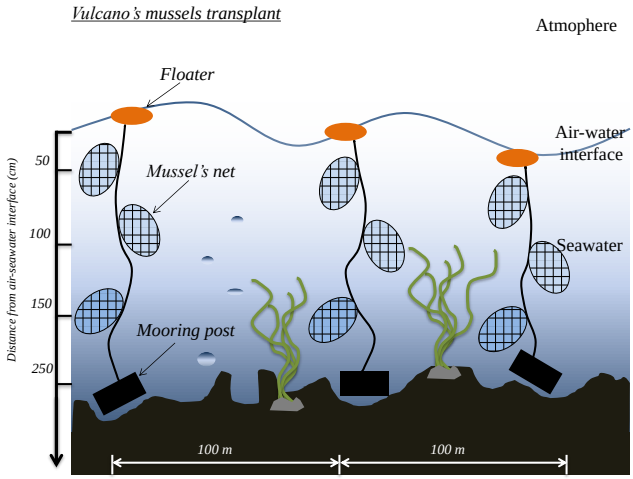

Fig. 42 - Mussel transplant scheme. Three points are 0-40, 40 and 100 in Appendix I

Three different depth nets were put in each sampling point (50 – 100 and 150 cm from the seawater surface to the bottom). Seawater samples were taken for the determination of chemical physical parameters and trace metal content. At the end of the exposition for each individual following biological parameters were recorded: whole weight, soft body weight, shell length and width (Appendix V and Tab. 3, Chapter 5). First the outer shells of the animals were carefully

Fig. 43 - Microwave oven MARSXpress.

cleaned with deionized water. After recording the biometric parameters, the shells opened with a stainless steel knife and the soft body was extracted with Teflon tools, the cavity fluid of the animals was drained and the soft body was carefully cleaned with Millipore-Q (Fig. 44). Mussels soft body dry weight was recorder after drying in the oven at 57 °C for 24^{h}. Each individual was powdered with an agate mortar, in order to prevent trace metal contamination mortar was cleaned for each sample. Afterwards, an aliquot of 0.3 g of dried- pulverized sample was mixed with 5 ml HNO_3/H_2O_2 (5:1) and mineralized in a microwave oven MARSXpress CEM (Burger at al., 2006; Capelli et al., 1978, ICRAM 2001). Teflon PFA reactors, equipped with a system of pressure regulation. A blank solution was prepared adding only HNO_3/H_2O_2 (5:1) in the vessel (Fig. 43).

After mineralization, the samples and the blank solution were brought to a volume of 20 ml with ultrapure water. All the labware was treated with a dilute solution of HNO_3 (0.1%) to prevent contamination. Samples thus obtained were analyzed for Fe, Mn, Zn, Cu, V, Ni, and Al by ICP-MS.

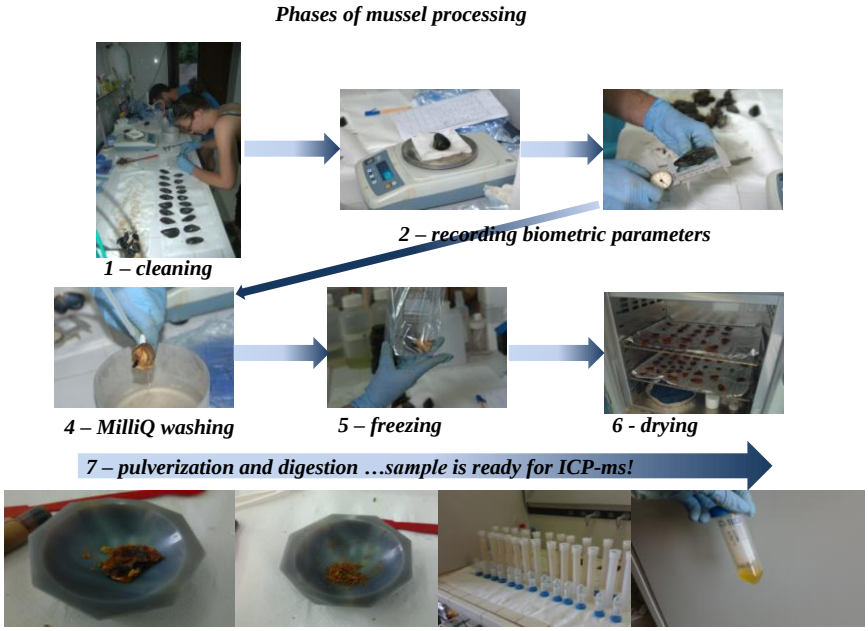

Fig. 44 - Preparation of mussel samples.

Inductively coupled plasma mass spectroscopy (ICP-MS) was used to simultaneously detect levels of nine trace metals (Fe, Al, Mn, Zn, Cu, V and Ni,) in seawater (Beauchemin et al., 1988) in the INGV's labs.

Chapter 5 - Results and Discussions.

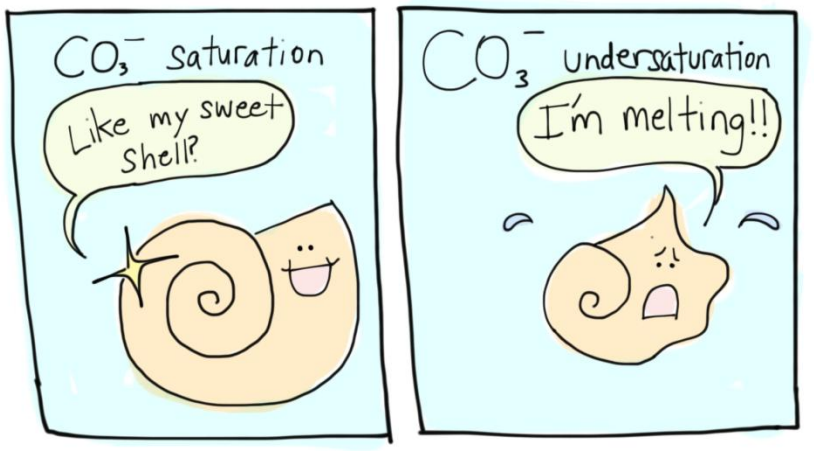

5.1. Results.

Water **temperatures** in the bay ranged between 16.0 and 18.6 °C for the first campaign, between 25.3 and 26.9 °C for the second campaign and between 17.9 and 23.3 °C for the third campaign (Tab. 2). Measured values are close to the mean values for surface waters of the Mediterranean Sea for the respective times of the year. **Electrical Conductivity**, measured only during April, didn't show great variations, being generally close to the mean value of 46.8 mS/cm. **Eh** and **pH** were greatly affected by the main vents. Eh values range from -152 to 170 mV in April and from -23 to 171 mV in September 2011 and from -39.7 to 181.3 in May 2012, while pH values range between 5.70 and 8.05 in April and from 6.05 to 8.03 in September 2011 and from 5.85 to 8.03 in May 2012. The lowest values for both Eh and pH are measured close to the main hydrothermal vents. The bubbling CO_2 produces a strong decrease in pH from the normal seawater value of 8.2 down to 5.6. Our maps of pH and Eh show that the area close to the main degassing vents is characterized by low pH and negative redox values (Fig.49 and 52), here macro-organisms were absent. Redox and pH values increase up to the normal sea water values at distances of about 350m from the main vents. In the northern part of the bay the composition of sampled gases does not differ significantly from that of seawater equilibrated with atmospheric air.

Continuous monitoring of seawater pH was made in 2010, it has revealed the short-term temporal variability of the shallow waters and allowed us to characterize in more detail the chemical environment surrounding the benthic shallow communities along the rocky shore

subjected on average to lowered pH conditions. During the whole period 807 measurements were recorded with values ranging from 6.62 to 8.06 pH units and an average value of 7.65.

The **composition of dissolved gas** sample collected in April 2011 and May 2012 at the most vigorous bubbling site has been reported in Table 2. All gases are mainly composed of CO_2 with concentrations generally above 95 - 99% by volume (Tab. 1). The main atmospheric gases (N_2 and O_2) are generally limited to few % with N_2 always in excess with respect to the N_2/O_2 ratio of the atmosphere. Typical hydrothermal gases (H_2, CH_4 and H_2S) are present with concentrations ranging from few ppm to few %.

Tab. 1 - Vulcano's seawater dissolved gases composition (%).

He	H_2	CO	CH_4	CO_2
%	%	%	%	%
0.003	0.7	0.0003	0.02	99.3

Since Baia di Levante is located in the Mediterranean Sea, which have an higher salinity than oceans (respectively 37‰ and 35‰), the composition of seawater **major elements** reflects the background literature seawater composition, in fact, concentration of elements is a bit higher with respect to the oceans' one. The concentrations of the major elements did not show great variation because they are conservative elements. All campaign samples, taken in 2011, shown that for *anions* concentration variations were the following: Cl^- from 18962 to 21465 mg/l, Br^- from 40 to 86 mg/l, SO_4^{2-} from 2652 to 2988 mg/l and HCO_3^- from 174 to 198 mg/l. For cations were: Na^+ from 10954 to 11825 mg/l, K^+ from 412 to 491 mg/l, Mg^{2+} from 1314 to 1444 mg/l and Ca^{2+} from 446 to 575 mg/l. TDS were from 21850 to 36348 mg/l. In campaign 2012 samples shown that for *anions* concentration variations were: Cl^- from 18989 to 21495 mg/l, Br^- from 40 to 86 mg/l, SO_4^{2-} from 2650 to 2986 mg/l and HCO_3^- from 185 to 469 mg/l. For cations were: Na^+ from 9428 to 13868 mg/l, K^+ from 348 to 511 mg/l, Mg^{2+} from 1166 to 1916 mg/l and Ca^{2+} from 367 to 538 mg/l. TDS were from 35275 to 40363 mg/l. Despite majors are conservative elements some of these shown fair variation in concentrations; higher variation were in Ca^{2+} and HCO_3^- (Tab. 2).

May 2012 campaign show that **trace metals** seawater abundances order in Vulcano samples was as follow: La<Ni<Cu<V<Zn<Fe<Al<Mn. In general the 50% of total amount of metals is represented by Mn, than 21% of Al, 15% of Fe and the rest the others with percentage less than

10%. Greatest variability in concentrations were in manganese from 0.0005 to 0.02 µg/l and iron from 0.0006 to 0.02 µg/l. Traces such as vanadium and copper shown high variation in concentration respect literature background levels respectively; from 0.0003 to 0.001 and from 0.0002 to 0.0005 µg/l (Tab 2).

Tab. 2 - Statistical table on chemical-physical parameters, dissolved gases, major and trace element in seawater sample of Vulcano. Table report the two years (2011-2012) data.

2011			"*Baia di Levante's seawater*" (Vulcano)					
			Av	Min	Max	S.D.	S.E.	*LQ*
Chemical-physical Parameters	pH		7.1	5.64	8.05	0.7	0.1	
	Cond.	mS/cm^2	47	45	50	1		
	Eh	mV	-4.7	-157.3	171.4	112	14	
	T	°C	19.2	16	26.9	4	0	
Dissolved gases	H_2	ml(STP)/l	0.02	0.001	0.1	0	0	-
	O_2	ml(STP)/l	3.3	0.04	4.9	1	0	-
	N_2	ml(STP)/l	9.2	5.2	11.2	2	0	-
	CO	ml(STP)/l	2.8E-05	6.9E-06	0.0001	0	0	-
	CH_4	ml(STP)/l	0.002	0.0001	0.01	0	0	-
	CO_2	ml(STP)/l	11.1	0.3	103.2	22	4	-
Majors	TA	(meq/L)	3	2.85	3.25	0.09783	0.0137	
	Cl^-	(mg/l)	20884	18962	21465	495	69	0.5
	Br^-	(mg/l)	67	40	86	11	1	0.05
	SO_4^{2-}	(mg/l)	2902	2652	2988	62	9	0.5
	HCO_3^-	(mg/l)	183	174	198	6	1	-
	Na^+	(mg/l)	10275	10954	11825	3587	502	0.6
	K^+	(mg/l)	386	412	491	135	19	0.03
	Mg^{2+}	(mg/l)	1358	1314	1444	26	4	0.2
	Ca^{2+}	(mg/l)	501	446	575	35	5	0.3
	TDS	(mg/l)	33501	21850	36348	10751	1505	-

n=60

Continued on the next page

From the previous page

2012			"*Baia di Levante's seawater*" (Vulcano)					
			Av	Min	Max	S.D.	S.E.	*LQ*
Chemical-physical	pH		7.5	5.85	8.03	0.5	0.1	
	Cond.	mS/cm^2	-	-	-	-		
	Eh	mV	129.6	-39.7	181.3	40	5	
	T	°C	19.7	17.9	23.3	2	0	
Dissolved gases	H_2	ml(STP)/l	0.07	0.0	0.837	0	0	-
	O_2	ml(STP)/l	5.3	1.9	6.63	1	0	-
	N_2	ml(STP)/l	12.2	9.4	17.2	2	1	-
	CO	ml(STP)/l	2.73869E-05	1.49583E-05	5.54128E-05	0	0	-
	CH_4	ml(STP)/l	0.002	0.0002	0.0114	0	0	-
	CO_2	ml(STP)/l	10	0.4	58	16	4	-
Majors	Cl^-	(mg/l)	20913	18989	21495	495	128	0.5
	Br^-	(mg/l)	67	40	86	11	3	0.05
	SO_4^{2-}	(mg/l)	2900	2650	2986	62	16	0.5
	HCO_3^-	(mg/l)	220	185	469	70	18	-
	Na^+	(mg/l)	11459	9428	13868	552	143	0.6
	K^+	(mg/l)	430	348	511	24	6	0.03
	Mg^{2+}	(mg/l)	1424	1166	1916	101	26	0.2
	Ca^{2+}	(mg/l)	448	367	538	26	7	0.3
	TDS	(mg/l)	37641	35275	40363	801	207	-
Trace elements	Al	(µg/l)	5.1	12.4	0.9	0.004	0.001	0.05
	V	(µg/l)	0.8	1.5	0.3	0.0004	0.0001	0.01
	Mn	(µg/l)	11.4	17.1	0.5	0.005	0.001	0.05
	Fe	(µg/l)	3.7	16.3	0.6	0.005	0.001	0.05
	Ni	(µg/l)	0.3	0.5	0.2	0.0001	0.00002	0.01
	Cu	(µg/l)	0.5	1.5	0.1	0.0005	0.0001	0.05
	Zn	(µg/l)	2.3	4.2	0.5	0.001	0.0003	0.01
	La	(µg/l)	5.2^{-3}	0.02	9.4^{-4}	0.00001	0.000001	0.001

n=62

Most of individuals of mussels have a size from 5 to 7 cm (Tab. 3 and Fig. 45).

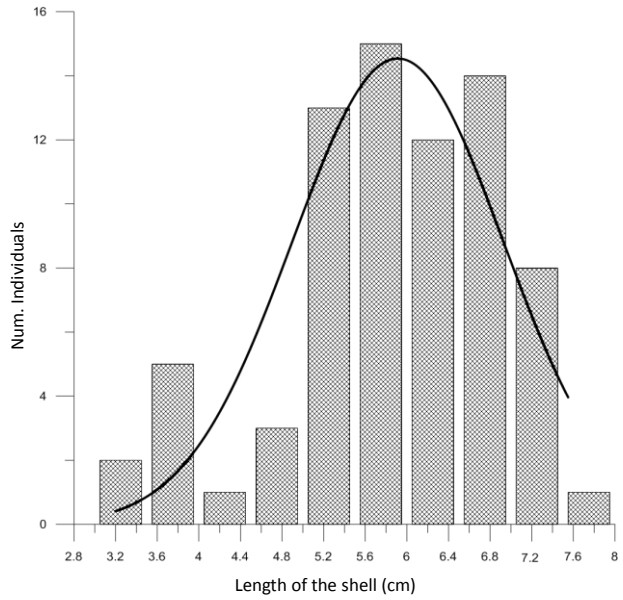

Fig. 45 - Statistical distribution of length in analysed mussel population.

Morphometric data of population shown that, has length (l) from 3.2 to 7.5 cm, soft body weight (Sb) from 1 to 10.3 gr, soft body dry weight (Dw) from 0.12 to 2.43 gr and ratio between Sb and Dw was in average 7 according to literature data. Ration Sb/Dw is an important parameter because it reflect the health state of population, and consequently mussels filtration and accumulation capability (Tab. 3) and is called condition index (C.I.).

Tab. 3 - Statistic on mussel biometric parameters.

n=74

	l* (cm)	L* (cm)	Sb* (gr)	Dw* (gr)	Sb/Dw -
Average	5.94	2.19	5.68	1.05	7
Min	3.20	0.91	0.98	0.12	5
Max	7.55	9.25	10.33	2.43	11
S.D.	1.0	1.1	2.5	0.6	1
S.E.	0.1	0.1	0.3	0.1	0.2
		R^2 *(Sb-Dw)*	0.8		
		R^2 *(l-Dw)*	0.6		

*l = length

*L = width

*Sb = Soft Body weight

*Dw = Dry weight

Many authors say that C.I. is an ecophysiological measure of the health status of the animals that summarizes their physiological activity (growth, reproduction, secretion, etc.) under given environmental conditions (Tsangaris et al 2013).

In general exposed individuals show the greatest accumulation ratio for iron, zinc and vanadium. The greatest accumulation variability was for Fe (from 1379 to 101 µg/g), Zn (from 177 to 25 µg/g), Al (from 91 to 7 µg/g) (Tab. 4).

Tab. 4 - Stats on heavy metal concentration in soft body exposed and not-exposed mussels.

	Ni µg/g	V µg/g	Cu µg/g	Mn µg/g	Al µg/g	Zn µg/g	Fe µg/g
Exposed							
Average	0.70	2.51	4.51	7.19	23.07	78.65	336.41
Min	0.17	0.73	1.77	2.98	7.39	25.20	101.77
Max	2.94	12.48	8.70	19.81	91.81	177.09	1379.16
S.D.	0.6	2.0	1.5	3.3	14.0	38.9	214.6
S.E.	0.1	0.2	0.2	0.4	1.7	4.7	25.8
n=60							
Not-Exposed							
Average	0.72	0.34	4.20	6.20	21.07	64.56	83.49
Min	0.42	0.22	2.68	3.53	12.00	40.69	52.41
Max	1.03	0.51	6.06	7.50	42.64	98.42	139.66
S.D.	0.2	0.1	1.4	1.3	11.4	22.0	31.4
S.E.	0.0	0.0	0.2	0.2	1.4	2.6	3.8
n=20							

Percentage of accumulation was calculated based on differences between average values on exposed *vs* not exposed metals concentrations, and shown that mussel had accumulated metals in the follow order: *Fe>Zn>V>Al>Mn>Cu>Ni* (Tab. 5).

Tab. 5 - Metals concentration-percentage on soft body mussels.

Fe %	Zn %	V %	Al %	Mn %	Cu %	Ni %
93	5	0.8	0.7	0.4	0.1	0

5.2. Discussion.

5.2.1. Chemical physical parameters and dissolved gases in the Bay of Levante.

About 3.6 tonnes of CO_2 bubble into Levant Bay per day (Inguaggiato et al., 2012) which strongly influences the seawater chemistry of the bay.

The composition of the free and dissolved gas sample collected in April 2011, at the most vigorous bubbling site is given in Table 7. All gases are mainly composed of CO_2 with concentrations generally above 95% by volume.

Tab. 7 - Comparison between free gas and dissolved gas at the Bubble.

	CO_2 %	*N_2 %*	*O_2 %*	*CH_4 ppm*	*H_2 ppm*	*H_2S ppm*
Free	98	1.5	0.21	1700	<5	400
Dissolved	13	64.5	0.17	430	<5	n.a.

The main atmospheric gases (N_2 and O_2) are generally limited to few % with N_2 always in excess with respect to the N_2/O_2 ratio of the atmosphere. Typical hydrothermal gases (H_2, CH_4 and H_2S) had concentrations ranging from few ppm to few %. Methane had the lowest variability (430–1710 ppm). The highly reactive species (H_2 and H_2S) had a greater variability and the April 2011 samples had values at the lowest end of the range we detected (Table 7).

Elevated seawater temperatures were found close to the vents due to heating by geothermal steam (Aiuppa et al., 2000). Moving away from the gas vents towards the northern part of the bay, N_2 and O_2 returned to normal values due to water-atmosphere exchange yet CO_2 remained elevated.

Accordingly, dissolution of CO_2 and CH_4 produces the observed enrichment in CO_2 and in a lesser extent in CH_4.

In the ternary diagram CH_4–N_2–CO_2 (Fig. 51), the variability of CH_4/CO_2 ratio could result from the preferential CO_2 dissolution and consequent conversion to carbonate and bicarbonate species. The dissolved gases do not reach equilibrium with the bubbling gases. The most CO_2-enriched dissolved gas sample was collected at the same site where the free-gas sample has been taken. Comparing the dissolved and the free-gas composition (Tab. 7), the former has a much lower content in CO_2 and a higher N_2 content with respect to the latter, confirming that equilibrium was not reached due to the short interaction time.

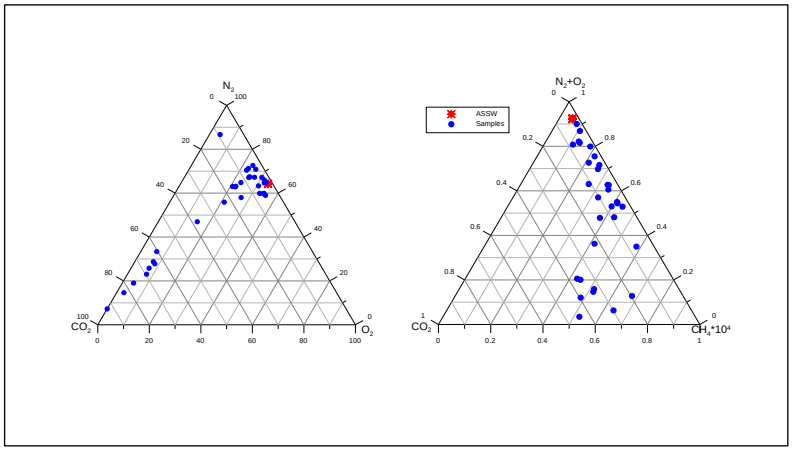

Fig. 46 - Ternary diagrams of the dissolved gases composition in the Bay of Levante seawater.

Dissolved gases (expressed as ml(STP)/l) are given in Table 2 for most of the collected samples. All the samples fall between two end members (Fig. 48): the air saturated seawater (hereafter ASSW) and CO_2 rich water. A clear alignment can be recognized thus suggesting that atmospheric contribution to dissolved gases always play an important role. However, if we look at N_2/O_2 ratio, many samples exhibit higher values with respect to the ASSW, probably due to the oxygen consumption occurring in reducing environments. Most of the samples are also enriched with respect to ASSW in methane and hydrogen (Fig. 48). The ternary diagram of CH4-(N_2+O_2)-CO_2 confirms the atmospheric contribution to dissolved gases and shows variable ratios between CH_4 and CO_2. Distribution of dissolved CO_2 and CH_4 along the bay clearly show a gradient from the main emission point (the bubble) until the northern part where the concentration decrease until the seawater background values (Fig. 47).

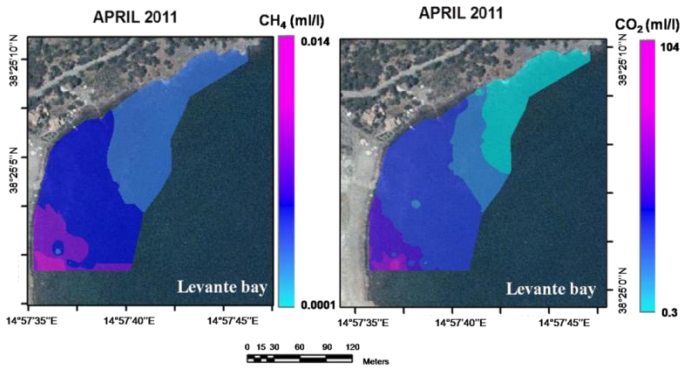

Fig. 47 - dissolved CH_4 and CO_2 distribution in the Bay of Levante.

As for the gas distribution also the pH formed a clear gradient from 5.65 at the main gas vents increasing to 8.1 (which is typical for Mediterranean seawater), in the north-eastern part of the bay.

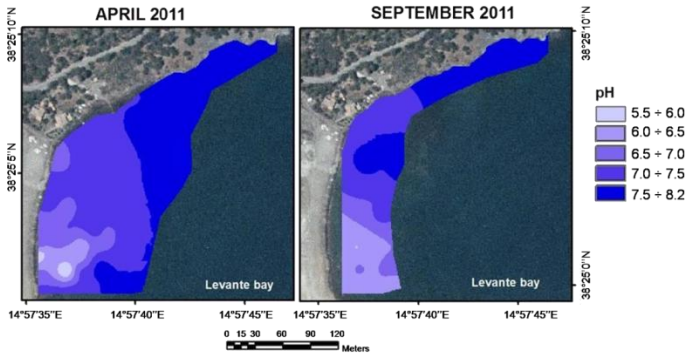

Fig. 48 - pH spatial distribution in the Bay of Levante.

The April 2011 Eh map shows a large area with negative values; during this campaign ambient conditions (light winds, calm seas) allowed only restricted water exchange between the bay and the open sea.

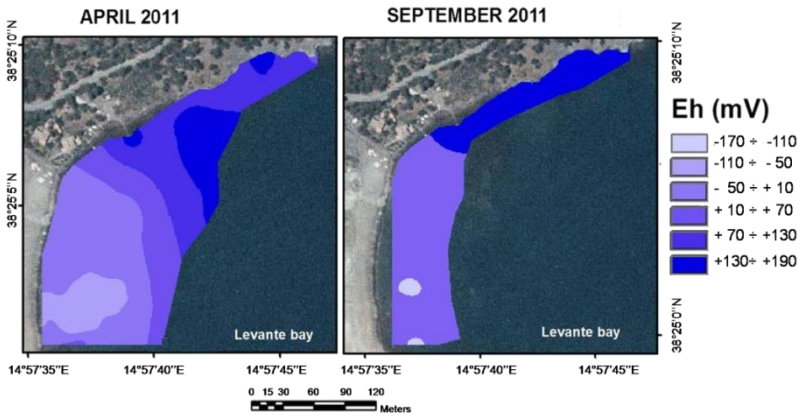

Fig. 49 - Eh spatial distribution in the Bay of Levante.

During the September 2011 campaign weather conditions were windier, with more water exchange with open sea. This is reflected in negative Eh values occurring very close to the main gas vents (Fig. 49).

The vent area had the lowest dissolved oxygen levels which, together with the lowest Eh values, could reflect oxygen consumption due to the oxidation of metals such as iron and reduced gases like H_2 and H_2S. Iron concentrations from the underwater CO_2 seeps in Levante Bay are about an order of magnitude higher than reported for other near-shore oligotrophic Mediterranean waters (Kadar et al., 2012), strongly indicating cold shallow

CO_2 seeps can supply significant input to the sea. Iron-rich (up to 2 mol kg^{-1}) shallow hydrothermal groundwaters are present in the Istmo area (Aiuppa et al., 2000). Alternatively, the high iron concentrations recorded in this area may also derive from an increased leaching from the sediments due to the extreme low pH levels, as recently suggested by Roberts et al. (2013).

Hydrogen sulphide is a low temperature product of hydrothermal activity whose dissolution in water could have severe consequences in living organisms (Hofmann et al., 2011).

Iron sulphides, mainly marcasite and pyrrhotite, coat rocks or occur as grains on Vulcano due to the effect of acid waters on sulphides according to the reaction:

$$FeS + 2H^{+} = Fe^{2+} + H_2S.$$

Sedwick and Stüben (1996) measured H_2S concentrations of 273 and 166 µmol kg^{-1} at the most intense bubbling sites while Amend et al. (2003) found values from 20 to 320 µmol kg^{-1} in the bay area. In April 2011, we found <55 µmol kg^{-1} in the bubbling area using Draeger tubes. Our Eh and pH data show that almost all samples fall in the stability field of sulphate and very few, close to the bubbling site, in that of hydrogen sulphide. Such data together with the low sulphide (S^{2-}) concentrations we recorded in the water at 5 m distances from the main vent area (<55 µmol kg^{-1}), suggest that due to the oxidation to non-toxic sulphate in the O_2-rich environment of the bay, only a small proportion of the H_2S brought by the hydrothermal fluids enters or remains into the aquatic phase.

Considering for sulphide a similar decay with the distance from the vents, as for dissolved CO_2, we consider that the northern transect, where the mussels transplant were situated, is not influenced by hydrogen sulphide. The positive Eh values measured in the area of the northern transect corroborate this assumption.

Our monitoring at shallow sites along the northern shore of Levante Bay allowed us to differentiate three carbonate chemistry zones influenced by the vent activity, and extending along ca. 200 m of coast.

Specifically, at sites >300 m from the intense CO_2 leakage site, we recorded reduced mean pH (< 7.6 pH units), and increased temporal pH variability, whereas ambient seawater pH/pCO_2 conditions were found at ca >400 m. pH was highly variable in the low pH zone (site 30), as showed during the 1 month hourly measurements.

The lowest pH was 6.62 and averaged 7.65 (±0.26), with two thirds of the measurements below 7.8 pH units, that is the projected average global sea surface pH value for the year 2100 (Caldeira and Wickett, 2003). At this value most subtidal calcifiers may disappear

in oligotrophic parts of the Mediterranean (Hall-Spencer et al., 2008). Daily and seasonal variations in seawater pH from 7.5 to 9.0 have been reported in coastal habitats (Middelboe and Hansen, 2007) and a compilation of high resolution time series of upper ocean pH has highlighted wide and rapid natural fluctuations in many coastal ecosystems, including vents (Hofmann et al., 2011). This natural variability was seldom considered in the early stages of ocean acidification research as perturbation experiments mainly investigated the responses of organisms to constant low pH. It may prove useful to incorporate natural pH variability in ocean acidification studies as ambient fluctuations in pH may have a large impact on marine organisms, affecting their performance (Hofmann et al., 2011).

Careful selection of study areas around CO_2 vent systems provide opportunities to examine the ecological effects of pH variability to forecast organism responses to acidification in habitats exposed to large natural diel, semi-diurnal and stochastic fluctuations in the carbonate system (Kerrison et al., 2011). Vulcano Island, like other volcanic sites in Southern Italy and Greece (Dando et al., 1999), shows how marine systems respond to long-term elevations in CO_2 such as those that could arise from geological sequestration leaks. As carbon capture and storage is being adopted as a CO_2 mitigation strategy, it is important to understand the associated risks such as leakage probability, strength of environmental perturbation, and any economic, and social impacts. Natural seabed CO_2 seeps clearly provide excellent opportunities for the development and testing of monitoring techniques for sub-seabed CO_2 leaks (Espa et al., 2010), and to assess the potential ecological impacts of marine CO_2 perturbations.

5.2.2. Saturation Index of calcite and aragonite.

The dissolution and precipitation of $CaCO_{3(s)}$ in the ocean is examined using the saturation state of the mineral, defined as SI or Ω.

$$\Omega = [Ca^{2+}]\,[CO_3^{2-}]/Ksp^*$$

The concentration of Ca^{2+}, a major constituent of seawater, changes only when the total salinity is increased or decreased. Ksp* in Equation is the measured solubility of $CaCO_{3(s)}$ in seawater at a given temperature, salinity, and pressure. There are three primary biogenic carbonate-containing mineral phases that occur in seawater: *aragonite*, *calcite* and *magnesian calcite*. Aragonite and calcite are naturally occurring polymorphs of calcium carbonate with differing crystal lattice structures and hence solubilities, the former being about 1.5 times more soluble than the latter at 25°C.

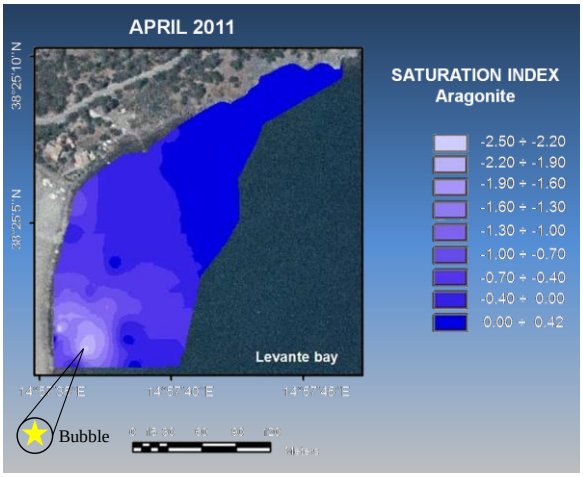

Fig. 50 - Saturation Index spatial distribution in the Bay of Levante seawater.

Aragonite is often referred to as a metastable form of calcium carbonate as it is not the form that would be expected at complete thermodynamic equilibrium. Nevertheless it is often convenient to treat the solubility of aragonite as a stable phase and to apply equation K_{sp} aragonite = $[Ca^{2+}]$ $[CO_3^{2-}]$ to investigate its saturation state.

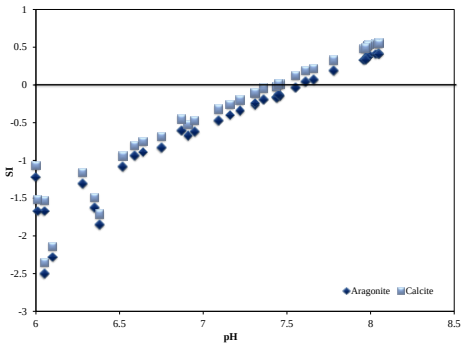

Fig. 51 - Saturation index (SI) of Calcite and Aragonite along the pH gradient.

Due to its relative thermodynamic instability, aragonite has a lower saturation state, ΩA, than calcite. Calcareous organisms secrete aragonite; thus its ΩA has to be considered when assessing future conditions for them. When ΩA > 1, the waters are supersaturated; when ΩA < 1, they are undersaturated; and when ΩA = 1, they are in equilibrium. Most ocean surface waters are supersaturated in aragonite while deep waters are undersaturated due to the decrease of $[CO_3^{2-}]$ and the increase of K_{sp}* with depth. As the surface oceans become more acidic, the values of ΩA in surface waters will decrease. Experimental measurements show that a decrease in ΩA or $[CO_3^{2-}]$ makes it more difficult for calcareous organisms like corals to produce CaCO3(s) (Langdon and Atkinson 2005;

Fabry et al. 2008). It is important to note that ΩA should not drop below 1, otherwise organisms will be negatively affected.

The map of ΩA values distribution (Fig. 50) shows that most of the samples are under-saturated with respect to calcite and aragonite minerals due to their low pH values (Fig. 51). Saturation in the bay is achieved only in the northern part where pH values exceed either 7.5 for calcite (not showed) or 7.6 for aragonite.

According to projections, 7.8 pH is the predicted average global sea surface pH value for the year 2100 (Caldeira & Wickett, 2003), and it is considered an ecological tipping point at which most subtidal calcifiers would disappear in the Mediterranean (Hall-Spencer et al. 2008).

5.2.3. Seawater major and trace elements of Vulcano.

Vulcano's seawater composition in terms of the major elements is close to that of Mediterranean surface waters even if salinity is a bit higher than oceans (Tab. 2 and Fig. 52); greater variability is recorded for dissolved Fe concentrations and trace metals distribution along the bay (Tab. 6).

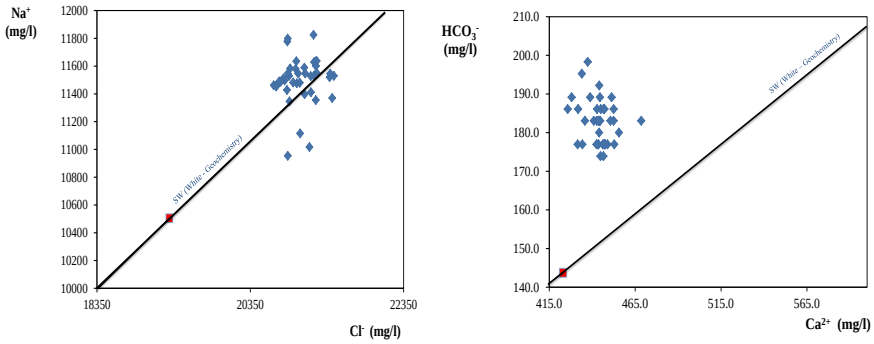

Fig. 52 - Major seawater composition in the Bay of Levante.

Graph Ca^{2+} *vs* HCO_3^- (in figure 52) shows that there is an higher concentration of HCO_3^- in Vulcano's seawater than background seawater. This fact is due to the presence of dissolved CO_2 that came from vents which dissolves calcium carbonates as previously said.

With regards to the dissolved trace element in seawater samples, they show different trends along the bay, in fact, some elements (Al and Cu) increase their concentration from the bubble to the offshore. Other elements (Mn, Fe, Zn and Ni) decrease their concentration along the bay (from bubble to the northern part). Elements such as La and V not shows high variation in concentration along the bay.

Tab. 6 - Bay's stat parameters compared with Pozzo Vasca, Bubble and Offshore.

n=15

	T °C	Eh (mV)	pH	Al ng/l	V ng/l	Mn ng/l	Fe ng/l	Ni ng/l	Cu ng/l	Zn ng/l	La ng/l
Pozzo Vasca	67	150	1.5	32339.6	51.5	69.1	51321.3	249.6	0.1	449.6	2.5
Bubble	22	-32	5.9	4.59	1.04	13.99	3.51	0.26	0.12	2.20	0.01
Offshore	21	171	8.0	0.95	1.46	0.51	0.63	0.20	0.21	0.56	0.004
Average	**22**	**124**	**7.3**	**5.14**	**0.77**	**11.42**	**3.68**	**0.31**	**0.50**	**2.32**	**0.004**
Min	21	-32	5.9	0.95	0.34	0.51	0.63	0.20	0.09	0.53	0.00001
Max	23	176	8.0	12.37	1.46	17.15	16.27	0.49	1.50	4.25	0.02
S.D.	*1*	*61*	*1*	*0*	*0*	*0*	*0*	*0*	*0*	*0*	*0*
S.E.	*0*	*16*	*0*	*0*	*0*	*0*	*0*	*0*	*0*	*0*	*0*

In the sediments of the Levante Bay Fe, Cu and Ni concentrations were close to or exceeded ERL and TEL limits. Sediments in fluid venting areas are generally characterized by conspicuous metal deposits of hydrothermal origin. This is a consequence of acid leaching from the underlying rocks which leads to the discharge of metal-rich hydrothermal fluids (Fig. 17, Chapter 1). Some of these elements in sediments (such as Cu, Fe, Mn and V) showed higher concentration values in sites at a distance of about 100-150 m upwards from the primary vent and decrease their concentration near the primary vent (The Bubble). Meanwhile, other elements (such as Ni and Zn) were more concentrated closer to the primary vent, reducing their concentration with distance, where clear positive Eh values were recorded (Vizzini et al., 2013). Complementary concentration trends of these metals in seawater and sediments, could be due to the fact that sediments represent an important sink/source for each elements depending from chemical-physical parameters.

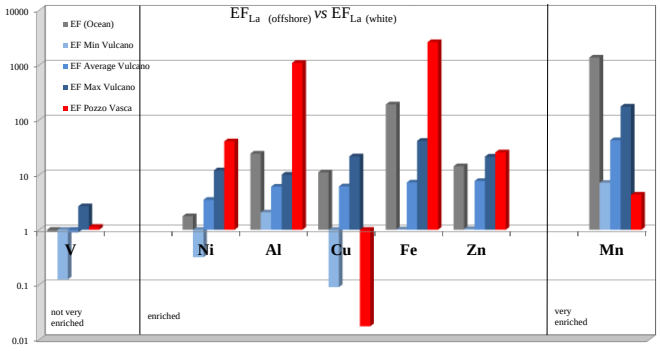

Fig. 53 - Elements EF_{La} are calculate using La as seawater background element, because it is considered a conservative element in seawater and it shouldn't been influenced from other sources.

Enrichment Factor (EF) respect offshore seawater were calculated for V, Ni, Al, Cu, Fe, Zn and Mn. EF is fundamental geochemical tool which tell us how much an element is enriched in our sample if compared with a background value:

$$EF_{La}=(X/La)/(X_{ref}/La_{ref})$$

Where numerator shows the ratio between *X* element and La in sample, and in denominator the same ratio between the same element and La in the reference medium. If EF value is one the element *X* is neither enriched nor depleted respect to the reference, if EF is greater than one the element *X* is enriched respect reference and there must be another source, if the EF is less than one, the element *X* is depleted so there must be a sink. The main source in the seawater of Baia di Levante is the hydrothermal reservoir and main sink are sediments.

In order to calculate EF it is necessary to choose an element which could be considered a background element in the studied geochemical sphere. We choose La because of the background level of La is close to the Mediterranean one and there aren't possible source for this element which can influence its concentration in our sample. Average La in the bay of Levante's seawater is $5.2*10^{-6}$ ppm, the values in the offshore of Vulcano is $4.3*10^{-6}$ ppm and the literature – White – background value is $5.7*10^{-6}$ ppm.

Such calculated EF of the Baia di Levante shows that all investigated element were enriched with respect to the background value (Fig. 53) except vanadium. To sum up, in general we can considered V as not very enriched, Ni, Al, Cu, Fe and Zn as medium enriched and Mn as very enriched, furthermore, EF show that trace metals are enriched in Bay of Levante probably because of the hydrothermal input.

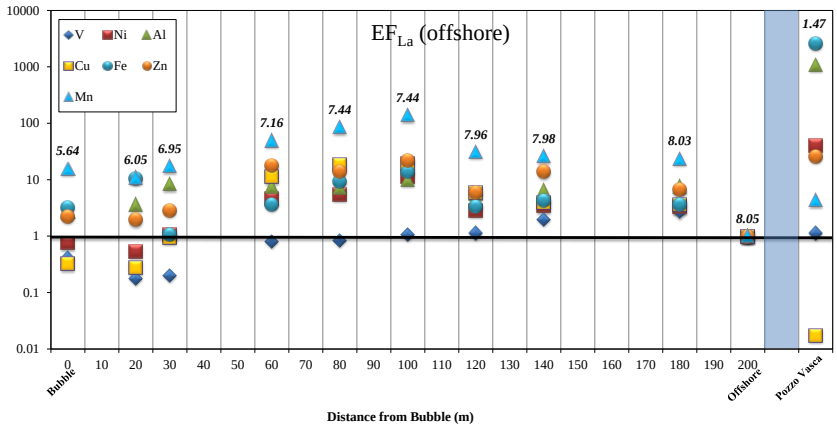

Fig. 54 - Elements EF_{La} along the Bay.

Plotting the EF_{La} values vs. the distance from the vent (in North direction) it is possible to see how in the first thirty meters from the vent seawater is impoverished in Ni, V and Cu and enriched for the other elements. That's probably because of the Eh and pH influence, this part of the bay being the most acidic and reducing. Once more this graph (Fig. 54) shows how the Pozzo Vasca is not enriched in Cu if compared with offshore sample, and not very enriched in Mn but very enriched for the other elements.

5.2.4. Seawater trace elements speciation and mussel accumulation.

The decrease of pH and Eh close to CO_2 vents may affect solubility, speciation and bioavailability of redox-sensitive trace elements (Öztürk, 1995; Hamilton-Taylor et al., 1996; Morford and Emerson, 1999; Kádár et al., 2012), with possible harmful effects on marine ecosystems. To evaluate these effects, we used blue mussels (*Mytilus galloprovincialis*) as they are considered good heavy metals accumulator and the huge literature define this species as a perfect biomonitor for the metals in their environment. Metals were accumulated during an exposition period of one month. We choose such short exposition period despite the fact that previous studies suggest to leave transplant from 3 to 12 months, because of nutrients in Vulcano's seawater are probably not enough to breed mussels and previous experiments on calcification rate, in this species, showed that mortality in this area increases after one month of exposition. Besides, a study of Incarbona et al. (2013) confirms that, due to the acidic condition, plankton (coccolithophores) populations are affected by an abundance decreasing in Baia di Levante seawater. Brand et al. (1983), suggests that for metals such as zinc, manganese and iron there are limitation for marine species of phytoplankton reproductive rates, these limits seems to be reached in the seawater of Vulcano (which are 10^{-7}M Log Activity of Fe, 10^{-11} for Zn and 10^{-11} for Mn) around the transplant area, that's could sustain the hypothesis that the one month period chosen to make the mussel's transplant was the most appropriate for.

Therefore, the period of transplant was chosen on one hand to not conditioning the accumulation rate because of the weakening of individuals, and on the other hand to assess if such short period is enough to evaluate the accumulation. Indeed data shown that only one month is enough for some metals. Besides, even if mussel alimentation rate is reduced in Vulcano's seawater (due to the loss of nutrients) Mikac et al. (1996) suggest that there is an accumulation which do not depend by feeding but only by respiration, despite the fact that most of metals accumulation is due to filter-feeding (they show that

for Hg, feeding contribute in the accumulation for about the 60% of the total accumulated Hg).

In general metal accumulation percentage in mussels exposed in normal pH (8.03) condition is higher in a range from 43-49% respect the other two pH points, except for Cu and Zn which not show differences. The fact that Cu and Zn hasn't shown differences could be due to the fact that mussel didn't show a conspicuous accumulation for both elements and the reason why, as suggested from White (2003), both elements are refractory elements and this mean that they are more accumulated in hard tissue than soft tissue. By contrast, as regards the other elements, the fact that mussels had accumulated more metals in normal pH condition could be in contrast which what we could aspect, because of the fact that in acidic conditions metals are more bio-available than in normal one and hydrothermal vents are enriched in various trace metals preponderantly in particulate phase, as stressed by Millero et., 2009 and Kadar et al., 2005.

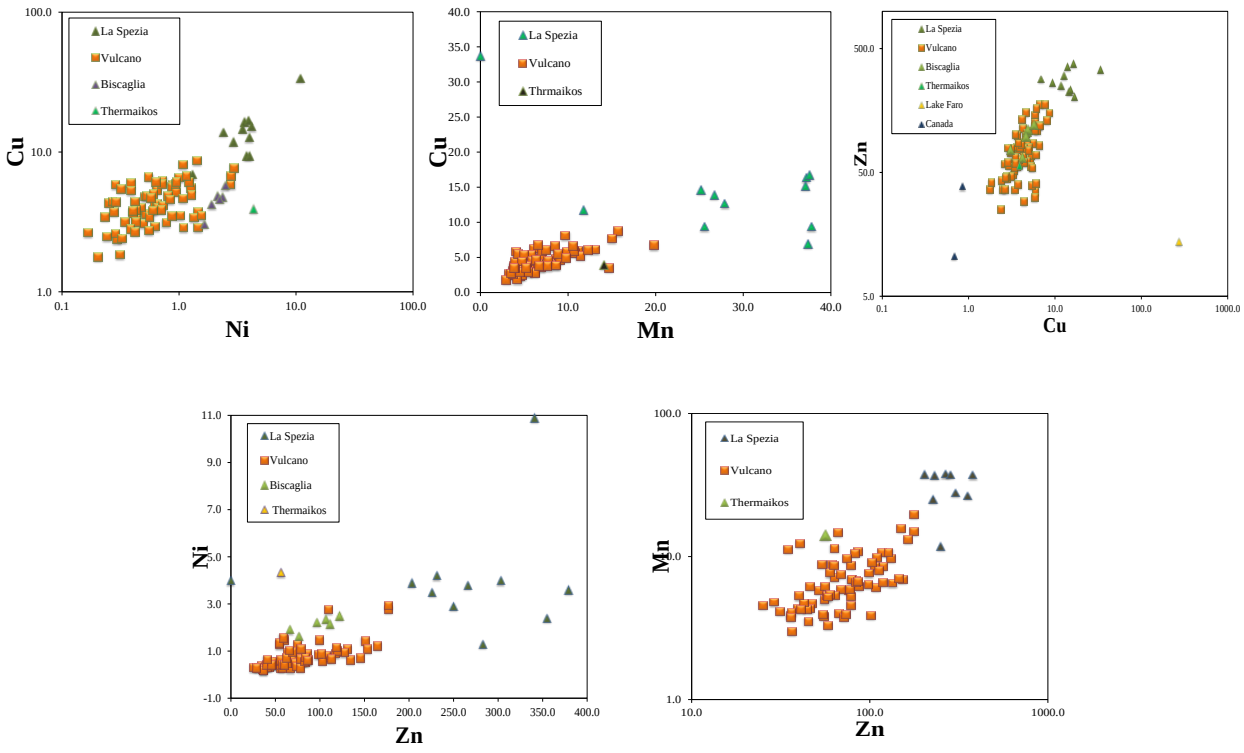

Fig. 55 - Comparison between exposed and literature metals mussel soft body concentrations, concentration in soft body are µg/g; Capelli et al. (1977), Rodriguez et al. (1995), Vassiliki et al. (2005), Licata et al. (2004), Fraser et al. (2011).

Literature data (Tab. 10 and Fig. 55) shows that in general (except that for Thermaikos, another volcanic area in Greece) the mussel's accumulation magnitude is higher with respect to our mussel probably due to the short exposition period.

The fact that mussels exposed in acidic condition has accumulated less than normal pH exposed, could depend from a physiological reason. Avoidance response via shell closure is known resilience strategy in mussels (Kadar et al., 2001 and 2002). As suggested from some authors, it could be possible that the acclimatization period at the acidic pH has slowed the filtration and thus accumulation rate with respect to the normal pH exposed mussels, which hadn't acclimate themselves. A longer exposition could mask the influence of this physiological process. This hypothesis could explain the unexpected differences between the different pH values. It should be better to repeat the experiment at the same conditions (but in another site where plankton is more abundant than at Vulcano, to lengthen the exposure time and control the accumulation rate after one, three and six months) in order to evaluate if adaptation period in lower pH can influence the accumulation rate in transplanted raft mussels. Actually, a study on mussels' physiology showed that for different level of salinity, temperature and pH, mussel respiration, which influence the accumulation rate of metals, is higher for lower temperature (22 vs. 28°C), normal pH (8.1 instead 7.2-7.4) and higher salinity (40 psu with respect to 34) (Chinellato et al., 2005). This fact could explain that mussel had a higher respiration rate in the normal pH than the respiration rate in acidic condition. The acclimation process results in alterations in the rate of ventilation and a concomitant reduction (or increase) in the metabolic cost of pumping water through the gills (Widdows, 1973). Thus, this process is reflected in the respiration, and is also a result of alterations in metabolism of the tissues (Gabbott, 1976). The standard metabolism is defined as the minimum amount of energy required to maintain the vital functions of the inactive organism. The routine metabolism corresponds to the energy required for a spontaneous activity, and the active metabolism relates to the consumption of energy or O_2 in maximum activity (Widdows, 1973). Bayne (1973) also describe these metabolisms related to the type of maintenance of the mussel *Mytilus edulis* and conclude that the standard metabolism is obtained after 30 days in a laboratory when the food offered is less than the needs of the organism. Resgalla et al. (2006) performed an acclimation experiment, using bivalves in controlled laboratory and environmental conditions than the natural. They observed that due to the physiological mechanism of adaptation the mussels tend to conserve energy and maintained their weight until the 20^{th} day of exposition to the new conditions, then lost

weight and demonstrated a greater variability in respiration rates (from the 25th day on). It would appear that the stabilization of their metabolic functions under laboratory conditions occurred after the 20th day, when the respiration rates became constant, the weight stabilized and there was a small increase in size. This may explain why our mussels exposed to lower pH than the physiological one accumulated less compared to those exposed to the normal pH which were already acclimatized.

Tab. 7 – Comparison between soft body metal concentration in exposed mussel and literature data.

	Exposition time days	Ni µg/g	V µg/g	Cu µg/g	Mn µg/g	Al µg/g	Zn µg/g	Fe µg/g	References
Vulcano 2012	**28**	**0.70**	**2.51**	**4.51**	**7.19**	**23.07**	**78.65**	**336.41**	**This Study**
Adak Island (Alaska)	*wild*	-	-	-	4.59	-	-	-	Burger et al., 2006
Adak Island (Alaska)	*wild*	-	-	-	25.5	-	-	-	Burger et al., 2006
Britain, SE Europe	*wild*	-	-	-	22.65	-	-	-	Burger et al., 2006
NE Asia, Pacific	*wild*	-	-	-	4.75	-	-	-	Burger et al., 2006
N America	*wild*	-	-	-	13	-	-	-	Burger et al., 2006
N Europe, White sea	*wild*	-	-	-	51.5	-	-	-	Burger et al., 2006
La Spezia (Italy)	*wild*	*4-5.9*	-	*13*	*30.4*	-	*23-283*	-	Capelli et al., 1977
Portofino (Italy)	*wild*	*1.78*	-	*3.78*	*7.35*	-	*130*	-	Capelli et al., 1977
N.Italy	*wild*	*1.3-11*	-	*6.9-33.7*	*9.8-37.8*	-	*139-381*	-	Capelli et al., 1978
Portugal	*wild*	-	-	6.2-13.4	-	-	140-542	305-1175	Coimba et al., 1991
New Brunswick (Canada)	*wild*	-	-	0.68	-	24	10.5	55.5	Fraser et al., 2011
Belleduene smelter	*wild*	-	-	0.85	-	19	38.5	52.5	Fraser et al., 2011
Gulf of Marine	*wild*	-	-	0.975	-	11.76	9.75	45.5	Fraser et al., 2011
France	*wild*	-	-	*0.92*	-	-	*14*	-	Fraser et al., 2011
USA	*wild*	-	-	1.2	-	-	17	-	Fraser et al., 2011
World	*wild*	-	-	1	-	-	17	-	Fraser et al., 2011
UK	*wild*	5.0-42.9	-	15.1-40.9	8.6-27	-	110-368	8.6-27	Giusti et al., 1999
Western part of Baltic	*wild*	0.005	-	-	-	-	0.31	1.51	Karbe et al., 1977
Bosporus (Turkey)	*wild*	-	-	2.97-5.65	-	-	31.9-45.4	-	Köklü et al., 2000
Lake Faro, Sicily (Italy)	*wild*	-	-	*0.27*	-	-	*0.01*	-	Licata et al., 2004
Italy	*wild*	-	-	*0.53-5.96*	*1.1-14.2*	-	*10.8-59*	*1.1-14.2*	Majori et al., 1991
Adriatic Sea (Mediterranean)	*wild*	*1.1*	-	*4*	*0.8*	-	*33*	*54*	Orescanin et al., 2006
Québec (Canada)	92	-	-	20	-	-	158	-	Pellerin et al., 2009
Spain	*wild*	-	-	1.1-3	-	-	17.3-75.8	-	Rodriguez et al., 1995
Western part of Baltic	*wild*	0.004	-	-	0.02	-	0.14	16.70	Schnier et al., 1978
Spain	*wild*	*1.6-2.4*	-	*3-5.7*	-	-	*66-121.8*	*110-660*	Soto et al., 1995
Bulgaria	*wild*	-	-	0.5-10.6	-	-	12.8-42	-	Stamov et al, 1988
Gulf of Gdansk	*wild*	0.01	-	0.00	0.08	-	0.328	1.2	Szefer and Szefer , 1985
Gulf of Gdansk	*wild*	0.01	-	0.01	0.04	-	0.2	0.56	Szefer and Szefer , 1990
Gulf of Gdansk	*wild*	0.01	-	0.003	0.07	-	0.13	1.26	Szefer and Szefer, 1990
Puck Bay	*wild*	-	-	0.02	0.05	-	-	0.54	Szefer et al., 1994
Gulf of Gdansk	*wild*	-	-	0.01	0.03	-	-	0.56	Szefera et al., 2002
Pomeranian Bay	*wild*	0.003	-	0.01	0.03	-	0.159	0.27	Szefera et al., 2002
Southern Baltic	*wild*	0.003	-	0.01	0.05	-	0.14	0.32	Szefera et al., 2003
Western part of Baltic	*wild*	0.00455	-	-	-	-	0.10	-	Theede et al., 1979
Black Sea (Turkey)	*wild*	*4.02-24.07*	-	*7.21-9.1*	*5.7-22.8*	-	*78-512*	*5.7-22.8*	Topcuoğlu et al., 2002
Pagassitikos Gulf, Greece	*90*	*2.7–5.0*	-	*6.6–10.0*	*8.6–27.1*	-	*228–364*	*355–1384*	Tsangaris et al., 2013
N. Evoikos Gulf, Greece	*90*	*47.0–50.3*	-	–	–	-	–	*842–898*	Tsangaris et al., 2013
Saronikos Gulf, Greece	*90*	–	-	*2.4–14.3*	–	-	*120–190*	–	Tsangaris et al., 2013
Greek coast	*90*	*2.9–6.8*	-	*2.5–4.8*	*2.1–7.8*	-	*83–184*	*49–113*	Tsangaris et al., 2013
North coast of Tunisia	*90*	–	-	*2.9–3.9*	–	-	*250–426*	*117–248*	Tsangaris et al., 2013
Bay of Cannes, France	*90*	–	-	*4.7–33.5*	–	-	*101–153*	–	Tsangaris et al., 2013
Arcachon Bay, France	*90*	*1.1–1.5*	-	*6.0–22.7*	–	-	*158–235*	–	Tsangaris et al., 2013
Balearic islands	90	1.9–3.35	-	0.16–0.26	4.29–5.19	-	1.56–3.37	0.51–1.25	Tsangaris et al., 2013
French Mediterranean coast	*90*	*0.47–2.48*	-	–	–	-	–	–	Tsangaris et al., 2013
West Mediterranean coast	*90*	*0.62–3.18*	-	-	–	-	–	–	Tsangaris et al., 2013
Thermaikos Gulf (Greece)	*wild*	*4.34*	-	*3.91*	*14.10*	-	*56.30*	*395*	Vassiliki et al., 2005

However, despite the fact that mussels were exposed for one month and in acidic condition they seem to accumulate less than normal one, data show that metals soft body accumulation in mussel soft body was evident for each metals except, as previously said, for Ni (Tab. 7).

As previously said shell (organism or individual) size can influence the accumulation capability, mostly because it is usually related to age, food acquisition capability and weight. Some studies report metal levels increasing with size of the mussel (Tewari et al., 2000; Wiesner et al., 2001) but it depend from metals because some metals (such as copper) decrease with shell size. In a study of Saavedra et al., 2004, they were no significant differences between metal concentration at different shell lengths were detected; in that study they has shown that metal concentrations in raft mussels are size independent probably owing to their rapid growth rates and that. But it was untypical in this aspect, raft cultured mussels seem to be different, because, although this kind of independence was found in some studies (Manly et al., 1996; Riget et al., 1996), in most cases, a negative relationship between metal concentration and size was observed in *Mytilus edulis*. Wright and Mason (1999) found that mercury levels increased with shell size, but cadmium and zinc did not.

Size has been shown to produce great differences in metal concentration in the tissues (Boyden, 1977; Cossa et al., 1980), with which the monitoring system must cope. In order to avoid this crucial influence, some authors transformed metal concentrations to metal content of standard mussel (Boyden, 1977; Riget et al., 1997) and others sampled mussels of uniform size (Popham et al., 1980). However, neither of the two methods has been completely satisfactory for monitoring purposes, owing to the limitations inherent to standardization methods (Boyden, 1974; Cossa et al., 1980; Cossa and Rondeau, 1985) and because sampling only one size class is an inadequate solution to guarantee public health when a wider range of sizes are commercialized.

In most of raft cultured mussels there is a negative relationship between metal concentration and size (Saavedra et al., 2004), due to the fact that smaller organisms presenting higher physiological rates than larger ones, and metabolic rates are strongly dependent on the size of the body, so in general smaller tend to accumulate more than bigger (Resgalla et al., 2006). According to literature data, it is possible to estimate the age class of the animal using shell length, although, accumulation rate depends mainly on the biomass of animal rather than on shell length. Some authors suggest to use soft body-weight to evaluate the accumulation rate capability because of biomass controlling the rapidity of mussel physiological processes. Furthermore, there is an inter-individual variability in ratio between biomass and length shell. For all these reasons, in order to understand if length and weight could be used as a good parameter to estimate the

accumulation rate, we have done a comparison between the two parameters as shown in following graph:

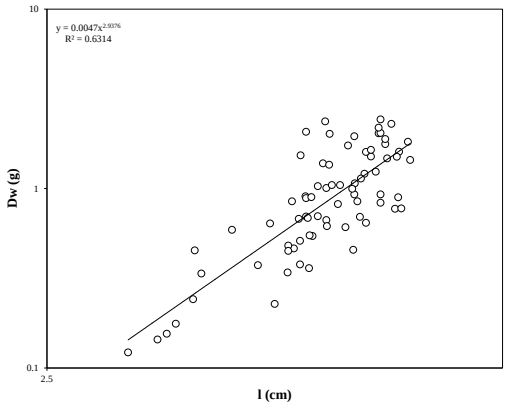

Fig. 56 - Dw (dry weight) vs l (length) in mussels.

Since there is a discrete correlation (R^2=0.6) between the parameters we decided to use Dw (dry weight) in order to define three bio-mass classes. Since there are data overestimation due to the size and season variability, in order to avoid it, some authors use the metal/shell-weight indices, which is the ratio between the metal concentration in the soft body per dry weight of soft tissue on dry shell weight. The so-called metal shell-weight index is independent of conditions such as nutritional stage, spawning, or tidal exposure (Fischer 1983) and of environmental factors such as temperature, salinity and oxygen levels (Fischer 1986) but only depend from biomass.

The use of Dw instead the l allows to reduce the variability due to the under mentioned reasons. Thus mussel population was subdivided follows; "***Class 1***" (C1) which includes individuals from 0 to 1 g (dry weight)," ***Class 2*** " (C2) from 1 to 3 g, "***Class 3***" (C3) from 2 to 3 g (Fig. 57). The different accumulation capacity for each investigated elements was evaluated on the dry weight.

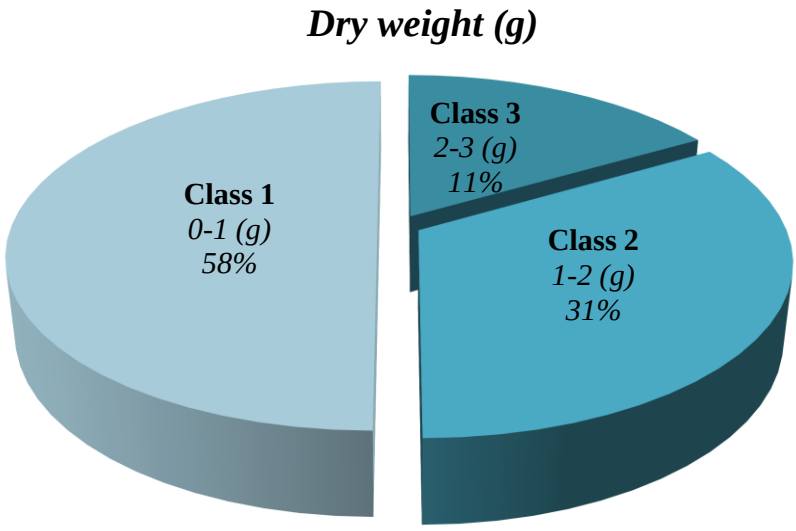

Fig. 57 - Biomass population composition divided in three classes. Market and consumed mussel populations are so composed: 58% Class1, 31% Class 2 and only 11% Class 3.

We must consider that the used mussels population is the typical marketable and consumed population. The analysis revealed that the 58% of the population is composed of small individuals (Dw - 0 to 1 gr), the 31% of medium individual (1-2 gr) and only the 11% is composed of the bigger (2-3 gr). For each investigated elements, the Class which shown the bigger accumulation rate is the most conspicuous of all, Class 1 (Tab. 10). This fact confirms what Saavedra et al., 2004 and Resgalla et al., 2006 said.

Tab. 8 - Stat on metals concentration in exposed soft body mussels. In general Class 1 accumulated about the 50% of the total amount accumulated from population for each elements. Besides, f*or all classes the preferred accumulated element seems to be Fe.*

n=60

	Al µg/g	V µg/g	Mn µg/g	Fe µg/g	Ni µg/g	Cu µg/g	Zn µg/g	
C1	33.74	2.80	8.55	361.35	0.99	5.02	95.01	
C2	20.82	1.28	5.49	186.40	0.47	3.77	57.32	
C3	11.58	1.27	3.94	200.19	0.31	3.01	42.35	
	Al %	V %	Mn %	Fe %	Ni %	Cu %	Zn %	
C1	***51***	***52***	***48***	***48***	***56***	***43***	***49***	
C2	31	24	31	25	27	32	29	
C3	18	24	22	27	18	26	22	
Sum	**100**	**100**	**100**	**100**	**100**	**100**	**100**	
	Al %	V %	Mn %	Fe %	Ni %	Cu %	Zn %	sum %
C1	7	1	2	***71***	0	1	19	**100**
C2	8	0	2	***68***	0	1	21	**100**
C3	4	0	1	***76***	0	1	16	**100**

In general Class 1 accumulated about the 50% of the total amount accumulated from population for each elements. For all classes the preferred accumulated element seems to be Fe, in fact, the 71% of the accumulated metals in Class 1 is iron, despite what predicted from White, which said that since iron is a refractory element it should be more accumulated in hard than in soft tissue. Similar percentage for other classes; the 68% of the accumulated metals in Class 2 is Fe and 76% for Class 3. But order of accumulation is different in each classes:

C1*: Fe>Zn>Al>Mn>V and Cu>Ni*

C2*: Fe>Zn>Al>Mn>Cu>V and Ni*

C3*: Fe>Zn>Al>Mn and Cu>V and Ni*

For all classes the accumulation follows the same order for iron, zinc, aluminum and nickel (which is always the lowest, but it shouldn't be surprising because as previously

said has not accumulated with respect to not-exposed). In C1 vanadium and copper have the same order of accumulation magnitude. In C2 copper is more accumulated than vanadium. In C3 copper and manganese have the same magnitude order accumulation which is bigger than vanadium.

In brief, despite the fact that they were exposed for a short period and that the physiological adaptation has probably influenced the accumulation process, we can affirm that mussels had accumulated all analyzed element.

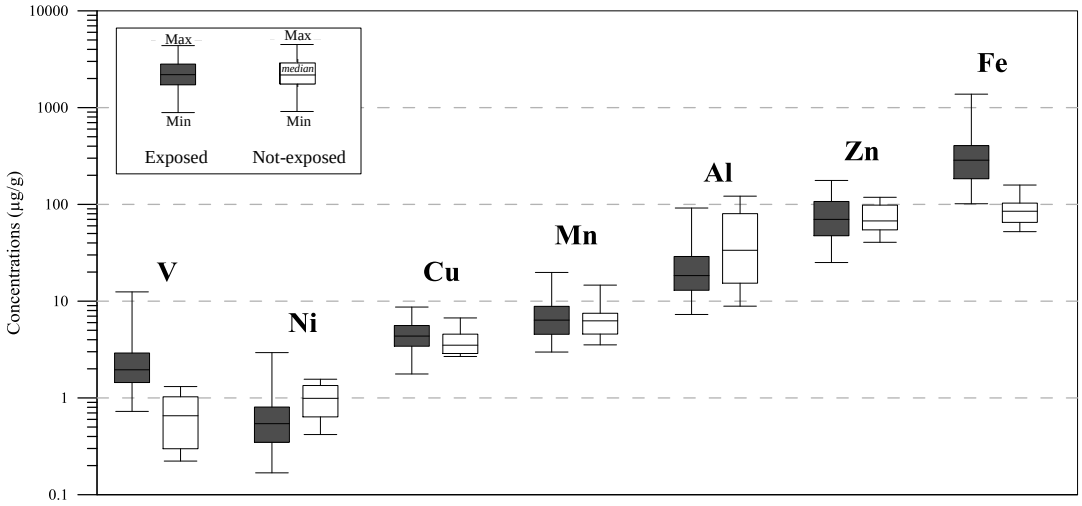

Fig. 58 - Metals concentration in exposed and not exposed soft body mussels (dry weight).

Figure 58 shows the accumulation for each metal in mussels, box plot reported the median, maximum and minimum values for exposed vs. not-exposed mussel. It is clear that there was an accumulation for almost all elements in the following order:

Fe>Zn>Al>Mn>Cu>V>Ni

Mussels are considered as good bio-monitors for pollutants in their environment, because they can represent the environmental background in amplified.

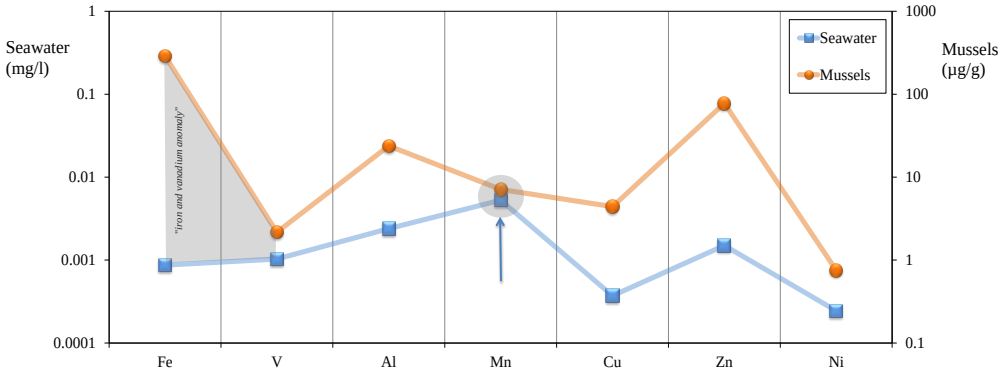

Fig. 59 - Comparison between trends metal accumulation in exposed mussels and concentration in seawater close to the mussel's transplant.

To confirm the above hypothesis we compared the average abundance for each investigated element in seawater and mussels. Trends are similar in both geochemical spheres, except that for iron and manganese (Fig. 59). It seems that mussel accumulated much more iron than what could be foreseen from measured seawater concentrations and less Mn.

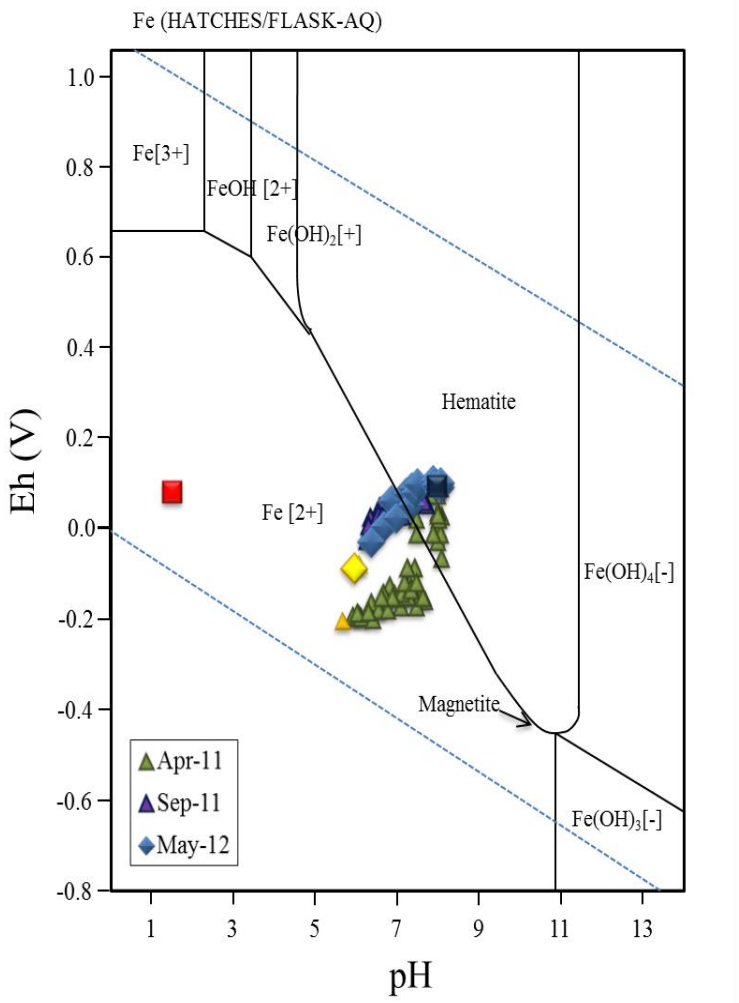

Fig. 60 - Eh/pH diagram shows the stability fields for the different iron species. Diagram from Atlas of Eh-pH diagrams (Takeno, 2005). Red square is the Bubble 2012, blue square is Offshore 2012, orange triangle is Bubble 2011.

Plotting our samples in a Eh/pH diagram, with stability field for chemical species, we can understand how seawater positive Eh and medium acid pH (7-7.5), that are the conditions of seawater around the mussel transplant, have as predominant species the Fe-oxide and hydroxides (Fig. 60). We are going to examine the speciation for each investigated element and its accumulation in mussels.

Iron.

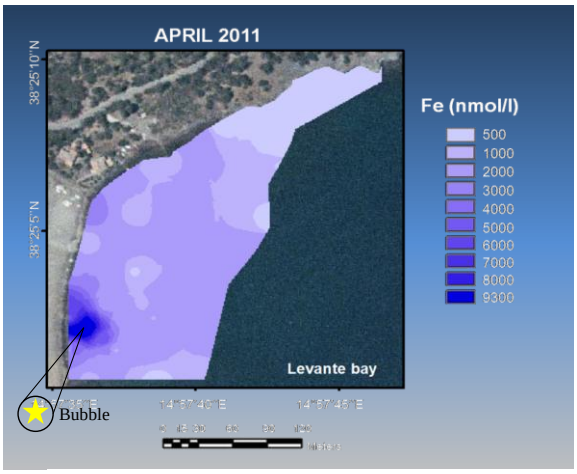

Fig. 61 - Spatial dissolved iron distribution along the Bay.

The distribution map of dissolved iron (Fig. 61) shows that the maximum values are all found along the coast of the Istmo area indicating a probable input correlated to hydrothermal fluids in liquid phase. Such iron-rich shallow hydrothermal waters in the Istmo area were also recorded by Aiuppa et al. (2000). The EF_{La} for iron also shows that the probable source is the hydrothermal vents fluid. In general seawater of Baia di Levante is enriched with respect to the background level (offshore). The hydrothermal end member (Pozzo Vasca) is very enriched with respect to the other samples, confirming the hypothesis that the principal source for Fe is hydrothermal reservoir (Fig. 62).

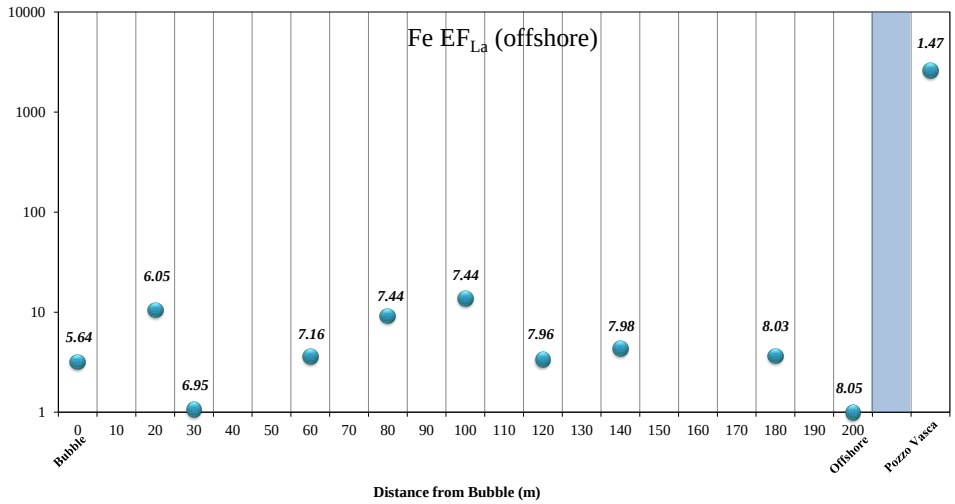

Fig. 62 - Fe-EF_{La} variation along the Bay.

Plotting dissolved Fe vs. pH in together with the saturation indexes (SI) of phases that could control iron solubility such as hydroxide and carbonates (Fig. 63), shows that Fe concentrations along the pH gradient are probably controlled by speciation. On the left part of the diagram, corresponding to lower pH values, dissolved iron concentration is controlled by a removal process in sulphides as suggested from speciation and chemical physical data (at pH 5.7, pyrite $SI_{(Log)}$ is -15.7 and calcite $SI_{(Log)}$ is 0.5, meanwhile at normal seawater pH, pyrite $SI_{(Log)}$ is -100.3 and calcite $SI_{(Log)}$ is 0.7).

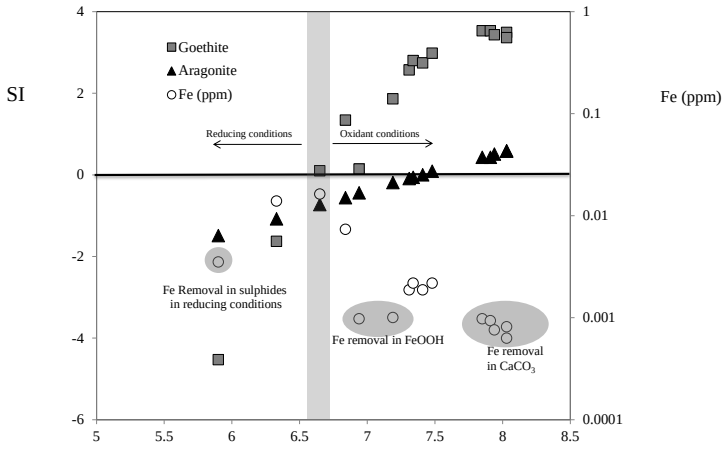

Fig. 63 - Dissolved iron concentration and SI of Aragonite and Goethite along pH gradient.

In the central part of diagram there are no possible sink for that reason the dissolved iron concentration is higher than other parts, because his speciation is mainly controlled by the pH, as predicted from Millero, 2009. On the right part of diagram dissolved iron concentrations decrease again probably because of removal in Fe-oxi-hydroxide (such as goethite and magnetite) and carbonates (such as $FeCO_3$ and aragonite).

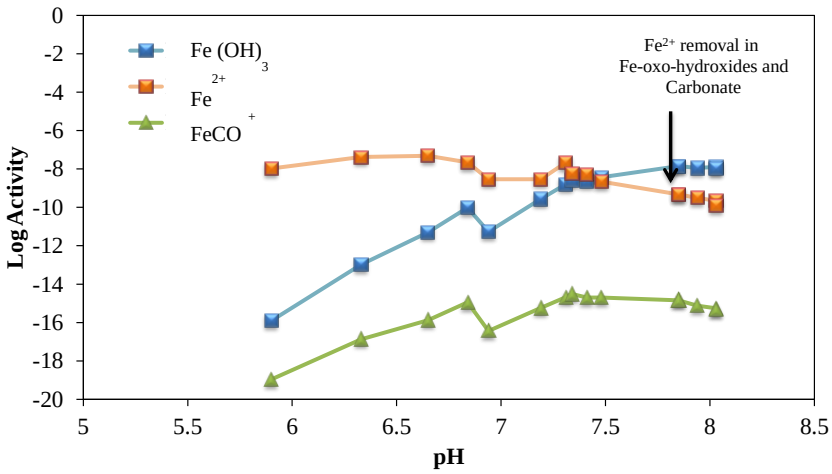

Fig. 64 - Log Activity of the different iron species along the pH gradient.

As confirmed from speciation data (Fig. 64), dissolved Fe^{2+} decreasing has an opposite trend with respect to the increase of hydroxide and carbonate species.

In the transplanted area we have measured the iron concentrations dissolved in seawater but not in the suspended particulate matter. In contrast mussels analysis include the bulk iron. Because these animals are filter feeder and can filtrate both suspended and dissolved matter in seawater, the concentrations in the mussel's body will include also particulate matter such as Fe-Hydroxides and carbonates. This may explane the "Fe-anomaly" in figure 59.

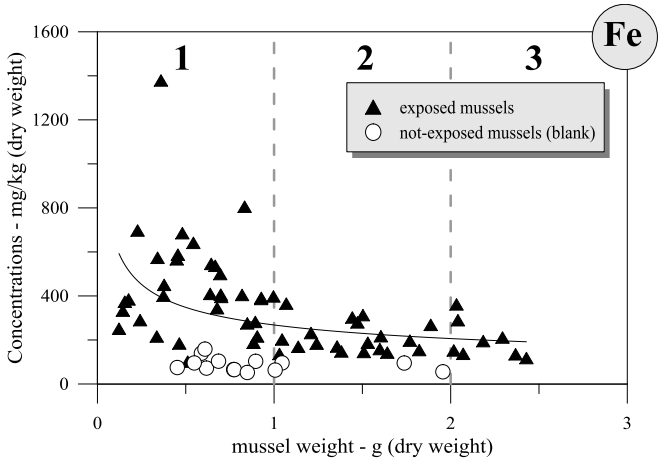

Fig. 65 - Iron concentration in exposed and not exposed soft body mussel.

Figure 65 shows that mussels accumulated a lot of iron with respect to not exposed mussel, and class 1 mussels accumulated more than other classes (as previously said).

***Vanadium*.**

Literature data highlight a strong correlation between the concentrations of iron and vanadium in natural waters. This correlation indicates that vanadium could have been incorporated as a trace element in the Fe-oxides through the adsorption mechanism (Kay et al., 2011). In the case of vanadium, it has been demonstrated that the rate of oxygenation of the vanadyl ion (VO^{2+}) is strongly enhanced by adsorption on to iron hydroxides. Scavenging of V by precipitation of iron hydroxides explains the low V content in the reduced Fe-rich Sea waters from Vulcano (this study). A similar process is responsible for the removal of Cu, Zn, and Pb from solution (Aiuppa et al., 2000). Trace metals such as V, Cr, As and Mo, are strongly associated with the fate of iron particles (Schaller et al., 1997). A study by Kim et al 2006 suggests the mechanism through the vanadium can be adsorbed by the surface of the Fe – oxide, they suggest that the adsorption is function of pH and redox condition of solution, because of as a result of electron donation from deposited vanadium to α-Fe_2O_3 surface layers. The de-polarization of a vanadium induced dipole moments due to an increasing interaction between the dipoles at a higher coverage. The vanadium deposits are oxidized after donating electrons to the α-Fe_2O_3 substrate. Another study highlights how in acid condition the concentration of V is inversely proportional to the Fe(II) because of the electronic interaction between V and Fe atoms in the oxide structure, changes in the oxidation states of V and Fe cations (Tsung Wang et al., 2010).

Baia di Levante seawater is not enriched in vanadium (0.7 µg/l) showing values close to literature background (1.7 µg/l - White, 2003). Pozzo Vasca (considered the hydrothermal end member) seems to show a bit higher value (51 µg/l), the source for this element could be hydrothermal vents in consideration that literature suggest that this elements derives from rocks weathering due to the acidic fluids.

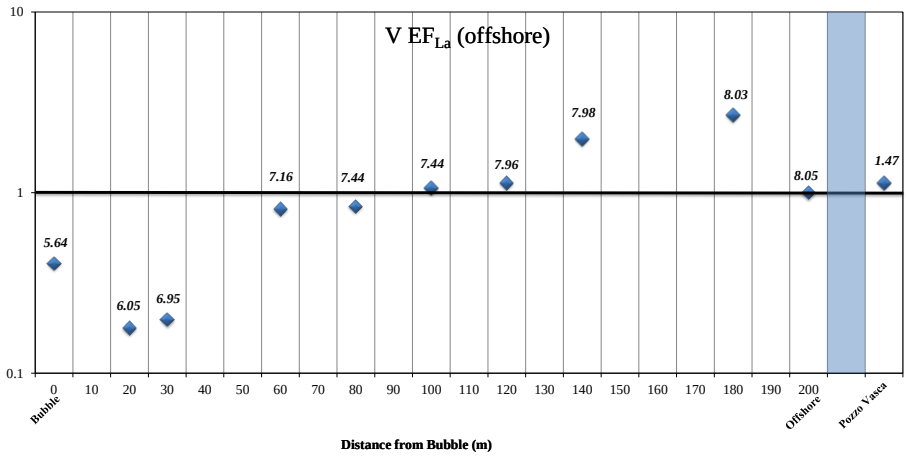

Fig. 66 - V-EF$_{La}$ variation along the Bay.

The samples closest to the vent have negative V-EF$_{La}$, that's mean that enrichment of vanadium in that point is less than the background seawater. The most enriched samples are at 140-180 m from the vent, in the area around the mussels transplant, indicating that there is no sink for V in that area.

The chemistry of vanadium is complex because this element can exist in oxidation states from −1 to +5 and frequently forms polymers. V(IV) and V(V) form many complexes in water that change in accordance with the solution pH, and their concentrations. This fact could explain the complex distribution of EF along the Bay. It is known that in the pH range 2–6, the main species of V(V) is the decavanadate anion $V_{10}O_{29}^{6-}$, which changes to the dioxovanadium(V) cation VO_2^+ below pH 2. In contrast, V(IV) exists as oxovanadium(IV) in acidic solution and this cation readily changes to the anion $V_{10}O_{42}^{12-}$ at about pH 4. The concentration of vanadium in natural waters is very low and usually in the range 0.5–2.5 µg/l (Coina et al., 2005).

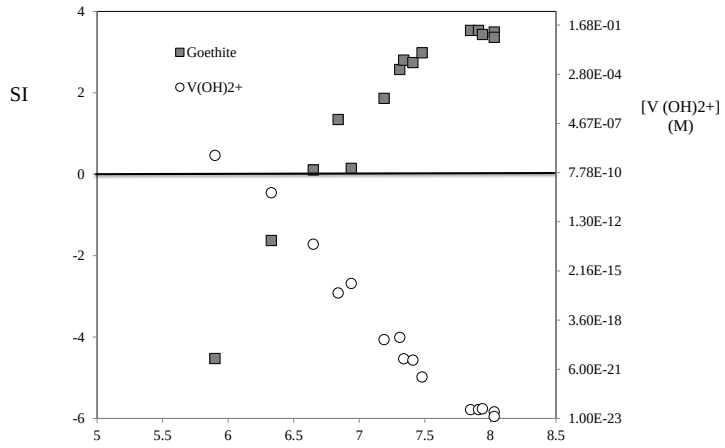

Fig. 67 - Vanadium idroxide concentration (M) and SI of Goethite along pH gradient, data processed through the help of Phreeqc.

Literature suggest that V(V) fate is tightly linked with Fe-hydroxide (for instance goethite) fate (Fig. 67), through an adsorption mechanism on to the hydroxide surface (Kay et al., 2011; Wang et al., 2010; Tavalli et al., 1998; Teshima et al., 1996; Kim et al., 2006; Aiuppa et al., 2000), actually, our data confirm a negative correlation between V and Fe hydroxides.

Eh can influence the formation of V-oxides as suggested from Theshima et al., 1996 and Schaller et al., 1997:

$$Fe^{3+} + V^{4-} \rightarrow Fe^{2+} + V^{3-}$$

$$Fe^{2+} + VO_2^{+} + H^{2+} \rightarrow Fe^{3+} + VO^{2+}\ H_2O$$

V-oxide make vanadium very mobile in seawater column, because it forms more stable species such as $H_2VO_4^-$ e HVO_4^{-2} which can be removed as carbonates and Fe-hydroxides.

The total dissolved vanadium and goethite SI are shown with respect to pH in Fig. 68. The decrease in vanadium concentration seems to correspond to positive goethite SI, confirming the hypothesis that the principal sink for V are Fe-hydroxides as literature suggest.

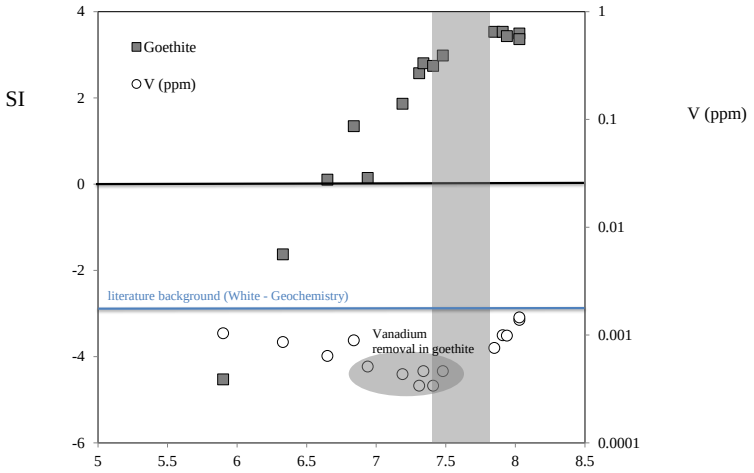

Fig. 68 – Dissolved vanadium concentration and SI of Goethite along pH gradient. Literature V background is in ppm.

Furthermore, Vizzini et al., 2013 confirm that, in the area where seawater is in the pH range 7-7.5, sediments are enriched in V with respect to those closest to the vent (where pH is acid and Eh negative, thus V is prevalent in dissolved form). The mechanism of adsorption on goethite surfaces as the main responsible for vanadium removal from the water column, can be confirmed by the fact that the sediments are also enriched in Fe.

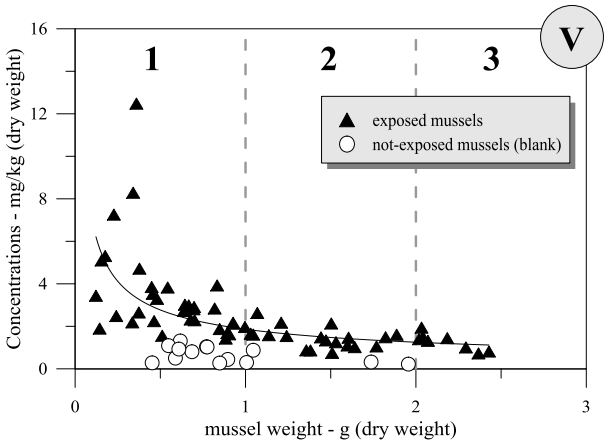

Fig. 69 – Vanadium concentration in exposed and not exposed soft body mussel.

This could explain why exposed mussels recorded a strong V accumulation (Fig 69) with respect to not exposed, despite the fact that vanadium abundance in seawater is not higher than in the background area. This highlights how speciation of non toxic metals, such as iron, can influence the fate of other toxic metals, such as vanadium and their

accumulation in animals which live in a such environment. In this case, the mussels have once more demonstrated that they can be used as biomonitor of their environment. But this fact has also demonstrated that the use of bioaccumulators, without the geochemical characterization of the environment, is not enough to explain the bio-geo-chemical mechanisms of accumulation in the food net for pollutants such as heavy metals.

To further confirm this hypothesis we compared the concentrations of iron and vanadium in the mussels soft body (data were normalized with respect to the dry weight in order to reduce variability). Fig. 70 confirms the good correlation between both metals, suggesting that iron drives vanadium fate also in the mussels' soft body.

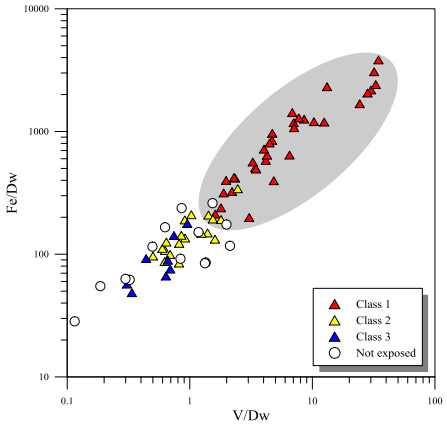

Fig. 70 - Fe and V ratio normalized in Dw, highlight a good correlation (R=0.87; p<0.001).

Once again graph confirm that exposed mussel are enriched in both elements respect not exposed and that C1 is the most enriched.

Manganese.

Mn is the most enriched element, Vulcano's seawater suggesting that this element have an hydrothermal origin (Fig.53 and 71).

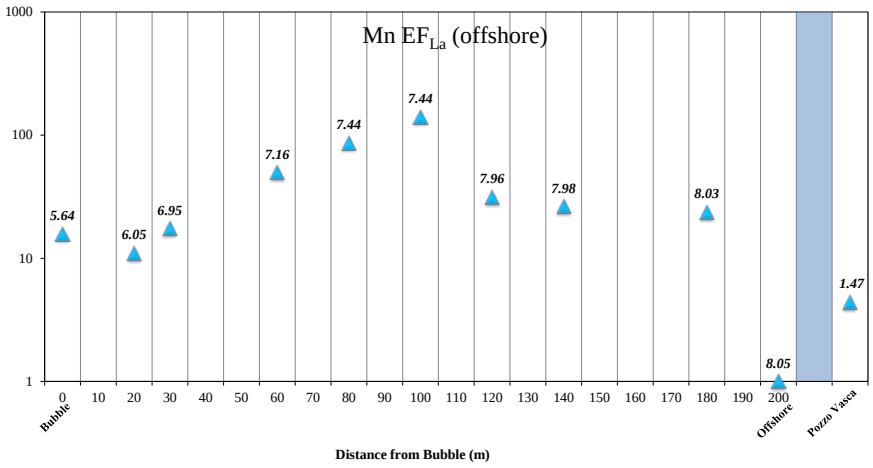

Fig. 71 - Mn-EF$_{La}$ variation along the Bay.

As suggest from literature (White, 2003) in oxidizing conditions Mn tends to form oxides which are removed in carbonates and Fe precipitation.

Figure 72 shows that dissolved Mn concentrations in seawater remain almost constant along the pH gradient, until pH 7.5 where SI of aragonite becomes positive, and from there it start to decrease probably because of carbonates precipitation. This fact could be confirmed by the distribution of Mn concentration in sediments (Vizzini et al., 2013) showed in figure 17. The map highlight that Mn values in the sediments are higher where seawater pH is in the range of 7-8, probably because of carbonate precipitations, and lower in sediments where the seawater pH is lower than 7.

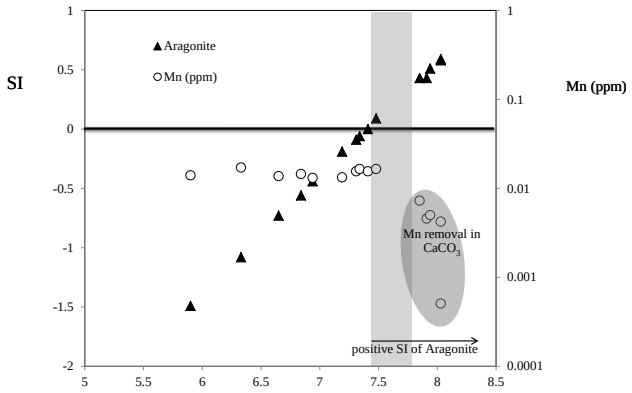

Fig. 72 – Dissolved manganese concentration and SI of Aragonite along pH gradient.

In figure 73 is shown the Mn concentration in exposed mussels. Despite manganese is very enriched in Vulcano's seawater, there was no accumulation for this element with respect to not exposed mussel.

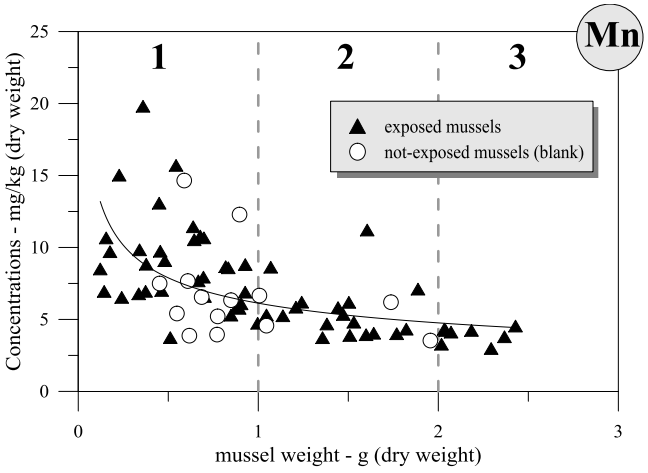

Fig. 73 – Manganese concentration in exposed and not exposed soft body mussel.

This could be explained with the carbonates removal, involving a physiological influence in this process. Particulate and dissolved carbonates are used by calcified constructor in order to build their shells. Since is not possible to appreciate the Mn accumulation in soft body, is probably due to the fact that it was mainly used by the animal to build its shell.

Copper.

Cu is a medium enriched element in the seawater of the Bay, comparison between Cu-EF_{La}(offshore) and Cu-EF_{La}(White) highlight that Vulcano's seawater are more enriched respect offshore background level (Fig. 53). Comparison with Pozzo Vasca EF highlight that this metal is not derived from the hydrothermal end member (Fig. 74).

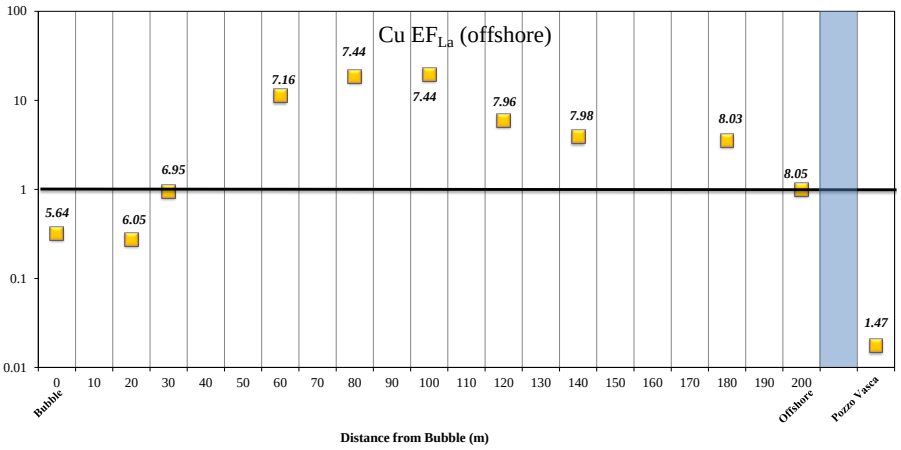

Fig. 74 – Cu-EF_{La} variation along the Bay.

The enrichment is probably due to the mobilization of this element which is influenced by the complex chemical physical parameters of the Bay.

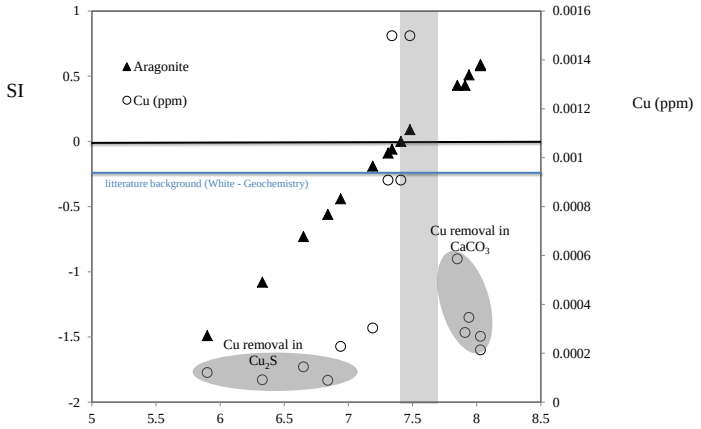

Fig. 75 – Dissolved copper concentration and SI of Aragonite along pH gradient. Literature Cu background is in ppm.

Along the pH gradient concentration of dissolved Cu undergoes large variations (Fig.75). In the most acidic and reducing area of the bay the low concentrations of Cu are probably due to sulphides precipitation, such also suggested by White. As highlighted by Kadar et

al. (2012), the sediments closest to the vent (pH 6-6.5) are enriched in Cu, confirming this hypothesis. Going towards higher pH values, after a strong increase of dissolved Cu at about pH 7.5, a new decrease, probably due to the removal in carbonate, can be observed. Vizzini et al., 2013 showed a map (Fig. 17) of copper concentration in sediment where the maximum values coincides with pH 8 (in figure 75), this confirm the hypothesis of Cu removal by precipitation of carbonates.

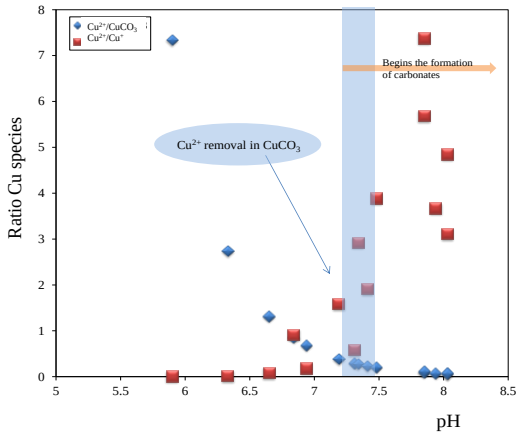

Fig. 76 - Calculated ratios copper species concentration along pH gradient.

Data on copper speciation (Fig. 76) confirm that for pH > 7.5 the $Cu^{2+}/CuCO_3$ ratio decrease. This fact could be explain with the removal of Cu^{2+} in carbonate.

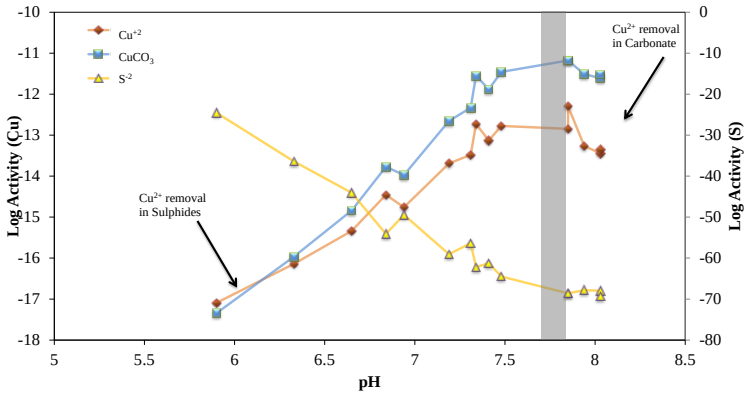

Fig. 77 - Calculated copper species and sulphur Log Activities along pH gradient.

Graph in figure 77 show the negative correlation between Cu species and S^{2-}, confirming what previously said.

Since the Cu fate is linked to carbonates, as it was for Mn, in mussels there shouldn't be accumulation for this element. The concentration of Cu in soft body mussels in shown in

figure 78; there isn't difference between exposed and not exposed mussels, despite the fact that copper is enriched in the seawater column. Once again a physiological reason can make clear this issue. As for the case of Mn as in this case, copper may be more accumulated in the shells because of carbonates construction than in soft body, for this reason probably mussel showed no copper accumulation, in soft tissue. Besides, as highlighter by White copper is considered a refractory elements and thus tend to be more accumulated in hard tissues than soft one.

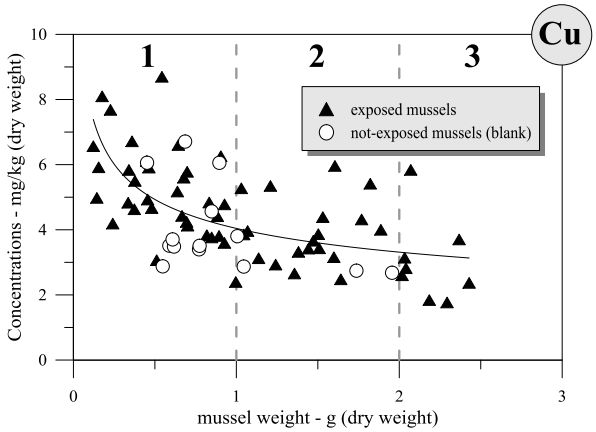

Fig. 78 - Copper concentration in exposed and not exposed soft body mussel.

In order to understand if Mn and Cu are linked we make a comparison between both in mussel soft body (Fig. 79).

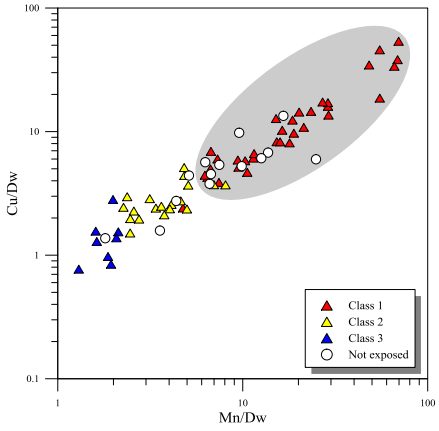

Fig. 79 - Cu and Mn ratio normalized in Dw, highlight a good correlation (R=0.75; p<0.001).

Graph 79 confirms that the elements are well correlated and that there isn't an appreciable difference compared with not exposed individuals.

Nickel.

Ni-EF_{La}(offshore) values are higher than Ni-EF_{La}(White) indicating that the Vulcano's seawaters are more enriched in Ni than the seawater literature background (Fig. 53). Since Ni-EF_{La}(Pozzo Vasca) shows higher values than others, it could be possible affirm that the hydrothermal reservoir is the main source for this metal (Fig. 80).

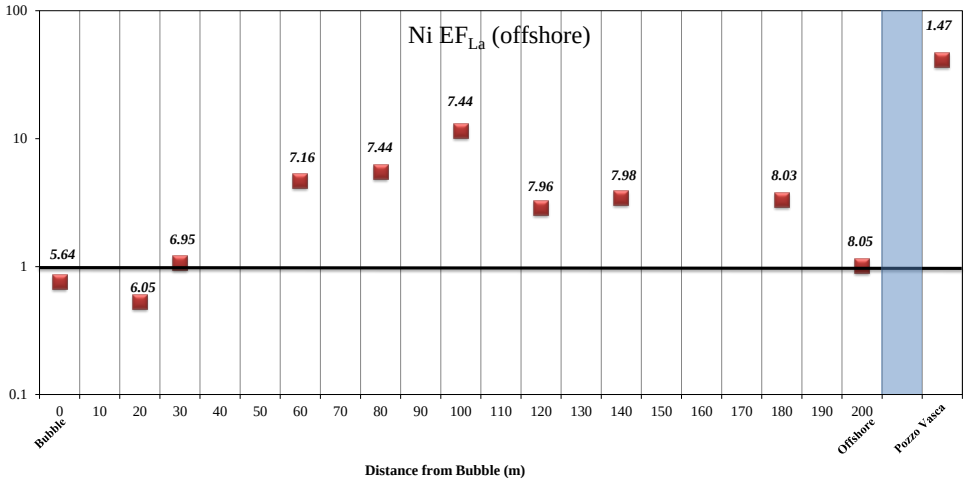

Fig. 80 – Ni-EF_{La} variation along the Bay.

As show in figure 80, along the bay seawater samples are enriched in Ni, except within the first 20 meters from vent. In the latter area, as for Cu, the sink could be sulphides in the acidic condition and reduced Eh (White – Geochemistry).

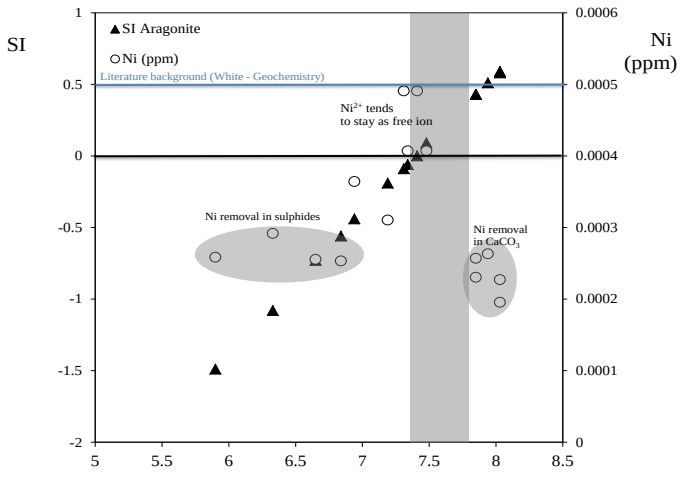

Fig. 81 – Dissolved nickel concentration and SI of Aragonite along pH gradient. Literature Ni background is in ppm.

Dissolved Ni concentration vs. pH data, shows a trend along the pH gradient very similar to that of Cu. On the most acidic part of the bay (close to the bubble, pH 5.6) dissolved

Ni concentration is low probably because of a removal in sulphides, in fact, Millero et al., 2009 suggests that for low values of pH, Ni tend to stay in form Ni^{2+} which tends to bind with sulphide complexes. This mechanism can be confirmed by data on Ni concentrations in sediments (Vizzini et al., 2013) which show the highest concentration in the area closest to the vent. In oxic-environments, nickel tends to form $NiCO_3$ (Calvert and Pedersen, 1993; Algeo and Maynard, 2004). As for Cu along the pH gradient, Ni concentrations increase until pH 7.35, then decrease again probably because of removal by carbonates. Speciation model seems to confirm the hypothesis because the decreasing of Ni starts at the same pH where aragonite SI becomes positive (figure 81).

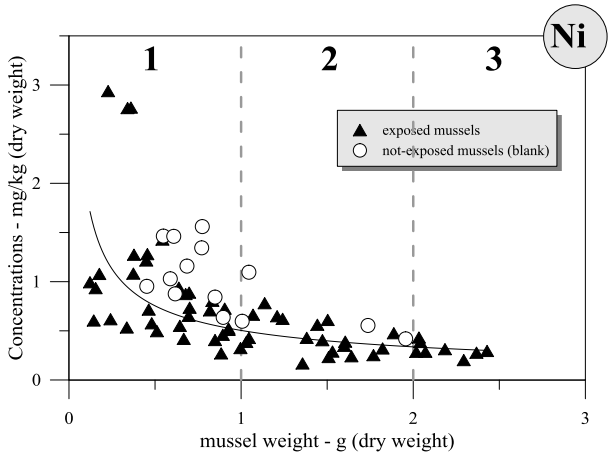

Fig. 82 – Nickel concentration in exposed and not exposed soft body mussel.

If Ni fate (for 7.5 pH) is linked to the carbonate fate, as for Cu and Mn also Ni shouldn't accumulate in mussels' soft body (Fig. 82). Effectively, nickel concentrations in the soft body of exposed and non-exposed mussels overlaps perfectly.

Aluminum.

Al-EF_{La}(Pozzo Vasca) is the higher among the others EF (Fig. 53), suggesting that the main source of Al is the hydrothermal reservoir, in fact, it is known that aluminum is deriving from rocks leaching and plagioclase weathering reactions (White – Geochemistry).

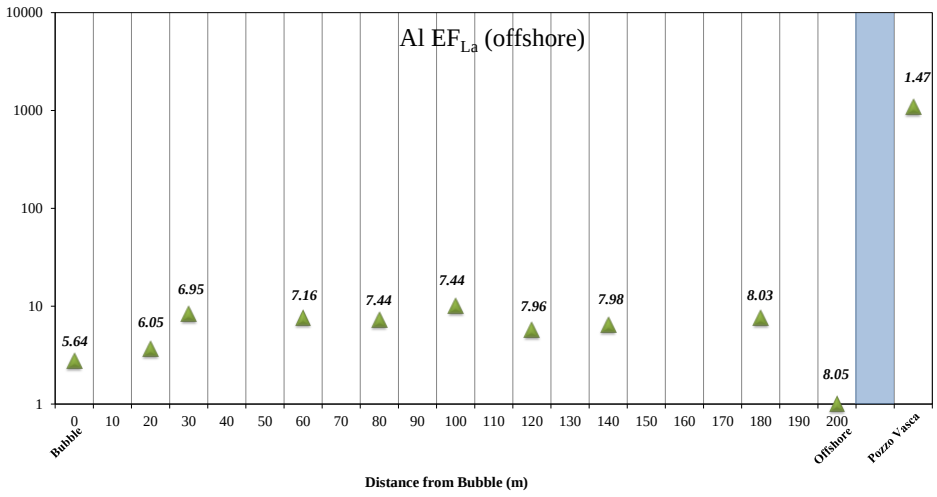

Fig. 83 - Al-EF$_{La}$ variation along the Bay.

As shown in figure 83, along the bay all samples are enriched in aluminum with respect to the off shore sample, Pozzo Vasca is the most enriched, as previously said.

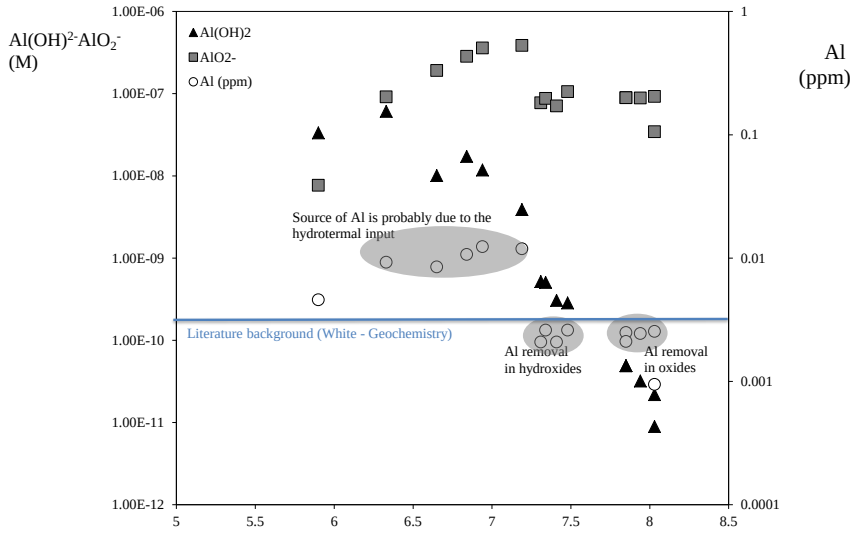

Fig. 84 - Dissolved aluminium concentration and calculated Al-oxi-hydroxides concentration along pH gradient (literature Al background is in ppm).

Analyzing the trend of dissolved aluminum concentration along the pH gradient (Fig. 84), there is the evidences that in general the Bay's seawater have an higher Al concentration respect to the natural background. The concentration tend to decrease when pH exceeds 7 probably because of the removal through oxides and hydroxides.

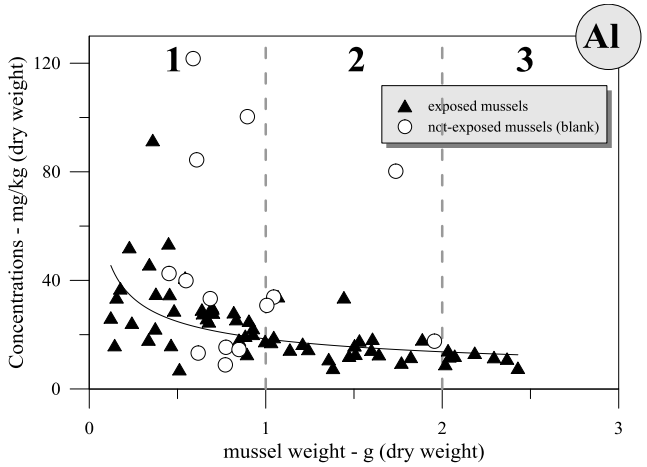

Fig. 85 – Aluminium concentration in exposed and not exposed soft body mussel.

Exposed mussels hadn't show a clear accumulation in Al with respect to not-exposed (Fig. 85). Besides, sometimes not-exposed mussel have more Al than exposed one.

Zinc.

Vulcano's seawater are more enriched in Zn than literature background seawater and off shore seawater too (Fig. 53), the fact that Zn-EF_{La}(Pozzo Vasca) is higher than the other makes clear that the main zinc source are hydrothermal fluids (Fig. 86).

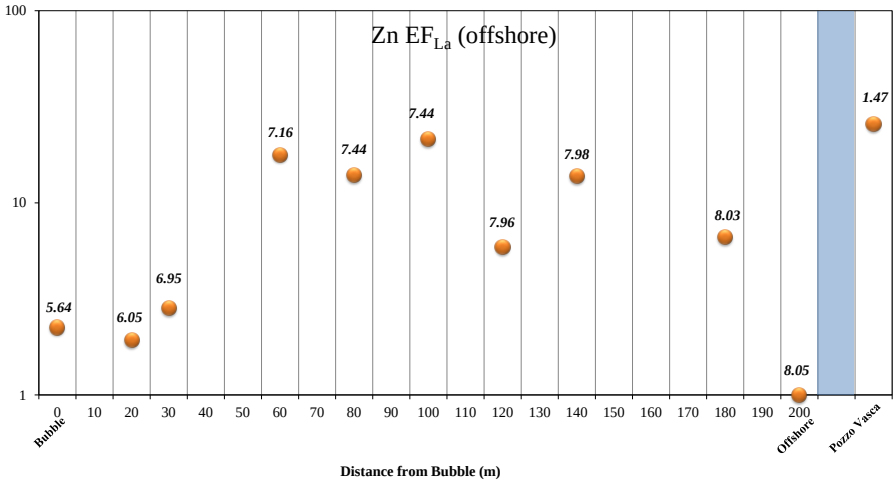

Fig. 86 – Zn-EF_{La} variation along the Bay.

Dissolved concentrations of zinc are higher than seawater literature background along the whole pH gradient. A decrease in concentration start from 7-8 pH and this is due to the removal in hydroxides (Fig. 87).

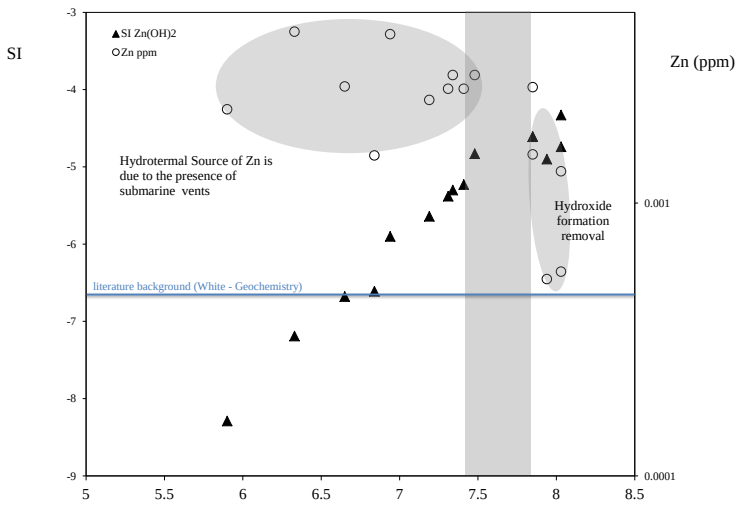

Fig. 87 – Dissolved zinc concentration and SI of Zn-hydroxide along pH gradient. Literature Zn background is in ppm.

The mechanism of zinc removal by precipitation seems to be proven by the higher concentration in sediments (Vizzini et al., 2013) around the 7.5 pH area (Fig 17). The fact that hydroxide are the possible way to remove the dissolved zinc is evidenced by the speciation of zinc (figure 88).

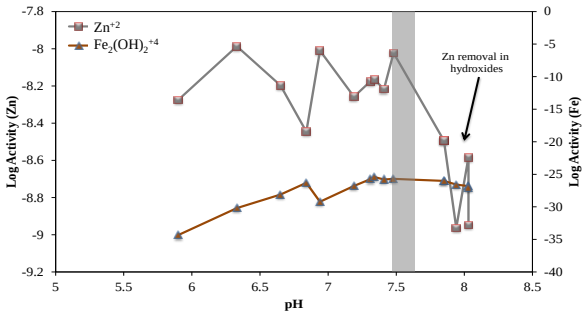

Fig. 88 – Hydroxide iron and zinc calculated Log Activities along pH gradient.

In graph 88, there is a negative trends between the Zn^{2+} and Fe-hydroxides Log Activities, the zinc decreasing start from about pH 7.5.

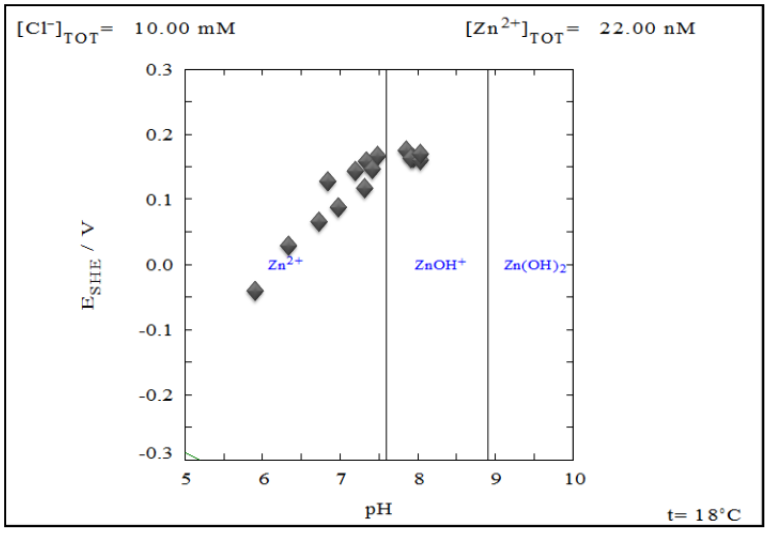

Fig. 89 - Eh/pH diagrams shows that stability fields for zinc is for almost all samples in the Zn^{2+} field, except that for the most high pH samples, where formation of hydroxide is possible.

Eh-pH diagram (figure 89) confirms that for these pH values Zn tend to stay more stable in hydroxides form.

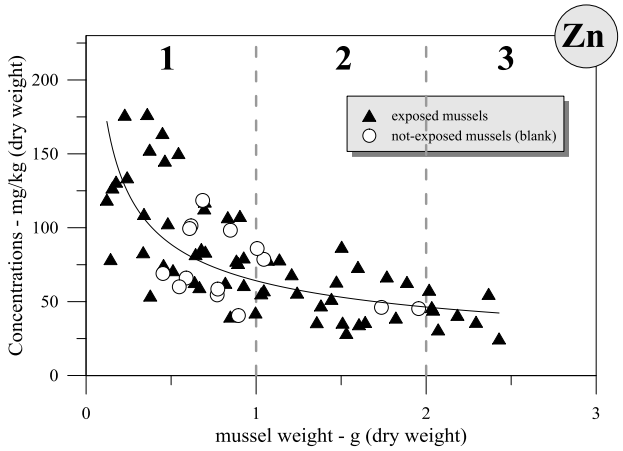

Fig. 90 - Zinc concentration in exposed and not exposed soft body mussel.

In figure 90 is show the zinc concentration in soft body mussel. Except for class C1, in general exposed mussel do not show an accumulation with respect to the not exposed. As suggest by White, since Zn is considered a refractory element, it tends to be more accumulated in hard tissue than in soft.

Chapter 6 - Conclusions.

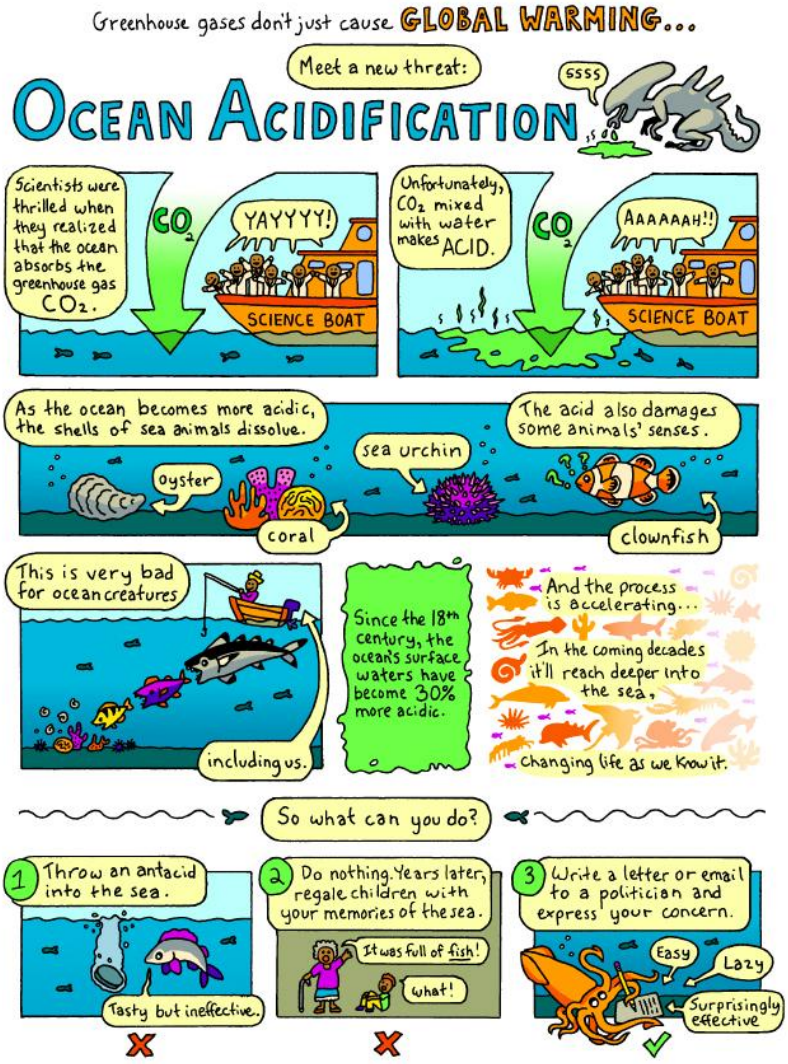

Data presented in this thesis highlight that even very large CO_2 seabed leakage has a relatively localized geochemical effect. Baia di Levante can be useful in predicting what physiological mechanisms could be affected when ocean chemistry alters due to ocean acidification, although, results must be interpreted with caution to avoid the confounding influence of other factors such as redox conditions, hydrothermal input of elevated metals levels such as Fe, Cu and Al, and widely toxic compounds such as H_2S. In the northern part of the bay, where the influence of hydrothermal fluids is less intense, pH values that mimic those predicted for the coming decades can be observed. The area close to the main vents is subjected to strong redox reactions, due to the input of reduced hydrothermal species (e.g. Fe^{2+} and H_2S) that dissolve and react in the oxidising sea-water. The area affected by these extreme conditions varies depending on wind driven water circulation within the bay. The northern part of the bay seems to be the most useful as a natural laboratory to perform ecological studies of the effects of increased CO_2 levels where the main ecosystem processes such as production, competition and predation can be observed. In

this part of the bay the saturation states of calcite and aragonite decrease gradually as CO_2 levels rise, and this is suitable for studies regarding the effects of carbon capture by seawater surface and on the chronic effects of OA.

The metals contents of Baia di Levante are mainly the result of a mixing of two end-members, Vulcano's seawater and the hydrothermal reservoir. Although the metal concentration in seawater is not simply the results of this fluid mixing, because chemical equilibrium between the two fluids is not instantly reached at the moment of the mixing. Changing environmental conditions, mainly pH and Eh, tends to shift equilibrium towards the stability fields of a series of phases forming solid or colloidal particles which finally settle on the sediments of the Bay representing the main sink for many metals.

Data on metal speciation, that we have calculated with the help of PHREEQC, explain relatively well the variation of metal concentrations in the water column along the bay and seems to confirm literature data on each metals in sediments.

Since sediments are the principal sink for these metals, the fact that higher concentrations in sediments coincide with less concentrations in seawater column, confirm the hypothesis that pH and Eh dependent speciation drive the metal flux between sediment and seawater column. For instance, the distribution map of dissolved iron in seawater obtained with our data is complementary to the same map in sediments (Vizzini et al., 2013 - Fig. 91).

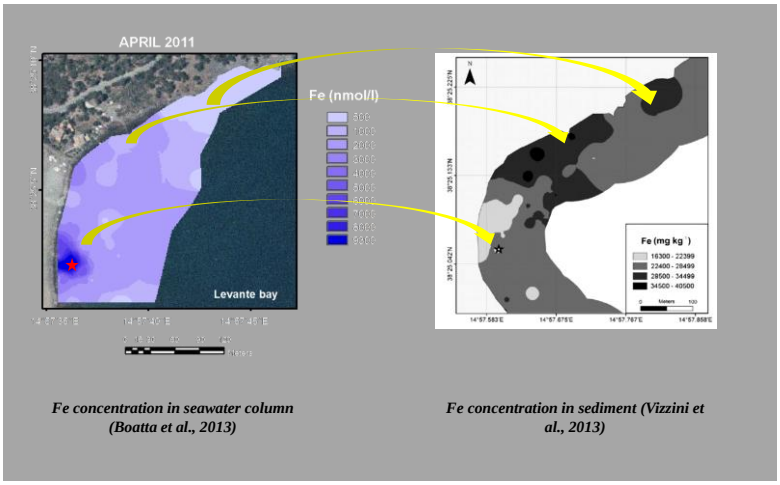

Fig. 91 - Comparison between iron distribution in seawater and sediments.

However, metal speciation is not only influenced by chemical-physical parameters (temperature, pH, Eh, salinity etc.) but also by the interaction between biota and its environment. Especially for carbonates species biota could represent an important sink, so the elements which mostly are linked to carbonates, such as Mn, Cu and Ni are in their speciation influenced too.

Since sediments are the principal sink for these metals, the fact that higher concentrations in sediments coincide with less concentrations in seawater column, confirm the hypothesis that pH and Eh dependent speciation drive the metal flux between sediment and seawater column. In the northern part of the bay chemical processes are mainly driven by smooth pH gradients and oxidizing conditions with 12 weak hydrothermal impact. Thus the northern part of the bay is more suitable for "*in situ OA experiments*" displaying pH conditions that could be reached within the end of the century.

According to literature data, mussels are good heavy metals bio-accumulator. Despite the fact that we had exposed mussels for only one month many elements showed strong accumulation with respect to those not exposed. The geochemical study of metal speciation in the seawater of the area where mussels have been transplanted is essential to obtain a correct data interpretation on the accumulation processes. To complete the picture it would be also important to investigate the heavy metal accumulation also in other animal's parts such as shells, for instance, to test if metals such as Cu follows the carbonates fate or if in general the refractory elements are more accumulated in hard tissue than soft one. It is fundamental to understand what sort of species to use in an in situ experiment before to start it. For the OA impact studies it is very useful the use of mussels, since they are a consumed species which can resist to the acidification and is considered a very good accumulator of metals.

Since mussels will be consumed by humans, also in an future acidic seawater scenario, they should be a risk to human health if we don't consider the possibility that OA could influence the concentration of pollutants in future food nets web, incrementing biomagnification of pollutants such as metals. This could be an indirect impact of the expected anthropogenic CO_2 atmospheric increase.

To sum up, this study confirms that an hydrothermal vent mixing zones inhabited by invertebrates is enriched in various trace metals, and supports the hypothesis that mixing-zone chemistry are not an exclusive result of fluid dilution in seawater but also it is the result of a combined chemical reactions, and the organism–habitat interactions accomplished under the extreme conditions typical to vent environments. Consequently, it opens up a number of questions that needs to be further addressed and complemented by chemical modeling of metal species.

1) It could be important estimate the not dissolved fraction for each metals.
2) With a longer exposure time, bioaccumulators such as mussels, can give us more information about the accumulation after an adaptation period, so it could be useful to

understand if in acidic condition bioaccumulator can accumulate faster than in normal pH condition.

In addition, the need for more samples in terms of replication for habitat type within one given vent site, and improved sampling and/or analytical techniques in order to discern a clearer pattern of distribution of metallic elements with particular emphasis on organism-habitat interaction is recommended.

Advantages and disadvantages of "in situ perturbation" experiments.

Thanks to this experiment we can highlight vantages and disadvantages of such techniques of scientific investigation.

Advantages	***Disadvantages***
Understanding of effectives relationships between species and community – ecosystem; this permit to make more realistic forecasting models on bioaccumulation mechanisms and dynamics. It is more environmentally relevant than bab-based studies.	It is harder to model the natural system because we have to evaluate a lot of natural variability and in case of bioaccumulation, there are many factors which influence it that are not possible to estimate.
Cheaper and easy to make. There are a lot of information available from the literature about mussels, so is possible to prevent a lot of problems during the realization of the experiment and results may be compared with the relevant literature.	Is fundamental to consider in advance all possible factors which can influence the experiment. Up to now some aspect have not been cleared by previous studies.
OA is tightly linked with metals speciation, and such link couldn't be exhaustively observed in laboratory because it is impossible to reproduce all natural conditions.	It is impossible to control disturbing factor such as stream, variation of temperature, winds etc., which some time not only influence results but also make more hard sampling and influence the health of transplanted mussels.

Finally, last consideration is that complementary approaches are needed in order to understand a natural process such as OA, so micro-mesocosms and in situ perturbation experiment should be used in parallel, because they provide us different information and points of view which are all fundamental in order to make an exhaustive model of the ecosystem dynamics. Choosing an approach or another depend from economic and time resources and more over the answer we are looking for. What really is important, is to provide models and answers to the policy makers in order to take the necessary measures that make us able to promise a worthy future for the next generations.

References.

Aiuppa, A., Allard, P., D'Alessandro, W., Michel, A., Parello., F., Treuil, M., Valenza, M., 2000. Mobility and fluxes of major, minor and trace metals during basalt weathering and groundwater transport as Mt.Etna volcano (Sicily). Geochimica et cosmochimica acta, vol 64, nr 11. GPII S0016-7037(00)00345-8.

Aiuppa, A., Dongarrà, G., Capasso, G., Allard, P., 2000. Trace elements in the thermal groundwaters of Vulcano Island (Sicily). J. Volcanol. Geoth. Res. 98, 189–207.

Amend, J.P., Rogers, K.L., Shock, E.L., Inguaggiato, S., Gurrieri, S., 2003. Energetics of hemolithoautotrophy in the hydrothermal system of Vulcano Island, southern Italy. Geobiology 1, 37–58.

Arnold, T., Mealey, C., Leahey, H., Miller, A.W., Hall-Spencer, J.M., Milazzo, M., Maers, K., 2012. Ocean acidification and the loss of protective phenolics in seagrasses. PLoS One 7 (4), e35107.

Barberi, F., Innocenti, F., Ferrara, G., Keller, J., Villari, L., 1974. Evolution of the Aeolian arc volcanism (Southern Tyrrhenian sea). Earth Planet Sci. Lett. 21, 269–276.

Beccaluva, L., Gabbianelli, G., Lucchini, R., Rossi, P.L., Savelli, C., 1985. Petrology and K/Ar ages of volcanic dredged from the Aeolian seamounts: implications for geodynamic evolution of the southern Tyrrhenian basin. Earth Planet Sci. Lett. 74, 187–208.

Brand, L. E., Sunda, W.G., Guillard, R.L., 1983. Limitation of marine phytoplankton reproductive rates by zinc, manganese, and iron. Limnol. Oceanogr., 28(6), 1983, 1182-1198.

Burger, J., Gochfeld, M., 2006. Locational differences in heavy metals and metalloids in Pacific Blue mussels Mytilus (edulis) trossulus from Adak Island in the Aleutian Chain, Alaska. Doi: 10.1016/j.scitotevn.2006.04.022.

Caldeira, K., Wickett, M.E., 2003. Anthropogenic carbon and ocean pH. Nature 425, 365.

Capaccioni, B., Tassi, F., Vaselli, O., 2001. Organic and inorganic geochemistry of low temperature gas discharges at the Baia di Levante beach, Vulcano Island, Italy. J. Volcanol. Geoth. Res. 108, 173–185.

Capelli, R., Contardi, V., Fassone, B., Zanicchi, G., 1978. Heavy metals in mussels (Mytilus galloprovincialis) from the gulf of La Spezia and from the Promontory of Portofino, Italy. Marine Chemistry, 6(1978) 179-185.

Carapezza, M.L., Barberi, F., Ranaldi, M., Ricci, T., Tarchini, L., Barrancos, J., Fisher, C., Perez, N., Weber, K., Di Piazza, A., Gattuso, A., 2011. Diffuse CO2 soil degassing and CO2 and H2S concentrations in air and related hazards at Vulcano Island (Aeolian arc, Italy). J. Volcanol. Geoth. Res. 204, 130–144.

Chinellato A., Munari M., Matozzo V., Bressan M., Marin M.G., 2010. (University of Padova, Italy) First attempts in evaluating acidification effects on physiological responses in Mytilus galloprovincialis. Abstracts / Comparative Biochemistry and Physiology, Part A 157 (2010) S15–S21. doi:10.1016/j.cbpa.2010.06.051.

Chiodini, G., Cioni, R., Marini, L., 1993. Reactions governing the chemistry of crater fumaroles from Vulcano Island, Italy, and implications for volcanic surveillance. Appl. Geochem. 8, 357–371.

Chiodini, G., Cioni, R., Marini, L., Panichi, C., 1995. Origin of the fumarolic fluids of Vulcano Island, Italy and implications for volcanic surveillance. Progr. Oceanogr. 57, 99–110.

Dando, P.R., Stüben, D., Varnavas, S.P., 1999. Hydrothermalism in the Mediterranean Sea. Progr. Oceanogr. 44, 333–367.

Doe, 1994. Handbook of methods for the analysis of the various parameters of the carbon dioxide system in sea water. Version 2. ORNL/CDIAC-74. In: Dickson, A.G., Goyet, C. (Eds.), Carbon Dioxide Information Analysis Center. Oak Ridge National Laboratory, US Department of Energy, Oak Ridge, Tennessee.

Doney, S.C., Tilbrook, B., Roy, S., Metzl, N., LeQue, C., Hood, M., Feely, R. A., Bakker, D., 2009. Surface-ocean CO_2 variability and vulnerability. Deep-Sea Research II 56 (2009) 504–511. doi:10.1016/j.dsr2.2008.12.016

Drever, J.I., 1997. The Geochemistry of Natural Waters: Surface and Groundwater Environments, third ed. Prentice Hall, Upper Saddle River, N.J.

Espa, S., Caramanna, G., Bouche, V., 2010. Field study and laboratory experiments of bubble plumes in shallow seas as analogues of sub-seabed CO2 leakages. Appl. Geochem. 25, 696–704.

Fabricius, K.E., Langdon, C., Uthicke, S., Humphrey, S., Noonan, S., Dèath, G., Okazaki, R., Muehllehner, N., Glas, M.S., Lough, J.M., 2011. Losers and winners in coral reefs acclimatized to elevated carbon dioxide concentrations. Nature Clim. Change 1, 165–169.

Fraser, M., Surette, C., Vaillancourt, C., 2011. Spatial and temporal distribution of heavy metal concentrations in mussels (Mytilus edulis) from the Baie des Chaleurs, New Brunswick, Canada. Doi: 10.1016/j.marpolbul.2011.03.036.

Frazzetta, G., La Volpe, L., Sheridan, M.F., 1984. Evolution of the Fossa cone, Vulcano. J. Volcanol. Geoth. Res. 17, 139–360.

Gattuso, J. P., Lavigne, H., 2009. Technical Note: Aproaches and software tools to investigate the impact of ocean acidification. Biogeosciences, 6, 2121–2133, 2009.

Giaccone, G., 1969. Associazioni algali e fenomeni secondari di vulcanismo nelle acque marine di Vulcano (Mar Tirreno). Giorn. Bot. Ital. 103, 353–366.

Hall-Spencer, J.M., Rodolfo-Metalpa, R., Martin, S., Ransome, E., Fine, M., Turner, S.M., Rowley, S.J., Tedesco, D., Buia, M., 2008. Volcanic carbon dioxide vents show ecosystem effects of ocean acidification. Nature 454, 96–99.

Hofmann, G.E., Smith, J.E., Johnson, K.S., Send, U., Levin, L.A., Micheli, F., Paytan, A., Price, N.N., Peterson, B., Takeshita, Y., Matson, P.G., Crook, E.D., Kroeker, K.J., Gambi, M.C., Rivest, E.B., Frieder, C.A., Yu, P.C., Martz, T.R., 2011. High-frequency dynamics of ocean pH: a multi-ecosystem comparison. PLoS One 6 (12), e28983, Epub 2011 Dec 19.

ICRAM Programma di monitoraggio per il controllo dell'ambiente marino e costiero (triennio 2001-2003). Metodologie analitiche di riferimento. Lo studio Ed. SrL, Roma 2001 ICRAM.

Inguaggiato, S., Mazot, A., Diliberto, I.S., Inguaggiato, C., Madonia, P., Rouwet, D., Vita, F., 2012. Total CO2 output from Vulcano Island (Aeolian Islands, Italy). Geochem. Geophys. Geosyst. 13, Q02012. http://dx.doi.org/10.1029/2011GC003920.

Italiano, F., 2009. Hydrothermal fluids vented at shallow depths at the Aeolian islands: relationships with volcanic and geothermal systems. FOG – Freiberg Online Geology, 22, 55–60.

Italiano, F., Nuccio, P.M., Sommaruga, C., 1984. Gas/steam and thermal energy release measured at the gaseous emissions of the Baia di Levante of Vulcano Island, Italy. Acta Vulcanologica 5, 89–94.

Langdon, C., et al., 2006. Impacts of Ocean Acidification on Coral Reefs and Other Marine Calcifiers: A Guide for Future Research. A report from a workshop sponsored by the National Science Foundation, the National Oceanic and Atmospheric Administration, and the U.S. Geological Survey. Contribution No. 2897 from NOAA/Pacific Marine Environmental Laboratory.

Johnson, V.R., Brownlee, C., Rickaby, R.E.M., Graziano, M., Milazzo, M., Hall-Spencer, J.M., 2013. Responses of marine benthic microalgae to elevated CO2. Mar. Biol. http://dx.doi.org/10.1007/s00227-011-1840-2.

Joung, D., Shiller, A. M., 2013. Trace metal distribution in the water column near the deepwater horizon well blowout. Doi: 10.1021/es303167p/environ.sci.technol.

Kadar E, Salánki J, Jugdaohsingh R, McCrohan CR, White KN. 2001. Avoidance reactions 30 of the swan mussel Anodonta cygnaea to sub-lethal aluminium concentrations, Aquat Tox 31 55: 137-148.

Kadar E, Salánki J, Powell JJ, White KN, McCrohan CR 2002. Effect of aluminium on the 33 filtration activity of the freshwater mussel Anodonta cygnea L at neutral pH, Acta Biol Hun, 34 53/4, pp. 485-493.

Kadar, E., Costa, V., Martins, I., Santos, R. S., Powell, J. J., 2005. Enrichment in trace metals (Al, Mn, Co, Cu, Mo, Cd, Fe, Zn, Pb and Hg) of macroinvertebrate habitats at hydrothermal vents along the Mid-Atlantic Ridge. Doi: 10.1007/s10750-005-4758-1.

Kadar E, Santos RS, Powell JJ. 2006a. Biological factors influencing tissue 4 compartmentalization of trace metals in the deep-sea hydrothermal vent bivalve 5 Bathymodiolus azoricus at geochemically distinct vent sites of the Mid-Atlantic Ridge. Env 6 Res 101: 221-229 7

Kadar E & Costa V. 2006b. First report on the micro-essential metal concentrations in 8 bivalve shells from deep-sea hydrothermal vents. J Sea Res 56: 37-44.

Kadar, E., Fisher, A., Stolpe, B., Harrison, R.M., Parello, F., Lead, J., 2012. Metallic nanoparticle enrichment at low temperature, shallow CO2 seeps in Southern Italy. Mar. Chem. 140–141, 24–32.

Kay, R. T., Groschen, G. E., Cygan, G., Dupré, D. H., 2011. Diel cycles in dissolvedbarium, lead, iron, vanadium, and nitrite in a stream draining a former zinc smelter site near Hegeler, Illinois. Doi: 10.1016/j.chemgeo.2010.10.009.

Keller, J., 1980. The Island of Vulcano. In: Villari, L. (Ed.), The Aeolian Islands, an Active Volcanic Arc in the Mediterranean Sea. Società Italiana di Mineralogia e Petrologia, Milano, pp. 29–74.

Kerrison, P., Hall-Spencer, J.M., Suggett, D.J., Hepburn, L.J., Steinke, M., 2011. Assessment of pH variability at a coastal CO2 vent for ocean acidification studies. Estuar. Coast Shelf S. 94, 129–137.

Kim, C.Y., Bedzyk, M.J., 2006. Study of growth and oxidation of vanadium films on α-Fe2O3 (0001). Science Direct. Doi: 10.1016/j.tsf.2006.04.015.

Licata, P., Trombetta, D., Cristani, M., Martino, D., Naccari, F., 2004. Organochlorine compounds and heavy metals in the soft tissue of the mussel Mytilus galloprovincialis collected from Lake Faro (Sicily, Italy). Doi: 10.1016/j.envint.2004.01.007.

Lidbury, I., Johnson, V., Hall-Spencer, J.M., Munn, C.B., Cunliffe, M., 2012. Community-level response of coastal microbial biofilms to ocean acidification in a natural carbon dioxide vent ecosystem. Mar. Poll. Bull. 64, 1063–1066.

Liotta, M., Martelli, M., 2012. Dissolved gases in brackish thermal waters: an improved analytical method. Geofluids 12, 236–244. http://dx.doi.org/10.1111/j.1468-8123.2012.00365.x.

Middelboe, A.L., Hansen, P.J., 2007. Direct effects of pH and inorganic carbon on macroalgal photosynthesis and growth. Mar. Biol. Res. 3, 134–144.

Mikaloff-Fletcher, S.E., Gruber, N., Jacobson, A.R., Doney, S.C., Dutkiewicz, S., Gerber, M., Follows, M., Joos, F., Lindsay, K., Menemenlis, D., Mouchet, A., Mueller, S.A.,

Sarmiento, J.L., 2006. Inverse estimates of anthropogenic CO2 uptake, transport, and storage by the ocean. Global Biogeochem. Cy. 20, GB2002.

Millero, F.J., Ditrolio, B., 2010. Use of thermodynamics in examining the effects of ocean acidification. Doi: 10.2113/gselements.6.5.299.

Millero, F.J., Schreiber, D.R., 1982. Use of the ion-pairing model to estimate activitycoefficients of the ionic components of natural-waters. Am. J. Sci. 282, 1508–1540.

Millero, F.J., Woosley, R., Ditrolio, B., Waters, J., 2009. Effect of Ocean Acidification on the Speciation of metals in Seawater. Oceanography Vol. 22, No.4.

Montegrossi, G., Tassi, F., Vaselli, O., Bidini, E., Minissale, A., 2006. A new, rapid and realiable method for determination of reduced sulphur (S2-) species in natural water discharges. Doi: 10.1016/j.apgeochem.2006.02.007.

Morley, N. H., Burton, J. D., Tankere, S. P. C., Martin, J. M., 1996. Distribution and behavior of some dissolved trace metals in the western Mediterranean Sea. Deep Sea research II vol 44. PII: s0967-0645(96)00098-7.

Olivieri, Y., 2011. Determinazione e studio delle terre rare presenti nelle acque idrotermali di Vulcano. MSc thesis in Chemistry – University of Palermo.

Pellerin J., Amiard, J. C., Comparison of bioaccumulation of metals and introduction of metallothioneins in two marine bivalves (Mytilus edulis and Mya arenaria). Doi: 10.1016/j.cbpc.2009.04.008.

Pierrot, D., Lewis, E., Wallace, D.W.R., 2006. MS Excel Program Developed for CO2 System Calculations. ORNL/CDIAC-105a. Carbon Dioxide Information Analysis Center, Oak Ridge National Laboratory, US Department of Energy, Oak Ridge, Tennessee.

Resgalla, C., Brasil, E.S., Laitano, K.S. , Reis Filho R.W., 2007. Physioecology of the mussel Perna perna (Mytilidae)in Southern Brazil. doi:10.1016/j.aquaculture.2007.05.019

Riebesell, U., Schulz, K.G., Bellerby, R.G.J., Botros, M., Fritsche, P., Meyerhöfer, M., Neill, C., Nondal, G., Oschlies, A., Wohlers, J., Zöllner, E., 2007. Enhanced biological carbon consumption in a high CO2 ocean. Nature 450, 545–548.

Riebessel, U., Fabry, V. J., Hansson, L., Gattuso, J. P., 2010. Guide to the best pratices for ocean acidification research and data reporting. EUR24328.

Rindi, F., Maltagliati, F., Rossi, F., Acunto, S., Cinelli, F., 1999. Algal flora associated with a Halophila stipulacela (Forsskål) Ascherson (Hydrocharitaceae, Helobiae) stand in the western Mediterranean. Oceanologica Acta 22, 421–429.

Roberts, D.A., Birchenough, S.N.R., Lewis, C., Sanders, M.B., Bolam, T., Sheahan, D., 2013. Ocean acidification increases the toxicity of contaminated sediments. Glob. Change Biol.. http://dx.doi.org/10.1111/gcb.12048.

Rodolfo-Metalpa, R., Houlbreque, F., Tambutte, E., Boisson, F., Baggini, C., Patti, F. P., Jeffree, R., Fine, M., Foggo, A., Gattuso, J-P., Hall-Spencer, J. M., 2011. Coral and mollusc resistance to ocean acidification adversely afected by warming. Doi: 10.1038/Nclimate1200.

Rogers, K.L., Amend, J.P., Gurrieri, S., 2007. Temporal changes in fluid chemistry and energy profiles in the Vulcano Island hydrothermal system. Astrobiology 7, 905–932. http://dx.doi.org/10.1089/ast.2007.0128.

Roy, R.N., Roy, L.N., Vogel, K.M., Porter-Moore, C., Pearson, T., Good, C.E., Millero, F.J., Campbell, D.M., 1993. The dissociation constants of carbonic acid in seawater at salinities 5–45 and temperatures 0–45 C. Mar. Chem. 44, 249–267.

Saavedra, Y., Gonzales, A., Fernandez, P., Blanco, J., 2004. The effect of size on trace metal levels in raft cultivated mussels (Mytilus galloprovincialis). Doi: 10.1016/S0048-9697(03)004029.

Sabine, C.L., Feely, R.A., Gruber, N., Key, R.M., Lee, K., Bullister, J.L., Wanninkhof, R., Wong, C.S., Wallace, D.W.R., Tilbrook, B., Millero, F.J., Peng, T., Kozyr, A., Ono, T., Rios, A.F., 2004. The oceanic sink for anthropogenic CO_2. Science 305, 367–371.

Schaller, T., Moor, C. H., Wehrli, B., 1997. Recostructing the iron cycle from the horizontal distribution of metals in the sediment of Baldeggersee. Aquat.sci.59 (1997) 326-344.

Sedwick, S., Stüben, D., 1996. Chemistry of shallow submarine warm springs in an arc-volcanic setting: Vulcano Island, Aeolian Archipelago, Italy. Mar. Chem. 53, 147–161.

Sezefer, P., Frelek, K., Szefer, K., Lee, C.B., Kim, B.S., Warzocha, J., Zdrojewska, I., Ciesielski, T., 2002. Distribution and relationships of trace metals in soft tissue, byssus and shells of marine Mytilus edulis trossulus from southern Baltic. PII: S0269-7991(02)00111-2.

Shi, D., Xu, Y., Hopkinson, B. M., Morel, F. M. M., 2010. Effect of ocean acidification on iron availability to marine phytoplankton. Doi: 10.1126/science.1183517.

Sicardi, L., 1940. Il recente ciclo dell'attività fumarolica dell'isola di Vulcano. Boll. Volcanol. 7, 85–139.

Silvestri, O., Mercalli, G., 1891. Modo di presentarsi e cronologia delle esplosioni eruttive di Vulcano cominciate il 3–8-1888. Ann. R. Uff. Cent. Meteor. Geodin. 4, 120–190.

Solomon, S., Qin, D., Manning, M., Chen, Z., Marquis, M., Averyt, K.B., Averyt, Tignor, M., Miller, H.L., 2007. Contribution of Working Group I to the Fourth Assessment Report of the Intergovernmental Panel on Climate Change. Cambridge, U.K., New York, USA.

Sommaruga, C., 1984. Le ricerche geotermiche svolte a Vulcano negli anni '50. Rendiconti della Soc. It. Mineral. Petrol. 39, 355–366.

Soto, M., Kortabitarte, M., Marigomez, I., 1995. Bioavailable heavy metals in estuarine water sas assessed by metal/shell-weight indices in sentinel mussels Mytilus galloprovincialis. Marine Ecology vol. 125:127-136, 1995.

Stipp, S.L.S., Hansen, M., Kristensen, R., Hochella, M.F., Bennedsen, L., Dideriksen, K., Balic-Zunic, T., Leonard, D., Matheieu, H. J., 2002. Behaviour of Fe-oxides relevant to contaminant uptake in the environment. Chemical Geology 190 (2002) 321-337. PII: S0009-2541(02)00123-7.

Szefera, P., Freleka, K. , Szeferb, K. , Leec, Ch.-B. , Kimc, B.-S. , Warzochad, J., Zdrojewskaa, I., Ciesielskia, T., 2002. Distribution and relationships of trace metals in soft tissue, byssus and shells of Mytilus edulis trossulus from the southern Baltic. Environmental Pollution 120 (2002) 423–444. PII: S0269-7491(02)00111-2.

Teshima, N., Aykawa, K., Kawashima, T., 1996. Simultaneous flow injection determination of iron (III) and vanadium (V) and of iron (III) and chromium (VI) based on redox reactions. Talanta 43(2006) 1755-1760. PII: S0039-9140(96)01966-2.

Tsangaris, C., Kaberi, H., Catsiki, V. A., 2013. Metal levels in sediments and transplanted mussels in Pagassitikos Gulf (AegeanSea, Easten Mediterranean). Doi: 10.1007/s10661-012-3008-z.

United Nations Environment Programme,
http://www.unep.org/newscentre/default.aspx?DocumentID=2716&ArticleID=9503

Vassiliki, A., Florou, H., 2006. Study on the behavior of the heavy metals Cu, Cr, Ni, Zn, Fe, Mn and Cs in an estuarine ecosystem using Mytilus galloprovincialis as a bioindicator species: the case of Thermaikos gulf, Greece. Doi: 10.1016/j.jenvrad.2005.07.005.

Vizzini, S., Di Leonardo, R., Costa, V., Tramati, C.D., Luzzu, F., Mazzola A., 2013. Trace element bias in the use of CO2-vents as analogues for low-pH environments: Implications for contamination levels in acidified oceans, Estuarine, Coastal and Shelf Science (2013), http://dx.doi.org/10.1016/ j.ecss.2013.09.015

Wang,T. C., Lai, D., Chen, M., T., 2010. Synthesis of iron doped vanadium-tin oxide nanocrystallites for CO gas sensing. Doi: 10.1016/j.matlet.2009.09.065.

Zuykov, M., Pelletier, E., Harper, D., 2013. Bivalve mollusks in metal pollution studies: from bioaccumulation to biomonitoring. Doi: 10.1016/j.chemosphere.2013.05.001.

Appendix I – *WGS84 Geographic coordinates of samples points*.

Id. Sample	E	N
0	14.960694	38.419306
Bubble	14.960093	38.417758
10	14.962755	38.420063
20	14.960968	38.419493
30	14.961386	38.419447
35	14.961506	38.419497
0-40	14.961061	38.419233
40	14.961207	38.419604
60	14.961612	38.419720
100	14.961389	38.415275
110	14.961906	38.419943
130	14.962128	38.420028
252	14.959717	38.417762
253	14.959767	38.417761
254	14.959719	38.417851
256	14.959771	38.417849
257	14.960058	38.417853
258	14.960059	38.417681
259	14.960174	38.417762
260	14.959715	38.417942
261	14.959771	38.417942
262	14.959887	38.417942
263	14.959716	38.418023
264	14.960289	38.417764
265	14.960494	38.417763
266	14.960576	38.418151
267	14.960287	38.417852
268	14.960493	38.417853
269	14.960278	38.418024
270	14.960541	38.418030
271	14.959923	38.417528

Id. Sample	E	N
272	14.960139	38.417529
273	14.959738	38.417528
274	14.960334	38.417529
275	14.960562	38.417525
276	14.959725	38.418150
277	14.960093	38.418150
278	14.960447	38.418149
279	14.960447	38.418401
280	14.960149	38.418402
281	14.960356	38.418401
282	14.959898	38.418645
283	14.960253	38.418645
284	14.960675	38.418645
285	14.959944	38.418870
286	14.960355	38.418871
287	14.960769	38.418872
288	14.961547	38.419116
289	14.961412	38.419383
290	14.961671	38.418787
291	14.961661	38.418631
292	14.961110	38.419293
293	14.962197	38.417959
310	14.960036	38.417650
320	14.959897	38.417703
60-100	14.961914	38.419600
CTL 4	14.968614	38.419720
CTL0	14.962755	38.420063
CTL1	14.953664	38.421220
CTL3	14.968612	38.424442
Offshore	14.417925	38.963444
Pozzo Vasca	14.960036	38.416017

Appendix II – *Bay of Levante seawaters samples(analyzed by Gas Chromatography, IC and ICP-MS).*

Date	Sample Id.	pH	Conduc. (mS/cm^3)	Eh	T °C	TA (meq/l)	He ml(STP)/l	H_2 ml(STP)/l	O_2 ml(STP)/l	N_2 ml(STP)/l	CO ml(STP)/l	CH_4 ml(STP)/l	CO_2 ml(STP)/l	HCO_3^{2-} (meq/l)	TDS (mg/l)	Cl (mg/l)	Br (mg/l)	Br (mg/l)	SO_4^{2-} (mg/l)	Na^+ (mg/l)	K^+ (mg/l)	Mg^{2+} (mg/l)	Ca^{2+} (mg/l)	Al (µg/l)	V (µg/l)	Mn (µg/l)	Fe (µg/l)	Ni (µg/l)	Cu (µg/l)	Zn (µg/l)	La (µg/l)
4-Apr	Bubble	5.64	47.1	-157.3	18	3	n.s	n.s	n.s	n.s	n.s	n.s	n.s	n.s	37803.7	592	0.9	76	2926	11485	428	1418	444	n.s	n.s	n.s	n.s	n.s	n.s	n.s	n.s
4-Apr	254	5.89	47.3	-144.3	18	2.9	n.s	n.s	n.s	n.s	n.s	n.s	n.s	n.s	35971.3	542	0.7	53	2890	11486	422	1419	446	n.s	n.s	n.s	n.s	n.s	n.s	n.s	n.s
4-Apr	260	6	46.3	-139	17	3.1	n.s	n.s	n.s	n.s	n.s	n.s	n.s	n.s	35358.2	583	0.8	60	2853	11466	425	1417	451	n.s	n.s	n.s	n.s	n.s	n.s	n.s	n.s
4-Apr	261	6.01	46.2	-137	17	2.9	n.s	n.s	n.s	n.s	n.s	n.s	n.s	n.s	37543.9	585	1.0	78	2907	11492	428	1416	447	n.s	n.s	n.s	n.s	n.s	n.s	n.s	n.s
4-Apr	256	6.05	47.1	-144	18	3.05	n.s	n.s	n.s	n.s	n.s	n.s	n.s	n.s	38126.6	598	0.9	74	2942	11556	434	1428	447	n.s	n.s	n.s	n.s	n.s	n.s	n.s	n.s
4-Apr	257	6.05	46.0	-148	17	2.9	n.s	n.s	n.s	n.s	n.s	n.s	n.s	n.s	40363.2	586	0.7	57	2864	13868	511	1714	538	n.s	n.s	n.s	n.s	n.s	n.s	n.s	n.s
4-Apr	258	6.1	45.9	-148	17	2.9	n.s	n.s	n.s	n.s	n.s	n.s	n.s	n.s	38042.8	597	0.8	63	2941	11535	429	1422	444	n.s	n.s	n.s	n.s	n.s	n.s	n.s	n.s
4-Apr	262	6.35	46.2	-114	17	2.95	n.s	n.s	n.s	n.s	n.s	n.s	n.s	n.s	37445.3	584	0.9	68	2901	11458	426	1419	456	n.s	n.s	n.s	n.s	n.s	n.s	n.s	n.s
4-Apr	259	6.38	45.4	-152	16	2.95	n.s	n.s	n.s	n.s	n.s	n.s	n.s	n.s	38273.2	603	0.8	66	2973	11525	430	1421	444	n.s	n.s	n.s	n.s	n.s	n.s	n.s	n.s
4-Apr	252	6.49	47.0	-128.6	18	2.9	n.s	n.s	n.s	n.s	n.s	n.s	n.s	n.s	37652.9	588	0.6	44	2887	11535	426	1425	449	n.s	n.s	n.s	n.s	n.s	n.s	n.s	n.s
4-Apr	253	6.52	47.2	-119.5	19	3.05	n.s	n.s	n.s	n.s	n.s	n.s	n.s	n.s	38114.1	594	0.8	67	2968	11594	451	1443	506	n.s	n.s	n.s	n.s	n.s	n.s	n.s	n.s
4-Apr	263	6.8	45.6	-73	17	3.05	n.s	n.s	n.s	n.s	n.s	n.s	n.s	n.s	35664.6	535	0.6	50	2650	11620	443	1436	476	n.s	n.s	n.s	n.s	n.s	n.s	n.s	n.s
5-Apr	269	6.28	47.1	-135	17	2.85	n.s	n.s	n.s	n.s	n.s	n.s	n.s	n.s	37445.3	585	0.8	60	2846	11495	422	1422	445	n.s	n.s	n.s	n.s	n.s	n.s	n.s	n.s
5-Apr	267	6.52	47.7	-131	17	2.85	n.s	n.s	n.s	n.s	n.s	n.s	n.s	n.s	37512	572	0.8	64	2829	11513	426	1916	451	n.s	n.s	n.s	n.s	n.s	n.s	n.s	n.s
5-Apr	285	6.59	47.3	-99.7	18	3.15	n.s	n.s	n.s	n.s	n.s	n.s	n.s	n.s	37932.9	594	0.7	53	2935	11552	429	1424	444	n.s	n.s	n.s	n.s	n.s	n.s	n.s	n.s
5-Apr	276	6.64	47.7	-91.3	18	3.1	n.s	n.s	n.s	n.s	n.s	n.s	n.s	n.s	37530.4	588	0.9	69	2885	11433	425	1417	444	n.s	n.s	n.s	n.s	n.s	n.s	n.s	n.s
5-Apr	270	6.75	46.9	-131.4	18	2.9	n.s	n.s	n.s	n.s	n.s	n.s	n.s	n.s	37890.4	588	1.1	85	2850	11782	429	1432	448	n.s	n.s	n.s	n.s	n.s	n.s	n.s	n.s
5-Apr	280	6.87	47.5	-99.7	17	3.25	n.s	n.s	n.s	n.s	n.s	n.s	n.s	n.s	38098.8	591	0.9	71	2925	11639	491	1467	524	n.s	n.s	n.s	n.s	n.s	n.s	n.s	n.s
5-Apr	266	6.91	46.2	-92.4	17	3	n.s	n.s	n.s	n.s	n.s	n.s	n.s	n.s	38347.1	603	1.1	86	2986	11551	433	1425	444	n.s	n.s	n.s	n.s	n.s	n.s	n.s	n.s
5-Apr	277	6.95	46.6	-102.2	17	3.1	n.s	n.s	n.s	n.s	n.s	n.s	n.s	n.s	37376.9	592	0.9	71	2936	11120	422	1369	428	n.s	n.s	n.s	n.s	n.s	n.s	n.s	n.s
5-Apr	264	7.07	47.0	-124	17	3.05	n.s	n.s	n.s	n.s	n.s	n.s	n.s	n.s	36369.2	591	0.9	69	2913	10353	384	1275	396	n.s	n.s	n.s	n.s	n.s	n.s	n.s	n.s
5-Apr	279	7.09	47.0	-90	18	3.05	n.s	n.s	n.s	n.s	n.s	n.s	n.s	n.s	37458.7	588	0.7	59	2890	11351	419	1406	443	n.s	n.s	n.s	n.s	n.s	n.s	n.s	n.s
5-Apr	283	7.16	47.0	-65.7	17	3	n.s	n.s	n.s	n.s	n.s	n.s	n.s	n.s	37710	590	0.6	51	2933	11487	426	1423	452	n.s	n.s	n.s	n.s	n.s	n.s	n.s	n.s
5-Apr	273	7.21	47.0	-75	18	n.d	n.s	n.s	n.s	n.s	n.s	n.s	n.s	n.s	n.d	n.d	n.d	n.d	n.d	n.d	n.d	n.d	n.d	n.s	n.s	n.s	n.s	n.s	n.s	n.s	n.s
5-Apr	274	7.21	47.2	-100.4	18	n.d	n.s	n.s	n.s	n.s	n.s	n.s	n.s	n.s	n.d	n.d	n.d	n.d	n.d	n.d	n.d	n.d	n.d	n.s	n.s	n.s	n.s	n.s	n.s	n.s	n.s
5-Apr	287	7.22	46.7	-29.7	17	3.1	n.s	n.s	n.s	n.s	n.s	n.s	n.s	n.s	37749.4	594	0.9	74	2916	11402	424	1406	439	n.s	n.s	n.s	n.s	n.s	n.s	n.s	n.s
5-Apr	278	7.24	47.0	-96.8	17	2.95	n.s	n.s	n.s	n.s	n.s	n.s	n.s	n.s	n.d	n.d	n.d	n.d	n.d	n.d	n.d	n.d	n.d	n.s	n.s	n.s	n.s	n.s	n.s	n.s	n.s
5-Apr	282	7.31	47.0	-76.9	18	3	n.s	n.s	n.s	n.s	n.s	n.s	n.s	n.s	37820.9	591	0.9	73	2888	11585	435	1427	443	n.s	n.s	n.s	n.s	n.s	n.s	n.s	n.s
5-Apr	284	7.31	46.2	-82.2	17	3.25	n.s	n.s	n.s	n.s	n.s	n.s	n.s	n.s	37841.5	592	0.9	75	2922	11551	430	1421	437	n.s	n.s	n.s	n.s	n.s	n.s	n.s	n.s
5-Apr	271	7.36	47.7	-49	18	3.05	n.s	n.s	n.s	n.s	n.s	n.s	n.s	n.s	37707.8	588	0.9	75	2872	11552	462	1425	452	n.s	n.s	n.s	n.s	n.s	n.s	n.s	n.s
5-Apr	272	7.41	46.7	-29.8	18	n.d	n.s	n.s	n.s	n.s	n.s	n.s	n.s	n.s	n.d	n.d	n.d	n.d	n.d	n.d	n.d	n.d	n.d	n.s	n.s	n.s	n.s	n.s	n.s	n.s	n.s
5-Apr	286	7.45	46.5	-64.8	17	3.05	n.s	n.s	n.s	n.s	n.s	n.s	n.s	n.s	37378.9	596	1.0	78	2930	11022	412	1361	426	n.s	n.s	n.s	n.s	n.s	n.s	n.s	n.s
5-Apr	268	7.46	46.7	-122	17	2.9	n.s	n.s	n.s	n.s	n.s	n.s	n.s	n.s	38210.6	598	0.9	68	2957	11642	432	1423	443	n.s	n.s	n.s	n.s	n.s	n.s	n.s	n.s
5-Apr	275	7.55	47.3	-99.6	17	3.05	n.s	n.s	n.s	n.s	n.s	n.s	n.s	n.s	37830.6	596	0.9	68	2921	11416	425	1398	432	n.s	n.s	n.s	n.s	n.s	n.s	n.s	n.s
5-Apr	281	7.61	46.2	-101	17	3.2	n.s	n.s	n.s	n.s	n.s	n.s	n.s	n.s	37833.4	598	0.9	70	2914	11360	424	1396	434	n.s	n.s	n.s	n.s	n.s	n.s	n.s	n.s
5-Apr	265	7.66	47.3	-107	17	3	n.s	n.s	n.s	n.s	n.s	n.s	n.s	n.s	36886.6	571	1.0	81	2782	11475	420	1417	441	n.s	n.s	n.s	n.s	n.s	n.s	n.s	n.s
5-Apr	Offshore	8.03	n.d	n.d	n.d	3.05	n.s	n.s	n.s	n.s	n.s	n.s	n.s	n.s	38338.3	605	0.8	64	2964	11535	438	1422	445	n.s	n.s	n.s	n.s	n.s	n.s	n.s	n.s
6-Apr	0	7.44	46.1	86	17	2.9	n.s	n.s	n.s	n.s	n.s	n.s	n.s	n.s	36979	588	0.7	54	2896	10958	414	1357	432	n.s	n.s	n.s	n.s	n.s	n.s	n.s	n.s
6-Apr	20	7.44	46.9	51	17	2.9	n.s	n.s	n.s	n.s	n.s	n.s	n.s	n.s	37687.9	591	0.8	67	2892	11481	427	1400	434	n.s	n.s	n.s	n.s	n.s	n.s	n.s	n.s
6-Apr	294	7.78	47.3	144	17	3	n.s	n.s	n.s	n.s	n.s	n.s	n.s	n.s	38049.1	596	0.9	75	2976	11533	437	1416	444	n.s	n.s	n.s	n.s	n.s	n.s	n.s	n.s
6-Apr	292	7.85	46.5	50	17	3	n.s	n.s	n.s	n.s	n.s	n.s	n.s	n.s	36807.7	606	0.9	69	2970	10190	380	1236	467	n.s	n.s	n.s	n.s	n.s	n.s	n.s	n.s
6-Apr	40	7.96	49.7	53.6	16	2.9	n.s	n.s	n.s	n.s	n.s	n.s	n.s	n.s	37557	587	0.5	40	2887	11501	429	1421	453	n.s	n.s	n.s	n.s	n.s	n.s	n.s	n.s
6-Apr	293	7.97	46.3	162	17	2.85	n.s	n.s	n.s	n.s	n.s	n.s	n.s	n.s	36452.6	557	0.9	74	2717	11588	427	1434	447	n.s	n.s	n.s	n.s	n.s	n.s	n.s	n.s
6-Apr	60	7.98	46.1	33	17	2.95	n.s	n.s	n.s	n.s	n.s	n.s	n.s	n.s	35275.1	591	1.0	84	2888	9428	348	1166	367	n.s	n.s	n.s	n.s	n.s	n.s	n.s	n.s
6-Apr	288	7.98	46.5	104	17	3	n.s	n.s	n.s	n.s	n.s	n.s	n.s	n.s	37755.5	589	0.8	64	2898	11588	431	1431	445	n.s	n.s	n.s	n.s	n.s	n.s	n.s	n.s
6-Apr	289	7.98	46.2	143	17	3.05	n.s	n.s	n.s	n.s	n.s	n.s	n.s	n.s	38163.3	598	0.8	63	2948	11606	437	1427	447	n.s	n.s	n.s	n.s	n.s	n.s	n.s	n.s
6-Apr	291	7.98	46.1	94.7	17	3	n.s	n.s	n.s	n.s	n.s	n.s	n.s	n.s	38328.4	597	0.7	54	2892	11830	440	1458	451	n.s	n.s	n.s	n.s	n.s	n.s	n.s	n.s
6-Apr	290	7.99	46.7	85	17	3	n.s	n.s	n.s	n.s	n.s	n.s	n.s	n.s	37985.6	588	0.7	57	2873	11803	440	1477	469	n.s	n.s	n.s	n.s	n.s	n.s	n.s	n.s
6-Apr	110	8.03	46.7	50	17	2.9	n.s	n.s	n.s	n.s	n.s	n.s	n.s	n.s	38183.1	598	1.0	78	2919	11638	433	1436	444	n.s	n.s	n.s	n.s	n.s	n.s	n.s	n.s
6-Apr	10	8.05	46.3	-7.2	17	2.9	n.s	n.s	n.s	n.s	n.s	n.s	n.s	n.s	38183.3	598	0.9	72	2918	11634	471	1430	447	n.s	n.s	n.s	n.s	n.s	n.s	n.s	n.s
6-Apr	130	8.05	46.7	94	17	3	n.s	n.s	n.s	n.s	n.s	n.s	n.s	n.s	38070.1	604	0.7	60	2918	11375	430	1402	436	n.s	n.s	n.s	n.s	n.s	n.s	n.s	n.s

2011

Continue in the next page

Date	Sample Id.	pH	Conduc. (mS/cm^3)	Eh	T °C	TA (meq/l)	He ml(STP)/l	H_2 ml(STP)/l	O_2 ml(STP)/l	N_2 ml(STP)/l	CO ml(STP)/l	CH_4 ml(STP)/l	CO_2 ml(STP)/l	HCO_3^{2-} (meq/l)	TDS (mg/l)	Cl (mg/l)	Br (mg/l)	Br^- (mg/l)	SO_4^{2-} (mg/l)	Na^+ (mg/l)	K^+ (mg/l)	Mg^{2+} (mg/l)	Ca^{2+} (mg/l)	Al (µg/l)	V (µg/l)	Mn (µg/l)	Fe (µg/l)	Ni (µg/l)	Cu (µg/l)	Zn (µg/l)	La (ng/l)
30-May	Pozzo Vasca	1.47	n.s	150	67	n.s	n.d.	1.11E-02	3.42E-01	6.28E+00	1.53E-03	1.01E-02	2.22E+02	0	n.s	n.s	n.s	n.s	n.s	n.s	n.s	n.s	n.s	32339.64	51.4663	69.1313	51321.26	249.61	0.11685	449.573	2505.72
30-May	Bubble	5.90	n.s	-32	22	n.s	1.65E-04	8.37E-01	1.93E+00	1.22E+01	5.54E-05	1.14E-02	5.80E+01	2.7-2.9	n.s	n.s	n.s	n.s	n.s	n.s	n.s	n.s	n.s	4.586053	1.03791	13.9906	3.5114	0.25835	0.1206	2.2044	7.50538
30-May	310	6.33	n.s	29.5	21	n.s	2.99E-04	6.01E-03	5.15E+00	1.72E+01	3.41E-05	5.54E-03	2.86E+01	2.7-1.3	n.s	n.s	n.s	n.s	n.s	n.s	n.s	n.s	n.s	9.254013	0.85922	17.1469	13.89147	0.29164	0.09109	4.245	20.2173
30-May	257	6.65	n.s	67.1	23	n.s	4.29E-04	1.59E-02	4.65E+00	1.25E+01	1.50E-05	3.83E-03	2.08E+01	2.9	n.s	n.s	n.s	n.s	n.s	n.s	n.s	n.s	n.s	8.478686	0.63794	13.7191	16.2713	0.25527	0.14394	2.67279	10.5447
30-May	320	6.84	n.s	129.1	22	n.s	2.64E-04	6.43E-02	5.65E+00	1.43E+01	2.27E-05	2.77E-03	1.06E+01	2.9	n.s	n.s	n.s	n.s	n.s	n.s	n.s	n.s	n.s	10.68488	0.89166	14.504	7.3337	0.25318	0.08917	1.4943	11.0218
30-May	262	6.94	n.s	89	23	n.s	n.d.	1.62E-03	5.34E+00	1.20E+01	2.24E-05	2.38E-03	9.70E+00	3	n.s	n.s	n.s	n.s	n.s	n.s	n.s	n.s	n.s	12.36691	0.50918	13.0974	0.97452	0.36404	0.22775	4.15733	6.50996
30-May	277	7.19	n.s	145	23	n.s	3.11E-04	6.41E-04	5.56E+00	1.18E+01	2.27E-05	1.12E-03	4.06E+00	3.2	n.s	n.s	n.s	n.s	n.s	n.s	n.s	n.s	n.s	11.87913	0.43278	13.2737	1.00332	0.31029	0.30287	2.38573	6.41109
30-May	30	7.31	n.s	118	22	n.s	2.14E-04	3.14E-04	6.04E+00	9.41E+00	2.02E-05	5.47E-04	3.09E+00	3.2	n.s	n.s	n.s	n.s	n.s	n.s	n.s	n.s	n.s	2.083813	0.33801	15.5355	1.868387	0.49082	0.90804	2.6235	0.93377
30-May	0	7.34	n.s	159	22	n.s	n.d.	1.76E-03	5.75E+00	1.07E+01	2.02E-05	5.46E-04	2.02E+00	3.2	n.s	n.s	n.s	n.s	n.s	n.s	n.s	n.s	n.s	2.603853	0.46164	16.4892	2.1798	0.40695	1.49875	2.9446	1.61877
30-May	20	7.41	n.s	148	22	n.s	n.d.	n.d.	5.93E+00	1.03E+01	2.07E-05	5.58E-04	2.56E+00	3	n.s	n.s	n.s	n.s	n.s	n.s	n.s	n.s	n.s	2.083813	0.33801	15.5355	1.868387	0.49082	0.90804	2.6235	0.93377
30-May	283	7.48	n.s	168	23	n.s	1.87E-04	1.13E-03	4.10E+00	1.11E+01	3.35E-05	6.20E-04	2.91E+00	3.1-3.3	n.s	n.s	n.s	n.s	n.s	n.s	n.s	n.s	n.s	2.603853	0.46164	16.4892	2.1798	0.40695	1.49875	2.9446	1.61877
30-May	40	7.85	n.s	176	22	n.s	n.d.	6.66E-03	5.21E+00	9.61E+00	2.14E-05	4.10E-04	6.98E-01	3.1	n.s	n.s	n.s	n.s	n.s	n.s	n.s	n.s	n.s	2.4859	0.75747	7.26627	0.97382	0.25675	0.58571	1.5076	1.96156
30-May	60	7.91	n.s	165	22	n.s	1.61E-04	1.40E-02	6.63E+00	1.36E+01	2.71E-05	5.51E-04	5.21E-01	2.9	n.s	n.s	n.s	n.s	n.s	n.s	n.s	n.s	n.s	2.106907	0.99394	4.57421	0.93332	0.23029	0.28434	2.6592	1.47089
30-May	35	7.94	n.s	165	22	n.s	2.75E-04	2.57E-04	5.94E+00	1.09E+01	4.12E-05	3.17E-04	5.73E-01	2.9	n.s	n.s	n.s	n.s	n.s	n.s	n.s	n.s	n.s	2.445813	0.98711	4.9968	0.75712	0.26316	0.34619	0.526	1.50443
30-May	110	8.03	n.s	161	22	n.s	9.63E-04	6.26E-04	5.37E+00	1.32E+01	3.35E-05	3.87E-04	5.44E-01	2.8-3	n.s	n.s	n.s	n.s	n.s	n.s	n.s	n.s	n.s	2.544533	1.38042	4.22915	0.8127	0.22694	0.26916	1.3072	1.51153
30-May	Offshore	8.03	n.s	171.3	21	n.s	2.75E-04	9.95E-03	5.81E+00	1.36E+01	2.06E-05	1.59E-04	4.42E-01	2.8	n.s	n.s	n.s	n.s	n.s	n.s	n.s	n.s	n.s	0.94596	1.45652	0.50724	0.628453	0.19536	0.21356	0.5602	4.27737

Follow from next page

Appendix III – *Metals speciation (data processed by PHREEQC), Molarity.*

		Bubble	310	257	320	262	277	30	0	20	283	40	60	35	110	Offshore		Pozzo Vasca
	pH	5.9	6.33	6.65	6.84	6.94	7.19	7.31	7.34	7.41	7.48	7.85	7.85	7.94	8.03	8.03	pH	1.47
	pe	-0.55	0.51	1.14	2.21	1.52	2.47	2.02	2.72	2.53	2.86	3.01	3.01	2.82	2.75	2.93	pe	2.77
	T (°C)	22.2	21.3	22.8	21.7	23.1	23.3	22.04	22.1	21.86	23.2	22.2	22.2	22.2	22.3	21.47	T (°C)	72.5
	Al	1.766E-07	3.564E-07	3.266E-07	4.115E-07	4.763E-07	4.575E-07	8.953E-08	1.003E-07	8.026E-08	1.177E-07	9.575E-08	9.575E-08	9.42E-08	9.801E-08	3.643E-08	Al	0.001203
	AlO2-	7.654E-09	9.128E-08	1.906E-07	2.835E-07	3.59E-07	3.847E-07	7.728E-08	8.723E-08	7.08E-08	1.056E-07	8.927E-08	8.927E-08	8.833E-08	9.233E-08	3.431E-08	Al+3	0.0009982
Al	HAlO2	2.161E-08	1.002E-07	9.287E-08	9.426E-08	8.838E-08	5.273E-08	8.559E-09	8.988E-09	6.285E-09	7.461E-09	2.828E-09	2.828E-09	2.275E-09	1.923E-09	7.451E-10	AlSO4+	0.0001913
	NaAlO2	3.09E-10	3.643E-09	7.755E-09	1.137E-08	1.466E-08	1.575E-08	3.114E-09	3.518E-09	2.846E-09	4.319E-09	3.604E-09	3.604E-09	3.567E-09	3.733E-09	1.372E-09	Al(SO4)2-	0.00001014
	Al(OH)2+	3.335E-08	6.084E-08	1.01E-08	1.724E-08	1.175E-08	3.892E-09	5.19E-10	5.067E-10	3.062E-10	2.842E-10	4.896E-11	4.896E-11	3.201E-11	2.185E-11	8.928E-12	AlOH+2	0.000003024
	C(4)	0.008198	0.00544	0.004564	0.004289	0.004175	0.003987	0.003929	0.003914	0.003885	0.003852	0.003719	0.003719	0.003683	0.003643	0.003648	Ca	0.0006532
	HCO3-	0.002492	0.002478	0.002488	0.00247	0.002479	0.002464	0.002442	0.002439	0.002427	0.002428	0.002328	0.002328	0.002293	0.002252	0.00225	Ca+2	0.0006093
C(4)	NaHCO3	0.0008258	0.0008357	0.0008146	0.0008265	0.0008072	0.0007991	0.0008115	0.0008096	0.0008097	0.0007888	0.0007714	0.0007714	0.0007598	0.0007447	0.0007562	CaSO4	0.00004349
	MgHCO3+	0.0004063	0.0004042	0.0004054	0.0004027	0.0004039	0.0004014	0.000398	0.0003975	0.0003957	0.0003954	0.0003792	0.0003792	0.0003735	0.0003667	0.0003665	CaCl+	0.000000427
	CO2	0.004398	0.001645	0.0007743	0.0005038	0.0003942	0.0002198	0.000168	0.0001564	0.000133	0.0001112	4.609E-05	4.609E-05	0.0000369	2.941E-05	0.00009529	CaCl2	1.269E-09
	Ca	0.0116	0.0116	0.0116	0.0116	0.0116	0.0116	0.0116	0.0116	0.0116	0.0116	0.0116	0.0116	0.0116	0.0116	0.0116	Cd	9.044E-10
	Ca+2	0.01031	0.01031	0.01031	0.01031	0.01031	0.0103	0.0103	0.0103	0.0103	0.0103	0.01029	0.01029	0.01029	0.01028	0.01028	CdCl+	5.063E-10
Ca	CaSO4	0.0008465	0.000846	0.0008468	0.0008462	0.0008468	0.0008467	0.0008461	0.0008461	0.0008459	0.0008464	0.0008453	0.0008453	0.000845	0.0008448	0.0008444	Cd+2	3.881E-10
	CaCl+	0.0002872	0.0002868	0.0002874	0.0002869	0.0002875	0.0002875	0.0002869	0.000287	0.0002868	0.0002874	0.0002867	0.0002867	0.0002866	0.0002865	0.0002862	CdCl2	9.829E-12
	CaCl2	0.0000849	8.567E-05	0.0000844	8.532E-05	8.415E-05	8.397E-05	0.000085	8.494E-05	8.514E-05	8.402E-05	8.476E-05	8.476E-05	8.473E-05	8.461E-05	0.00008532	MgCl+	0.000003131
	Cl(-1)	0.6122	0.6122	0.6122	0.6122	0.6122	0.6122	0.6122	0.6122	0.6122	0.6122	0.6122	0.6122	0.6122	0.6122	0.6122	Cl(1)	2.443E-39
	Cl-	0.585	0.5851	0.5849	0.585	0.5849	0.5848	0.585	0.585	0.585	0.5849	0.585	0.585	0.585	0.585	0.585	HClO	2.443E-39
Cl(-1)	NaCl	0.02063	0.02051	0.02071	0.02056	0.02075	0.02078	0.02061	0.02062	0.02058	0.02077	0.02063	0.02063	0.02063	0.02064	0.02053	Cu(2)	3.27E-10
	MgCl+	0.006038	0.006063	0.006021	0.006051	0.006013	0.006007	0.006041	0.006039	0.006046	0.006009	0.006034	0.006034	0.006033	0.006029	0.006052	Cu+2	3.03E-10
	CaCl+	0.0002872	0.0002868	0.0002874	0.0002869	0.0002875	0.0002875	0.0002869	0.000287	0.0002868	0.0002874	0.0002867	0.0002867	0.0002866	0.0002865	0.0002862	CuSO4	2.203E-11
	Cl(1)	0	0	0	0	0	1.114E-39	0	3.478E-39	1.665E-39	1.713E-38	9.139E-38	9.139E-38	5.486E-38	6.015E-38	9.696E-38	CuCl+	1.947E-12
Cl(1)	HClO	0	0	0	0	0	6.856E-40	0	1.849E-39	8.471E-40	9.401E-39	6.767E-38	2.372E-38	1.217E-38	1.131E-38	7.872E-38	CuCl2	3.406E-15
	ClO-	0	0	0	0	0	4.279E-40	0	1.629E-39	8.18E-40	7.724E-39	2.372E-38	6.767E-38	4.27E-38	4.883E-38	1.824E-38	Fe(2)	0.0009221
	Cu(1)	1.972E-09	1.49E-09	2.354E-09	1.458E-09	3.725E-09	4.953E-09	2.159E-08	2.451E-08	1.485E-08	1.658E-08	9.57E-09	9.57E-09	5.658E-09	4.399E-09	3.489E-09	Fe+2	0.0008759
Cu(1)	CuCl3-2	1.784E-09	1.348E-09	2.13E-09	1.319E-09	3.37E-09	4.481E-09	1.953E-08	2.217E-08	1.343E-08	1.5E-08	8.658E-09	8.658E-09	5.118E-09	3.98E-09	3.156E-09	FeSO4	0.00004406
	CuCl2-	1.879E-10	1.421E-10	2.242E-10	1.39E-10	3.547E-10	4.715E-10	2.057E-09	2.335E-09	1.415E-09	1.579E-09	9.12E-10	9.12E-10	5.391E-10	4.191E-10	3.326E-10	FeCl+	0.000002206
	Cu+	2.129E-14	1.608E-14	2.541E-14	1.574E-14	4.021E-14	5.348E-14	2.33E-13	2.645E-13	1.602E-13	1.79E-13	1.033E-13	1.033E-13	6.107E-14	4.748E-14	3.765E-14	FeCl2	5.546E-11
Cu+	Cu(2)	5.63E-17	5.795E-16	4.553E-15	4.107E-14	2.287E-14	3.775E-13	7.351E-13	4.387E-12	1.949E-12	5.04E-12	8.668E-12	8.668E-12	3.976E-12	3.159E-12	3.901E-12	FeOH+	4.679E-12
	CuCO3	4.535E-18	1.087E-16	1.457E-15	1.695E-14	1.063E-14	2.211E-13	4.67E-13	2.837E-12	1.309E-12	3.503E-12	6.651E-12	6.651E-12	3.076E-12	2.451E-12	3.027E-12	FeCl4-2	1.199E-14
	Cu+2	3.327E-17	2.975E-16	1.906E-15	1.44E-14	7.16E-15	8.428E-14	1.36E-13	7.723E-13	3.046E-13	6.949E-13	5.861E-13	7.615E-13	2.237E-13	1.475E-13	1.822E-13	Fe(OH)2	8.884E-22
Cu+2	CuOH+	4.85E-19	1.168E-17	1.561E-16	1.829E-15	1.144E-15	2.393E-14	5.098E-14	3.101E-13	1.437E-13	3.848E-13	7.615E-13	5.861E-13	3.576E-13	2.901E-13	3.585E-13	Fe(OH)3-	1.285E-30
	CuCl+	1.207E-17	1.08E-16	6.905E-16	5.225E-15	2.593E-15	3.052E-14	4.935E-14	2.802E-13	1.105E-13	2.517E-13	2.126E-13	2.126E-13	8.114E-14	5.351E-14	6.615E-14	Fe(OH)4-2	0
	Fe(2)	6.534E-08	2.585E-07	3.028E-07	1.363E-07	1.813E-08	1.834E-08	1.367E-07	3.744E-08	3.204E-08	1.369E-08	3.018E-09	3.018E-09	2.025E-09	1.455E-09	7.876E-10	Fe(3)	4.137E-13
	Fe+2	4.339E-08	1.716E-07	2.006E-07	9.025E-08	1.198E-08	1.208E-08	8.986E-08	2.459E-08	2.1E-08	8.951E-09	1.935E-09	1.935E-09	1.289E-09	9.181E-10	4.966E-10	Fe+3	3.348E-13
	FeHCO3+	1.38E-08	5.431E-08	6.364E-08	2.846E-08	3.787E-09	3.793E-09	2.8E-08	7.651E-09	6.508E-09	2.769E-09	5.748E-10	5.748E-10	3.77E-10	2.637E-10	1.427E-10	FeSO4+	4.483E-14
	FeCl+	4.139E-09	1.633E-08	1.917E-08	8.598E-09	1.146E-09	1.156E-09	8.569E-09	2.345E-09	2.002E-09	8.563E-10	1.846E-10	1.846E-10	1.229E-10	8.761E-11	4.728E-11	FeOH+2	3.246E-14
	FeSO4	3.963E-09	1.579E-08	1.824E-08	8.278E-09	1.087E-09	1.093E-09	8.22E-09	2.248E-09	1.924E-09	8.109E-10	1.768E-10	1.768E-10	1.177E-10	8.382E-11	4.565E-11	FeCl+2	1.134E-15
Fe(2)	FeCO3	3.52E-11	3.731E-10	9.129E-10	6.326E-10	1.059E-10	1.886E-10	1.837E-09	5.377E-10	5.374E-10	2.685E-10	1.307E-10	1.307E-10	1.055E-10	9.077E-11	4.912E-11	FeCl2+	2.08E-16
	FeOH+	3.878E-12	4.131E-11	1.008E-10	7.029E-11	1.173E-11	2.103E-11	2.065E-10	6.053E-11	6.077E-11	3.039E-11	1.541E-11	1.541E-11	1.263E-11	1.107E-11	5.992E-12	Fe(OH)2+	1.706E-16
	FeCl4-2	1.234E-11	4.834E-11	5.741E-11	2.553E-11	3.441E-12	3.476E-12	2.551E-11	6.983E-12	5.95E-12	2.573E-12	5.501E-13	5.501E-13	3.664E-13	2.613E-13	1.402E-13	Fe(SO4)2-	7.002E-17
	FeCl2	5.346E-12	2.101E-11	2.483E-11	1.108E-11	1.486E-12	1.5E-12	1.106E-11	3.027E-12	2.582E-12	1.111E-12	2.384E-13	2.384E-13	1.588E-13	1.132E-13	6.088E-14	Fe(OH)3	1.907E-21
	Fe(OH)2	1.604E-17	4.6E-16	2.344E-15	2.533E-15	5.321E-16	1.696E-15	2.196E-14	6.896E-15	8.134E-15	4.777E-15	5.683E-15	5.683E-15	5.728E-15	6.176E-15	3.344E-15	FeCl4-	4.198E-24
	Fe(OH)3-	7.422E-22	5.729E-20	6.101E-19	1.021E-18	2.701E-19	1.531E-18	2.612E-17	8.79E-18	1.218E-17	8.408E-18	2.344E-17	2.344E-17	2.907E-17	3.856E-17	2.088E-17	Fe2(OH)2+4	1.271E-25
	Fe(OH)4-2	2.338E-30	4.853E-28	1.082E-26	2.799E-26	9.343E-27	9.418E-26	2.115E-24	7.627E-25	1.241E-24	1.009E-24	6.582E-24	6.582E-24	1.004E-23	1.639E-23	8.863E-24	Fe(OH)4-	1.741E-29
	Fe(3)	6.346E-16	2.681E-13	8.74E-12	1.411E-10	7.449E-12	3.341E-10	1.865E-09	3.125E-09	2.725E-09	4.133E-09	1.51E-08	1.51E-08	1.206E-08	1.367E-08	1.091E-08	Fe3(OH)4+5	1.921E-38
	Fe(OH)3	1.229E-16	1.058E-13	5.041E-12	9.569E-11	5.404E-12	2.747E-10	1.598E-09	2.701E-09	2.398E-09	3.693E-09	1.409E-08	1.409E-08	1.128E-08	1.278E-08	1.02E-08	K	0.0002461
	Fe(OH)2+	7.074E-18	1.614E-13	3.681E-12	4.51E-11	2.024E-12	5.786E-11	2.552E-10	4.026E-10	3.042E-10	3.989E-10	6.49E-10	6.49E-10	4.224E-10	3.888E-10	3.102E-10	K+	0.000244
	Fe(OH)4-	3.587E-20	8.313E-17	8.28E-15	2.434E-13	1.731E-14	1.565E-12	1.199E-11	2.172E-11	2.266E-11	4.101E-11	3.666E-10	3.666E-10	3.612E-10	5.033E-10	4.015E-10	KSO4-	0.00000184
	FeOH+2	5.044E-16	8.396E-16	9.186E-15	7.257E-14	2.591E-15	4.166E-14	1.392E-13	2.049E-13	1.318E-13	1.473E-13	1.021E-13	1.021E-13	5.401E-14	4.042E-14	3.221E-14	KHSO4	2.404E-07
	FeCO3+	1.6E-19	2.013E-17	1.989E-16	1.686E-15	5.475E-17	8.627E-16	3.12E-15	4.569E-15	2.974E-15	3.026E-15	2.157E-15	2.157E-15	1.124E-15	8.204E-16	6.928E-16	KCl	6.147E-08
Fe(3)	FeCl2+	7.007E-21	3.096E-19	1.616E-18	8.262E-18	2.336E-19	2.111E-18	5.366E-18	7.372E-18	4.037E-18	3.828E-18	1.135E-18	1.135E-18	4.879E-19	2.967E-19	2.37E-19	KOH	1.997E-17
	Fe+3	3.098E-21	1.365E-19	7.156E-19	3.647E-18	1.036E-19	9.364E-19	2.371E-18	3.258E-18	1.783E-18	1.698E-18	5.016E-19	5.016E-19	2.157E-19	1.312E-19	1.045E-19	La(3)	9.663E-10
	FeSO4+	8.031E-23	3.448E-21	1.888E-20	9.319E-20	2.756E-21	2.507E-20	6.12E-20	8.423E-20	4.577E-20	4.532E-20	1.301E-20	1.301E-20	5.594E-21	3.413E-21	2.654E-21	LaSO4+	7.039E-10
	FeCl+2	7.432E-23	3.132E-21	1.769E-20	8.535E-20	2.598E-21	2.372E-20	5.644E-20	7.777E-20	4.205E-20	4.28E-20	1.203E-20	1.203E-20	5.175E-21	3.164E-21	2.418E-21	La+3	2.551E-10
	Fe(SO4)2-	3.583E-24	1.602E-22	8.197E-22	4.252E-21	1.181E-22	1.064E-21	2.75E-21	3.775E-21	2.073E-21	1.932E-21	5.804E-22	5.804E-22	2.496E-22	1.516E-22	1.224E-22	La(SO4)2-	4.106E-12
	FeCl4-	1.123E-24	4.965E-23	2.587E-22	1.324E-21	3.739E-23	3.378E-22	8.599E-22	1.181E-21	6.469E-22	6.127E-22	1.818E-22	1.818E-22	7.817E-23	4.754E-23	3.799E-23	LaCl+2	3.187E-12
	Fe2(OH)2+4	2.218E-32	3.117E-28	3.747E-26	2.331E-24	2.984E-27	7.718E-25	8.586E-24	1.861E-23	7.689E-24	9.643E-24	4.62E-24	4.62E-24	1.293E-24	7.243E-25	4.59E-25	Mg	0.001634
	Fe3(OH)4+5	0	1.416E-37	3.898E-34	2.962E-31	1.708E-35	1.264E-31	6.181E-30	2.113E-29	6.594E-30	1.088E-29	8.458E-30	8.458E-30	1.541E-30	7.947E-31	4.01E-31	Mg+2	0.001226
	K	0.01148	0.01148	0.01148	0.01148	0.01148	0.01148	0.01148	0.01148	0.01148	0.01148	0.01148	0.01148	0.01148	0.01148	0.01148	MgSO4	0.0004049
	K+	0.0112	0.0112	0.0112	0.0112	0.0112	0.0112	0.0112	0.0112	0.0112	0.0112	0.0112	0.0112	0.0112	0.0112	0.0112	MgCl+	0.000003131
K	KSO4-	0.0001973	0.0001978	0.000197	0.0001976	0.0001968	0.0001967	0.0001974	0.0001974	0.0001975	0.0001968	0.0001973	0.0001973	0.0001974	0.0001973	0.0001978	Mn(2)	0.000001263
	KCl	8.097E-05	7.956E-05	8.191E-05	8.019E-05	8.239E-05	8.271E-05	8.072E-05	8.081E-05	8.044E-05	8.255E-05	8.097E-05	8.097E-05	8.097E-05	8.113E-05	0.00007983	Mn+2	0.000001085
	KOH	1.322E-10	5.076E-11	1.06E-10	1.642E-10	2.066E-10	3.674E-10	4.846E-10	5.193E-10	6.102E-10	7.165E-10	1.68E-09	1.68E-09	2.067E-09	2.543E-09	2.544E-09	MnSO4	1.589E-07

Follow in the next page

Continue from previous page

		Bubble	310	257	320	262	277	30	0	20	283	40	60	35	110	Offshore		Pozzo Vasca
	pH	5.9	6.33	6.65	6.84	6.94	7.19	7.31	7.34	7.41	7.48	7.85	7.85	7.94	8.03	8.03	pH	1.47
	pe	-0.55	0.51	1.14	2.21	1.52	2.47	2.02	2.72	2.53	2.86	3.01	3.01	2.82	2.75	2.93	pe	2.77
	T (°C)	22.2	21.3	22.8	21.7	23.1	23.3	22.04	22.1	21.86	23.2	22.2	22.2	22.2	22.3	21.47	T (°C)	72.5
	La(3)	5.615E-11	1.513E-10	7.889E-11	8.246E-11	4.87E-11	4.796E-11	9.107E-12	1.211E-11	6.986E-12	1.351E-11	1.468E-11	1.468E-11	1.126E-11	1.131E-11	3.2E-11	MnCl+	1.916E-08
	LaCO3+	2.02E-12	1.387E-11	1.353E-11	2.005E-11	1.383E-11	1.941E-11	4.259E-12	5.838E-12	3.6E-12	7.328E-12	9.382E-12	9.382E-12	7.223E-12	7.19E-12	2.039E-11	MnCl3-	1.989E-14
La(3)	LaSO4+	2.555E-11	6.434E-11	3.086E-11	2.908E-11	1.633E-11	1.303E-11	2.132E-12	2.734E-12	1.434E-12	2.555E-12	1.426E-12	1.426E-12	9.058E-13	7.479E-13	2.087E-12	Mn(3)	1.088E-27
	La+3	1.876E-11	4.803E-11	2.242E-11	2.155E-11	1.18E-11	9.379E-12	1.57E-12	2.011E-12	1.06E-12	1.842E-12	1.047E-12	1.047E-12	6.649E-13	5.48E-13	1.552E-12	Mn+3	1.088E-27
	LaCl+2	6.354E-12	1.6E-11	7.676E-12	7.231E-12	4.063E-12	3.241E-12	5.303E-13	6.8E-13	3.567E-13	6.355E-13	3.545E-13	3.545E-13	2.252E-13	2.495E-12	5.187E-13	Na	0.006816
	Mg	0.05996	0.05996	0.05996	0.05996	0.05996	0.05996	0.05996	0.05996	0.05996	0.05996	0.05996	0.05996	0.05996	0.05996	0.05996	Na+	0.006779
	Mg+2	0.04519	0.04528	0.04512	0.04524	0.04509	0.04506	0.0452	0.04519	0.04521	0.04507	0.04516	0.04516	0.04515	0.04513	0.04522	NaSO4-	0.00003057
Mg	MgSO4	0.008325	0.008206	0.008405	0.008259	0.008445	0.008471	0.008303	0.008311	0.008279	0.008457	0.008322	0.008322	0.008321	0.008333	0.008224	NaCl	0.000005727
	MgCl+	0.006038	0.006063	0.006021	0.006051	0.006013	0.006007	0.006041	0.006039	0.006046	0.006009	0.006034	0.006034	0.006033	0.006029	0.006052	S(3)	3.192E-23
	MgHCO3+	0.0004063	0.0004042	0.0004054	0.0004027	0.0004039	0.0004014	0.000398	0.0003975	0.0003957	0.0003954	0.0003792	0.0003792	0.0003735	0.0003667	0.0003665	S2O4-2	1.596E-23
	Mn(2)	2.647E-07	3.244E-07	2.595E-07	2.744E-07	2.478E-07	2.511E-07	4.787E-07	3.119E-07	2.939E-07	2.018E-07	1.375E-07	1.375E-07	9.452E-08	8E-08	9.595E-09	S(4)	1.402E-07
	Mn+2	1.873E-07	2.304E-07	1.828E-07	1.941E-07	1.739E-07	1.756E-07	3.362E-07	2.188E-07	2.061E-07	1.403E-07	9.449E-08	9.449E-08	6.458E-08	5.424E-08	6.531E-09	SO2	2.818E-08
Mn(2)	MnCl+	4.926E-08	5.932E-08	4.877E-08	5.045E-08	4.674E-08	4.74E-08	8.808E-08	5.742E-08	5.376E-08	3.779E-08	2.485E-08	2.485E-08	1.699E-08	1.43E-08	1.688E-09	S4O6-2	2.581E-08
	MnSO4	2.561E-08	3.135E-08	2.509E-08	2.647E-08	2.391E-08	2.416E-08	4.593E-08	2.991E-08	2.813E-08	1.93E-08	1.293E-08	1.293E-08	8.835E-09	7.425E-09	8.897E-10	H2SO3	4.745E-09
	MnCO3	1.539E-09	3.089E-10	5.129E-10	8.389E-10	1.426E-09	1.69E-09	4.236E-09	2.951E-09	3.251E-09	2.595E-09	3.936E-09	3.936E-09	3.26E-09	3.307E-09	3.983E-10	HSO3-	4.022E-09
Mn(3)	Mn(3)	1.064E-32	1.4E-31	5.328E-31	6.1E-30	1.245E-30	1.137E-29	7.004E-30	2.296E-29	1.37E-29	2.213E-29	1.948E-29	1.948E-29	8.597E-30	6.193E-30	1.058E-30	SO3-2	5.791E-15
	Mn+3	1.064E-32	1.4E-31	5.328E-31	6.1E-30	1.245E-30	1.137E-29	7.004E-30	2.296E-29	1.37E-29	2.213E-29	1.948E-29	1.948E-29	8.597E-30	6.193E-30	1.058E-30	S5O6-2	6.002E-20
	Na	0.5198	0.5198	0.5198	0.5198	0.5198	0.5198	0.5198	0.5198	0.5198	0.5198	0.5198	0.5198	0.5198	0.5198	0.5198	S3O6-2	3.649E-23
	Na+	0.4906	0.4907	0.4906	0.4907	0.4906	0.4906	0.4906	0.4906	0.4907	0.4906	0.4907	0.4907	0.4907	0.4907	0.4907	S2O6-2	1.717E-23
Na	NaCl	0.02063	0.02051	0.02071	0.02056	0.02075	0.02078	0.02061	0.02062	0.02058	0.02077	0.02063	0.02063	0.02063	0.02064	0.02053	S(5)	5.322E-22
	NaSO4-	0.007684	0.007733	0.007651	0.007712	0.007634	0.007624	0.007693	0.00769	0.007704	0.00763	0.007686	0.007686	0.007687	0.007682	0.007728	S2O5-2	2.661E-22
	NaHCO3	0.0008258	0.0008357	0.0008146	0.0008265	0.0008072	0.0007991	0.0008115	0.0008096	0.0008097	0.0007888	0.0007714	0.0007714	0.0007598	0.0007447	0.0007562	S(6)	0.01395
	S(-2)	5.861E-17	1.315E-29	7.426E-38	0	0	0	0	0	0	0	0	0	0	0	0	HSO4-	0.01161
	HS-	5.808E-18	2.938E-30	2.872E-38	0	0	0	0	0	0	0	0	0	0	0	0	SO4-2	0.001599
S(-2)	H2S	5.28E-17	1.021E-29	4.554E-38	0	0	0	0	0	0	0	0	0	0	0	0	MgSO4	0.0004049
	CoHS+	1.205E-21	8.176E-34	0	0	0	0	0	0	0	0	0	0	0	0	0	AlSO4+	0.0001913
	S-2	1.431E-24	1.83E-36	0	0	0	0	0	0	0	0	0	0	0	0	0	FeSO4	0.00004406
	S2-2	7.146E-34	0	0	0	0	0	0	0	0	0	0	0	0	0	0	CaSO4	0.00004349
	S(4)	3.788E-16	1.779E-19	1.532E-21	3.647E-24	5.333E-23	1.815E-25	7.506E-25	2.576E-26	4.327E-26	7.013E-27	5.722E-28	5.722E-28	8.966E-28	8.128E-28	3.453E-28	NaSO4-	0.00003057
	SO3-2	5.629E-17	5.725E-20	7.564E-22	2.205E-24	3.49E-23	1.398E-25	6.14E-25	2.133E-26	3.679E-26	6.085E-27	5.376E-28	5.376E-28	8.521E-28	7.796E-28	3.314E-28	Al(SO4)2-	0.00001014
S(4)	HSO3-	3.225E-16	1.206E-19	7.76E-22	1.442E-24	1.843E-23	4.162E-26	1.366E-25	4.433E-27	6.488E-27	9.277E-28	3.456E-29	3.456E-29	4.453E-29	3.315E-29	1.396E-29	KSO4-	0.00000184
	H2SO3	2.7E-20	3.797E-24	1.146E-26	1.396E-29	1.391E-28	1.762E-31	4.46E-31	1.349E-32	1.686E-32	2.017E-33	3.247E-35	3.247E-35	3.4E-35	2.055E-35	8.746E-36	ZnSO4	0.000001035
	SO2	1.978E-20	2.693E-24	8.579E-27	1.004E-29	1.052E-28	1.342E-31	3.247E-31	9.846E-33	1.22E-32	1.531E-33	2.378E-35	2.378E-35	2.49E-35	1.511E-35	6.241E-36	KHSO4	2.404E-07
	S(6)	0.0314	0.0314	0.0314	0.0314	0.0314	0.0314	0.0314	0.0314	0.0314	0.0314	0.0314	0.0314	0.0314	0.0314	0.0314	MnSO4	1.589E-07
	SO4-2	0.01434	0.01441	0.0143	0.01438	0.01427	0.01426	0.01436	0.01435	0.01437	0.01427	0.01435	0.01435	0.01435	0.01434	0.0144	VSO4+	6.884E-08
	MgSO4	0.008325	0.008206	0.008405	0.008259	0.008445	0.008471	0.008303	0.008311	0.008279	0.008457	0.008322	0.008322	0.008321	0.008333	0.008224	VOSO4	5.737E-08
	NaSO4-	0.007684	0.007733	0.007651	0.007712	0.007634	0.007624	0.007693	0.00769	0.007704	0.00763	0.007686	0.007686	0.007687	0.007682	0.007728	LaSO4+	7.039E-10
	CaSO4	0.0008465	0.000846	0.0008468	0.0008462	0.0008468	0.0008467	0.0008461	0.0008461	0.0008459	0.0008464	0.0008453	0.0008453	0.000845	0.0008448	0.0008444	CuSO4	2.203E-11
	KSO4-	0.0001973	0.0001978	0.000197	0.0001976	0.0001968	0.0001967	0.0001974	0.0001974	0.0001975	0.0001968	0.0001973	0.0001973	0.0001974	0.0001973	0.0001978	La(SO4)2-	4.106E-12
	MnSO4	4.161E-07	1.517E-07	7.496E-08	4.727E-08	3.869E-08	2.416E-08	4.593E-08	2.991E-08	2.813E-08	1.93E-08	1.293E-08	1.293E-08	8.835E-09	7.425E-09	3.038E-09	FeSO4+	4.483E-14
	HSO4-	2.561E-08	3.135E-08	2.509E-08	2.647E-08	2.391E-08	2.185E-08	1.614E-08	1.508E-08	1.277E-08	1.118E-08	4.67E-09	4.67E-09	3.796E-09	3.093E-09	8.897E-10	Fe(SO4)2-	7.002E-17
	ZnSO4	7.481E-09	1.579E-08	1.824E-08	8.278E-09	4.649E-09	2.636E-09	8.22E-09	3.21E-09	2.839E-09	4.536E-09	1.51E-09	1.51E-09	5.124E-10	1.232E-09	5.269E-10	VO2SO4-	1.823E-17
	FeSO4	3.963E-09	4.788E-09	3.011E-09	1.672E-09	1.087E-09	1.093E-09	3.136E-09	2.248E-09	1.924E-09	8.109E-10	3.267E-10	3.267E-10	3.348E-10	2.886E-10	2.495E-10	V(3)	3.193E-07
S(6)	KHSO4	1.376E-09	3.966E-10	1.598E-10	5.473E-11	1.929E-11	1.303E-11	5.117E-12	4.785E-12	4.04E-12	3.599E-12	1.484E-12	1.484E-12	1.206E-12	9.839E-13	2.087E-12	V+3	2.362E-07
	LaSO4+	1.127E-09	3.727E-10	3.179E-11	2.908E-11	1.633E-11	7.989E-12	2.357E-12	2.734E-12	1.751E-12	2.555E-12	1.426E-12	1.426E-12	9.058E-13	7.479E-13	9.565E-13	VSO4+	6.884E-08
	La(SO4)2-	1.817E-11	3.733E-11	2.373E-12	1.934E-12	1.343E-12	8.203E-13	1.769E-13	1.794E-13	9.487E-14	1.593E-13	6.003E-14	6.003E-14	3.596E-14	3.401E-14	8.187E-14	VOH+2	1.419E-08
	AlSO4+	5.302E-12	6.029E-12	2.252E-12	1.764E-12	1.035E-12	5.942E-13	1.402E-13	1.52E-13	7.877E-14	1.184E-13	5.168E-14	5.168E-14	2.954E-14	2.482E-14	4.855E-14	V(OH)2+	4.933E-11
	CuSO4	1.67E-12	3.952E-12	1.159E-12	5.729E-13	7.272E-13	3.586E-13	4.755E-14	1.021E-13	4.033E-14	5.599E-14	2.251E-14	2.251E-14	1.383E-14	8.329E-15	1.709E-14	V2(OH)2+4	4.731E-15
	Al(SO4)2-	5.863E-13	7.933E-13	5.47E-13	2E-13	1.434E-13	1.124E-13	2.015E-14	2.799E-14	1.27E-14	1.686E-14	7.656E-15	7.656E-15	4.574E-15	3.288E-15	6.863E-15	V(4)	6.945E-07
	VOSO4	9.631E-16	1.894E-15	2.503E-16	1.763E-15	9.383E-16	4.863E-17	2.185E-17	6.714E-18	3.619E-18	1.056E-18	1.364E-19	1.364E-19	9.646E-20	7.294E-20	7.797E-20	VO+2	6.371E-07
	VO2SO4-	3.58E-16	5.399E-17	2.482E-16	1.16E-16	3.47E-17	6.087E-18	1.411E-18	2.516E-18	1.168E-18	9.165E-19	4.509E-20	4.509E-20	2.979E-20	1.967E-20	2.9E-20	VO2SO4-	1.823E-17
	H2SO4	3.033E-16	4.974E-17	1.127E-17	4.737E-18	2.959E-18	9.345E-19	5.426E-19	4.724E-19	3.428E-19	2.46E-19	2.249E-20	2.249E-20	1.272E-20	8.057E-21	1.978E-20	VO(OH)3	8.401E-18
	FeSO4+	2.401E-16	3.957E-17	2.059E-18	1.693E-18	9.786E-19	6.124E-19	6.12E-20	8.423E-20	4.577E-20	4.532E-20	1.758E-20	1.758E-20	1.116E-20	7.361E-21	5.85E-21	H2VO4-	4.944E-19
	Fe(SO4)2-	2.385E-18	6.373E-19	3.268E-20	5.227E-20	2.756E-21	1.586E-21	2.75E-21	3.775E-21	1.487E-21	1.932E-21	5.804E-22	5.804E-22	2.496E-22	1.516E-22	1.224E-22	VO2(OH)2-	3.057E-20
	VSO4+	8.031E-23	1.602E-22	1.541E-22	1.108E-23	6.047E-24	5.098E-27	3.985E-27	2.121E-28	1.3E-28	1.035E-29	2.705E-32	2.705E-32	2.003E-32	8.947E-33	4.922E-33	HVO4-2	4.333E-25
	V(3)	7.348E-09	5.634E-11	6.949E-14	1.208E-16	4.187E-16	2.813E-19	3.786E-19	2.315E-20	1.955E-20	2.169E-21	3.091E-23	3.091E-23	3.463E-23	2.343E-23	1.282E-23	VO3OH-2	2.221E-25
	V(OH)2+	7.195E-09	5.59E-11	6.923E-14	1.205E-16	4.179E-16	2.81E-19	3.783E-19	2.313E-20	1.954E-20	2.168E-21	3.09E-23	3.09E-23	3.463E-23	2.343E-23	1.281E-23	VO4-3	1.051E-37
V(3)	VOH+2	1.525E-10	4.396E-13	2.61E-16	2.93E-19	8.084E-19	3.057E-22	3.118E-22	1.779E-23	1.279E-23	1.21E-24	7.346E-27	7.346E-27	6.691E-27	3.68E-27	2.011E-27	Zn	0.000006899
	V+3	2.534E-13	2.71E-16	7.723E-20	5.585E-23	1.227E-22	2.611E-26	2.015E-26	1.073E-27	6.563E-28	5.297E-29	1.37E-31	1.37E-31	1.014E-31	4.534E-32	2.473E-32	Zn+2	0.00000556
	VSO4+	5.003E-14	5.399E-17	1.516E-20	1.108E-23	2.401E-23	5.098E-27	3.985E-27	2.121E-28	1.3E-28	1.035E-29	2.705E-32	2.705E-32	2.003E-32	8.947E-33	4.922E-33	ZnSO4	0.000001035
	V2(OH)2+4	2.009E-18	1.666E-23	5.9E-30	7.41E-36	5.664E-35	0	0	0	0	0	0	0	0	0	0	ZnCl+	3.041E-07
	V(4)	1.354E-08	1.709E-09	1.542E-11	4.095E-13	3.771E-13	3.738E-15	2.134E-15	6.988E-16	4.364E-16	1.297E-16	5.589E-18	5.589E-18	4.949E-18	3.512E-18	2.774E-18	ZnCl2	7.23E-10
	VOOH+	8.499E-09	8.93E-10	1.073E-11	3.194E-13	3.08E-13	3.319E-15	1.947E-15	6.416E-16	4.056E-16	1.219E-16	5.438E-18	5.438E-18	4.841E-18	3.449E-18	2.725E-18		
V(4)	VO+2	3.913E-09	7.197E-10	4.145E-12	7.958E-14	6.107E-14	3.701E-16	1.645E-16	5.058E-17	2.721E-17	6.969E-18	1.325E-19	1.325E-19	9.587E-20	5.553E-20	4.382E-20		
	VOSO4	1.127E-09	9.619E-11	5.47E-13	1.06E-14	8.037E-15	4.863E-17	2.185E-17	6.714E-18	3.619E-18	9.165E-19	1.758E-20	1.758E-20	1.272E-20	7.361E-21	5.85E-21		
	(VO)2(OH)2+2	1.732E-12	9.01E-14	1.302E-17	1.153E-20	1.074E-20	1.247E-24	4.288E-25	4.654E-26	1.86E-26	1.681E-27	3.345E-30	3.345E-30	2.65E-30	1.345E-30	8.388E-31		
	V(5)	2.821E-10	1.576E-08	1.3E-08	1.819E-08	1.039E-08	8.829E-09	4.335E-09	9.418E-09	6.895E-09	1.015E-08	1.545E-08	1.545E-08	2.014E-08	2.816E-08	2.971E-08		
	VO3OH-2	4.255E-11	5.142E-09	6.224E-09	1.07E-08	6.467E-09	6.391E-09	3.357E-09	7.369E-09	5.538E-09	8.208E-09	1.355E-08	1.355E-08	1.784E-08	2.514E-08	2.668E-08		
	H2VO4-	1.333E-10	5.644E-09	3.603E-09	3.726E-09	1.957E-09	1.101E-09	4.048E-10	8.326E-10	5.243E-10	7.21E-10	4.761E-10	4.761E-10	5.095E-10	5.874E-10	1.967E-09		
	VO2(OH)2-	1.021E-10	4.589E-09	2.653E-09	2.951E-09	1.413E-09	7.852E-10	3.134E-10	6.42E-10	4.222E-10	5.173E-10	3.647E-10	3.647E-10	3.903E-10	4.47E-10	4.751E-10		
V(5)	HVO4-2	3.341E-12	3.735E-10	5.145E-10	8.05E-10	5.485E-10	5.513E-10	2.599E-10	5.737E-10	4.108E-10	7.021E-10	1.064E-09	1.064E-09	1.401E-09	1.991E-09	5.908E-10		
	VO(OH)3	8.602E-13	1.437E-11	3.975E-12	2.855E-12	1.086E-12	3.392E-13	1.027E-13	1.964E-13	1.07E-13	1.146E-13	3.448E-14	3.448E-14	2.999E-14	2.792E-14	2.968E-14		
	VO4-3	1.911E-18	6.203E-16	1.574E-15	4.183E-15	3.191E-15	5.61E-15	3.874E-15	9.114E-15	8.042E-15	1.405E-14	5.423E-14	5.423E-14	8.783E-14	1.523E-13	1.614E-13		
	VO2+	3.365E-15	2.088E-14	2.766E-15	1.282E-15	3.875E-16	6.807E-17	1.563E-17	2.79E-17	1.293E-17	1.18E-17	1.513E-18	1.513E-18	1.07E-18	8.097E-19	8.604E-19		
	VO2SO4-	3.033E-16	1.894E-15	2.482E-16	1.16E-16	3.47E-17	6.087E-18	1.411E-18	2.516E-18	1.168E-18	1.056E-18	1.364E-19	1.364E-19	9.646E-20	7.294E-20	7.797E-20		
	Zn	3.503E-08	6.746E-08	4.248E-08	2.375E-08	6.607E-08	3.792E-08	4.56E-08	4.68E-08	4.169E-08	6.698E-08	2.396E-08	2.396E-08	8.36E-09	2.078E-08	8.903E-09		
	Zn+2	2.183E-08	4.231E-08	2.613E-08	1.471E-08	4.02E-08	2.274E-08	2.746E-08	2.809E-08	2.492E-08	3.917E-08	1.319E-08	1.319E-08	4.478E-09	1.076E-08	4.645E-09		
Zn	ZnCl4-2	4.591E-09	8.863E-09	5.511E-09	3.086E-09	8.493E-09	4.809E-09	5.772E-09	5.906E-09	5.232E-09	8.28E-09	2.775E-09	2.775E-09	9.418E-10	2.263E-09	9.738E-10		
	ZnCl+	4.116E-09	7.569E-09	5.102E-09	2.693E-09	7.989E-09	4.572E-09	5.13E-09	5.266E-09	4.606E-09	7.83E-09	2.488E-09	2.488E-09	8.444E-10	2.04E-09	8.393E-10		
	ZnSO4	2.497E-09	4.788E-09	3.011E-09	1.672E-09	4.649E-09	2.636E-09	3.136E-09	3.21E-09	2.839E-09	4.536E-09	1.51E-09	1.51E-09	5.124E-10	1.232E-09	5.269E-10		

Appendix IV – *SI of Mineralogical phase (data processed by PHREEQC).*

Formula	Phase	Bubble	310	257	320	262	277	30	0	20	283	40	60	35	110	Offshore
	pH	5.9	6.33	6.65	6.84	6.94	7.19	7.31	7.34	7.41	7.48	7.85	7.85	7.94	8.03	8.03
Al	Al	-93.44	-97.49	-99.97	-104.04	-101.92	-105.69	-105.83	-107.98	-107.84	-108.61	-110.86	-110.9	-110.65	-110.76	-111.93
Al	Al(g)	-144.7	-148.92	-151.1	-155.39	-152.99	-156.73	-157.11	-159.25	-159.16	-159.66	-162.11	-162.1	-161.9	-161.99	-163.33
Al2(SO4)3	Al2(SO4)3	-44.75	-46.03	-47.97	-49.13	-49.74	-51.68	-54.02	-54.16	-54.9	-55.12	-58.22	-58.22	-58.95	-59.63	-60.48
Al2(SO4)3:6H2O	Al2(SO4)3:6H2O	-27.21	-28.4	-30.47	-31.54	-32.27	-34.23	-36.46	-36.6	-37.32	-37.67	-40.67	-40.67	-41.4	-42.09	-42.87
MnS	Alabandite	-18.49	-30.27	-38.04	-48.05	-43.44	-53.04	-50.06	-56.09	-55.15	-58.58	-62.86	-62.86	-62.23	-62.47	-64.79
KAl(SO4)2:12H2O	Alum-K	-11.21	-11.74	-12.89	-13.34	-13.81	-14.8	-15.82	-15.9	-16.24	-16.51	-17.94	-17.94	-18.31	-18.66	-18.99
CaSO4	Anhydrite	-0.91	-0.92	-0.9	-0.91	-0.9	-0.9	-0.91	-0.91	-0.91	-0.9	-0.91	-0.91	-0.91	-0.91	-0.91
CaCO3	Aragonite	-1.49	-1.08	-0.73	-0.56	-0.44	-0.19	-0.09	-0.06	0	0.09	0.43	0.43	0.51	0.59	0.58
CaCO3	Calcite	-1.35	-0.93	-0.59	-0.42	-0.3	-0.05	0.05	0.08	0.15	0.24	0.57	0.57	0.66	0.74	0.73
Cu2S	Chalcocite	-4.13	-16.13	-23.61	-33.9	-28.62	-38.01	-33.86	-39.6	-39.03	-42.38	-46.84	-46.84	-46.49	-46.89	-48.38
CuSO4	Chalcocyanite	-22.75	-21.83	-20.97	-20.13	-20.38	-19.3	-19.14	-18.39	-18.8	-18.39	-18.5	-18.5	-18.92	-19.1	-19.04
CuFeS2	Chalcopyrite	-15.3	-37.42	-52.04	-71.45	-63.47	-81.63	-75.02	-86.52	-85.03	-91.71	-100.57	-100.6	-99.56	-100.23	-103.12
PbCl2	Cotunnite	-7.42	-7.84	-7.62	-7.84	-8.01	-7.49	-7.62	-7.8	-8.06	-7.6	-7.78	-7.78	-7.95	-8.24	-7.52
Fe	Fe	-23.12	-24.71	-25.78	-28.36	-27.74	-29.62	-27.95	-29.91	-29.62	-30.54	-31.59	-31.59	-31.38	-31.38	-32.07
Fe(OH)2	Fe(OH)2	-10.25	-8.84	-8.05	-8.08	-8.68	-8.16	-7.12	-7.62	-7.56	-7.72	-7.7	-7.7	-7.7	-7.66	-7.97
Fe(OH)3	Fe(OH)3	-9.69	-6.8	-5.05	-3.82	-5	-3.29	-2.58	-2.35	-2.42	-2.16	-1.63	-1.63	-1.73	-1.67	-1.81
Fe2(SO4)3	Fe2(SO4)3	-54.51	-51.35	-49.7	-48.44	-51.34	-49.4	-48.76	-48.48	-49.04	-48.89	-50.09	-50.09	-50.82	-51.24	-51.55
FeO	FeO	-9.88	-8.48	-7.68	-7.72	-8.31	-7.79	-6.76	-7.26	-7.2	-7.35	-7.34	-7.34	-7.33	-7.29	-7.61
FeOOH	Goethite	-4.53	-1.63	0.1	1.34	0.14	1.86	2.57	2.8	2.74	2.98	3.53	3.53	3.43	3.49	3.36
Fe2O3	Hematite	-8.08	-2.28	1.19	3.66	1.27	4.7	6.13	6.59	6.47	6.95	8.03	8.03	7.84	7.96	7.7
FeAl2O4	Hercynite	-7.56	-4.8	-4.11	-4.1	-4.79	-4.73	-5.24	-5.69	-5.94	-5.98	-6.78	-6.78	-6.96	-7.07	-8.19
FeS2	Pyrite	-15.71	-36.68	-50.81	-68.99	-62.05	-79.38	-73.91	-84.76	-83.25	-89.59	-98.1	-98.1	-97.06	-97.68	-100.33
FeS	Pyrrhotite	-26.81	-23.01	-20.36	-17.58	-18.42	-15.49	-15.8	-14.46	-14.62	-13.66	-12.19	-12.19	-12.37	-12.21	-12.89
FeCO3	Siderite	-4.69	-3.68	-3.27	-3.45	-4.2	-3.94	-2.98	-3.51	-3.51	-3.79	-4.12	-4.12	-4.21	-4.28	-4.56
SO2	SO2(g)	-19.92	-23.8	-26.28	-29.23	-28.18	-31.07	-30.71	-32.23	-32.14	-33.02	-34.84	-34.84	-34.82	-35.04	-35.44
FeS	Troilite	-15.67	-26.94	-34.56	-44.92	-41.16	-50.77	-47.19	-53.59	-52.69	-56.33	-61.1	-61.1	-60.48	-60.79	-62.45
V	V	-55.51	-61.83	-66.98	-73.54	-70.86	-77.35	-76.35	-79.71	-79.4	-81.23	-84.46	-84.46	-84.02	-84.14	-85.1
V2O4	V2O4	-2.78	-3.26	-6.36	-9.11	-8.84	-12.26	-12.57	-13.47	-13.75	-14.56	-16.59	-16.59	-16.51	-16.62	-16.88
V3O5	V3O5	-3.79	-7.48	-14.06	-20.68	-19.13	-26.67	-26.44	-29.26	-29.42	-31.47	-35.53	-35.53	-35.21	-35.42	-36.15
V4O7	V4O7	-6.28	-10.22	-18.34	-26.34	-24.65	-33.89	-33.83	-37.09	-37.4	-39.85	-44.93	-44.93	-44.57	-44.83	-45.7
ZnO	Zincite	-7.83	-6.73	-6.22	-6.15	-5.44	-5.18	-4.92	-4.85	-4.77	-4.36	-4.15	-4.15	-4.44	-3.87	-4.28
Zn	Zn	-33.29	-35.22	-36.52	-39.03	-37.06	-39.18	-38.34	-39.73	-39.43	-39.74	-40.62	-40.62	-40.71	-40.18	-41
Zn(ClO4)2:6H2O	Zn(ClO4)2:6H2O	-308.14	-285.11	-268.28	-249.72	-257.01	-237.82	-244.55	-232.79	-235.05	-226.82	-220.19	-220.2	-222.26	-221.44	-219.94
Zn	Zn(g)	-50.12	-52.13	-53.31	-55.91	-53.82	-55.93	-55.19	-56.57	-56.29	-56.5	-57.46	-57.46	-57.55	-57.01	-57.89
Zn(OH)2	Zn(OH)2(beta)	-8.56	-7.46	-6.96	-6.88	-6.17	-5.91	-5.65	-5.58	-5.5	-5.1	-4.88	-4.88	-5.17	-4.61	-5.01
Zn(OH)2	Zn(OH)2(epsilon)	-8.29	-7.19	-6.68	-6.61	-5.9	-5.64	-5.38	-5.3	-5.23	-4.83	-4.61	-4.61	-4.9	-4.33	-4.74

Appendix V – *Soft body trace metal concentration in mussels.*

Sample Id.	Site	Date from	Date to	Exposition	l	L	Wo	Sb	Dw	Sb/Dw	pH	Al	V	Mn	Fe	Ni	Cu	Zn
		dd	dd	days	(cm)	(cm)	(g)	(g)	(g)			µg/g	µg/g	µg/g	µg/g	µg/g	µg/g	µg/g
0-40-a-1	0-40	16-May	13-Jun	28	7.3	2.6	29.29	7.59	1.605	5	7.31	1.86E+01	1.47E+00	1.12E+01	2.17E+02	3.90E-01	5.96E+00	3.49E+01
0-40-a-2	0-40	16-May	13-Jun	28	5.79	2.58	26.8	7.07	1.3813	5	7.31	7.89E+00	8.69E-01	4.68E+00	1.48E+02	4.29E-01	3.32E+00	4.76E+01
0-40-a-3	0-40	16-May	13-Jun	28	6.9	1.4	26.43	8.95	2.4289	4	7.31	7.93E+00	8.19E-01	4.54E+00	1.18E+02	2.95E-01	2.37E+00	2.52E+01
0-40-a-4	0-40	16-May	13-Jun	28	5.83	1.43	28.52	8.94	2.3675	4	7.31	1.13E+01	7.28E-01	3.80E+00	1.35E+02	2.78E-01	3.70E+00	5.54E+01
0-40-a-6	0-40	16-May	13-Jun	28	5.5	0.92	19.66	4.44	0.6982	6	7.31	2.98E+01	2.91E+00	1.07E+01	4.06E+02	8.88E-01	5.78E+00	1.18E+02
0-40-a-7	0-40	16-May	13-Jun	28	5.5	1.51	28.21	8.93	2.0707	4	7.31	1.24E+01	1.32E+00	4.12E+00	1.37E+02	2.87E-01	5.84E+00	3.13E+01
0-40-a-8	0-40	16-May	13-Jun	28	5.38	0.92	21.08	3.77	0.6778	6	7.31	2.50E+01	2.33E+00	1.08E+01	3.44E+02	8.74E-01	5.60E+00	8.57E+01
0-40-a-9	0-40	16-May	13-Jun	28	5.91	1.47	19.8	9.06	2.0177	4	7.31	9.30E+00	1.40E+00	3.28E+00	1.53E+02	2.87E-01	2.60E+00	5.82E+01
0-40-a-10	0-40	16-May	13-Jun	28	5.49	0.93	22.14	5.73	0.9048	6	7.31	2.53E+01	1.63E+00	6.09E+00	2.16E+02	7.26E-01	6.26E+00	1.08E+02
0-40-a-12	0-40	16-May	13-Jun	28	4.93	0.91	20.53	4.34	0.6384	7	7.31	2.94E+01	2.73E+00	1.14E+01	4.10E+02	9.39E-01	5.18E+00	6.34E+01
0-40-c-1	0-40	16-May	13-Jun	28	7.28	2.52	26.92	7.84	0.8938	9	7.31	1.30E+01	1.69E+00	5.77E+00	2.82E+02	4.60E-01	3.81E+00	7.63E+01
0-40-c-2	0-40	16-May	13-Jun	28	6.57	2.3	25.87	6.97	1.2092	6	7.31	1.68E+01	2.17E+00	5.85E+00	2.32E+02	6.49E-01	5.35E+00	6.87E+01
0-40-c-5	0-40	16-May	13-Jun	28	6.9	2.16	24.39	5.77	0.9271	6	7.31	2.04E+01	2.17E+00	6.90E+00	3.86E+02	5.23E-01	3.60E+00	8.00E+01
0-40-c-11	0-40	16-May	13-Jun	28	6.37	2.24	13.71	5.6	0.9276	6	7.31	2.25E+01	2.13E+00	8.81E+00	3.91E+02	5.09E-01	4.78E+00	6.14E+01
0-40-c-12	0-40	16-May	13-Jun	28	5.61	2	15.82	3.72	0.5433	7	7.31	4.12E+01	3.83E+00	1.57E+01	6.41E+02	1.43E+00	8.70E+00	1.51E+02
0-40-c-13	0-40	16-May	13-Jun	28	7.13	2.63	32.81	10.33	2.2935	5	7.31	1.18E+01	1.01E+00	2.98E+00	2.11E+02	2.03E-01	1.77E+00	3.65E+01
0-40-c-14	0-40	16-May	13-Jun	28	7.04	2.51	29.41	7.73	1.4724	5	7.31	1.23E+01	1.34E+00	5.35E+00	2.80E+02	4.05E-01	3.67E+00	6.37E+01
0-40-c-15	0-40	16-May	13-Jun	28	7	2.64	30.57	8.29	1.769	5	7.31	9.84E+00	1.06E+00	4.01E+00	1.97E+02	2.53E-01	4.32E+00	6.72E+01
0-40-c-16	0-40	16-May	13-Jun	28	7.25	2.38	21.61	6.88	1.5032	5	7.31	1.62E+01	2.14E+00	6.19E+00	3.13E+02	6.11E-01	3.87E+00	8.72E+01
0-40-c-20	0-40	16-May	13-Jun	28	4.75	1.64	11.43	2.92	0.374	8	7.31	2.24E+01	2.65E+00	6.95E+00	4.02E+02	1.08E+00	4.63E+00	1.53E+02
40-a-2	40	16-May	13-Jun	28	7.5	2.6	33.84	9.37	1.822	5	7.85	1.19E+01	1.49E+00	4.33E+00	1.54E+02	3.21E-01	5.42E+00	3.93E+01
40-a-4	40	16-May	13-Jun	28	5.2	1.9	12.65	2.72	0.3405	8	7.85	4.60E+01	8.29E+00	9.84E+00	5.74E+02	2.77E+00	5.84E+00	1.09E+02
40-a-5	40	16-May	13-Jun	28	5.7	2.2	16.28	5.2	1.0306	5	7.85	1.74E+01	1.65E+00	4.97E+00	1.37E+02	3.87E-01	5.28E+00	5.57E+01
40-a-7	40	16-May	13-Jun	28	5.4	2.5	14.01	3.59	0.5111	7	7.85	7.39E+00	1.56E+00	3.74E+00	1.02E+02	4.97E-01	3.07E+00	7.14E+01
40-a-9	40	16-May	13-Jun	28	4	2.2	6.93	1.99	0.336	6	7.85	1.83E+01	2.19E+00	6.78E+00	2.16E+02	5.34E-01	4.83E+00	8.36E+01
40-a-12	40	16-May	13-Jun	28	3.9	2.2	6.25	1.66	0.2415	7	7.85	2.46E+01	2.49E+00	6.53E+00	2.90E+02	6.18E-01	4.19E+00	1.34E+02
40-a-14	40	16-May	13-Jun	28	3.7	1.5	5.71	1.74	0.1764	10	7.85	3.73E+01	5.31E+00	9.71E+00	3.85E+02	1.08E+00	8.10E+00	1.31E+02
40-a-17	40	16-May	13-Jun	28	3.6	1.2	4.03	1.2	0.1551	8	7.85	3.40E+01	5.10E+00	1.07E+01	3.74E+02	9.34E-01	5.92E+00	1.27E+02
40-a-18	40	16-May	13-Jun	28	3.2	1.3	3.71	0.98	0.1221	8	7.85	2.66E+01	3.45E+00	8.51E+00	2.51E+02	9.94E-01	6.57E+00	1.19E+02
40-a-19	40	16-May	13-Jun	28	3.5	1.2	3.78	1.2	0.144	8	7.85	1.64E+01	1.90E+00	6.95E+00	3.34E+02	6.05E-01	4.98E+00	7.90E+01
40-c-1	40	16-May	13-Jun	28	7.55	2.7	27.5	8.12	1.443	6	7.85	3.39E+01	1.49E+00	5.82E+00	3.02E+02	5.62E-01	3.42E+00	5.20E+01
40-c-2	40	16-May	13-Jun	28	7	2.6	32.58	9.16	1.8872	5	7.85	1.84E+01	1.61E+00	7.11E+00	2.69E+02	4.76E-01	4.00E+00	6.35E+01
40-c-3	40	16-May	13-Jun	28	6.7	2.5	25.01	7.83	1.5086	5	7.85	1.31E+01	7.55E-01	3.89E+00	1.46E+02	2.34E-01	3.43E+00	3.59E+01
40-c-4	40	16-May	13-Jun	28	6.6	2.35	18.4	8.11	1.5989	5	7.85	1.46E+01	1.10E+00	3.94E+00	1.59E+02	3.48E-01	3.16E+00	7.36E+01
40-c-6	40	16-May	13-Jun	28	6.5	2.4	24.61	6.65	1.1369	6	7.85	1.46E+01	1.59E+00	5.26E+00	1.69E+02	7.81E-01	3.13E+00	7.87E+01
40-c-7	40	16-May	13-Jun	28	6.8	2.2	24.29	6.6	1.2413	5	7.85	1.49E+01	1.55E+00	6.20E+00	1.84E+02	6.22E-01	2.93E+00	5.62E+01
40-c-8	40	16-May	13-Jun	28	6.1	2.5	20.86	5.96	1.0455	6	7.85	1.92E+01	1.61E+00	5.31E+00	2.02E+02	4.28E-01	3.86E+00	5.78E+01
40-c-10	40	16-May	13-Jun	28	6.7	2.7	26.32	7.31	1.6413	4	7.85	1.29E+01	1.02E+00	4.04E+00	1.43E+02	2.42E-01	2.48E+00	3.64E+01
40-c-16	40	16-May	13-Jun	28	5.5	2	16.21	4.45	0.8841	5	7.85	1.97E+01	1.43E+00	5.92E+00	1.88E+02	2.71E-01	4.42E+00	7.79E+01
40-c-19	40	16-May	13-Jun	28	5.3	2	14.02	3.1	0.4635	7	7.85	1.63E+01	2.25E+00	7.02E+00	1.84E+02	7.16E-01	5.91E+00	1.46E+02
100-a-1	100	16-May	13-Jun	28	6.86	2.64	31.48	10.21	2.0331	5	8.03	1.44E+01	1.94E+00	4.32E+00	3.62E+02	4.32E-01	3.14E+00	4.64E+01
100-a-6	100	16-May	13-Jun	28	6.9	2.72	30.74	9.82	2.041	5	8.03	1.21E+01	1.52E+00	4.24E+00	2.90E+02	3.86E-01	2.82E+00	4.47E+01
100-a-8	100	16-May	13-Jun	28	6.9	2.33	25.58	6	0.8334	7	8.03	2.58E+01	3.93E+00	8.59E+00	8.06E+02	8.06E-01	4.84E+00	1.07E+02
100-a-9	100	16-May	13-Jun	28	6.48	2.24	22	4.68	0.6953	7	8.03	3.04E+01	2.81E+00	7.94E+00	5.00E+02	6.53E-01	4.24E+00	1.13E+02
100-a-13	100	16-May	13-Jun	28	6.38	2.42	24.6	6.3	1.0693	6	8.03	3.43E+01	2.63E+00	8.63E+00	3.65E+02	6.64E-01	3.96E+00	7.85E+01
100-a-14	100	16-May	13-Jun	28	6.6	2.02	19.11	4.01	0.6442	6	8.03	2.80E+01	3.02E+00	1.05E+01	5.46E+02	5.51E-01	6.61E+00	8.23E+01
100-a-15	100	16-May	13-Jun	28	6.33	2.41	24.04	6.05	0.9966	6	8.03	1.78E+01	1.97E+00	4.74E+00	3.98E+02	3.25E-01	2.40E+00	4.28E+01
100-a-17	100	16-May	13-Jun	28	5.85	2.22	17.62	4.95	0.6668	7	8.03	2.62E+01	2.99E+00	7.68E+00	5.37E+02	4.19E-01	4.43E+00	5.99E+01
100-a-18	100	16-May	13-Jun	28	5.55	1.86	15.43	3.31	0.3598	9	8.03	9.18E+01	1.25E+01	1.98E+01	1.38E+03	2.77E+00	6.72E+00	1.77E+02
100-a-20	100	16-May	13-Jun	28	5.21	1.82	13.39	2.94	0.4808	6	8.03	2.90E+01	3.30E+00	9.09E+00	6.85E+02	5.77E-01	4.67E+00	1.03E+02
100-c-6	100	16-May	13-Jun	28	5.4	2.1	14.82	3.03	0.3776	8	8.03	3.52E+01	4.72E+00	8.84E+00	4.51E+02	1.27E+00	5.50E+00	5.42E+01
100-c-7	100	16-May	13-Jun	28	5	1.72	9.38	2.27	0.2274	10	8.03	5.24E+01	7.26E+00	1.50E+01	6.98E+02	2.94E+00	7.68E+00	1.77E+02
100-c-8	100	16-May	13-Jun	28	6.86	2.6	28.68	9.03	2.1843	4	8.03	1.35E+01	1.45E+00	4.24E+00	1.95E+02	3.14E-01	1.84E+00	4.12E+01
100-c-9	100	16-May	13-Jun	28	5.9	9.25	20.74	6.62	1.3569	5	8.03	1.11E+01	8.74E-01	3.73E+00	1.71E+02	1.68E-01	2.66E+00	3.62E+01
100-c-10	100	16-May	13-Jun	28	5.7	2.14	17.79	4.03	0.7012	6	8.03	2.82E+01	2.29E+00	6.60E+00	3.96E+02	7.35E-01	4.13E+00	8.40E+01
100-c-11	100	16-May	13-Jun	28	5.21	1.86	13.18	3.26	0.4493	7	8.03	5.37E+01	3.85E+00	1.31E+01	5.67E+02	1.22E+00	6.11E+00	1.64E+02
100-c-13	100	16-May	13-Jun	28	6.43	2.31	24.83	5.64	0.8485	7	8.03	1.82E+01	1.88E+00	5.30E+00	2.76E+02	4.07E-01	3.77E+00	4.00E+01
100-c-15	100	16-May	13-Jun	28	6.35	2.16	20.71	5.12	0.4555	11	8.03	3.51E+01	3.53E+00	9.74E+00	5.88E+02	1.28E+00	4.93E+00	7.49E+01
100-c-16	100	16-May	13-Jun	28	6.06	2.18	20.25	6.66	0.8189	8	8.03	2.84E+01	2.84E+00	8.67E+00	4.05E+02	7.08E-01	3.84E+00	6.29E+01
100-c-17	100	16-May	13-Jun	28	5.41	1.82	14.88	5.14	1.5309	3	8.03	1.80E+01	1.25E+00	4.81E+00	1.88E+02	2.89E-01	4.39E+00	2.90E+01
blk15	-	16-May	16-May	0	6.25	2.84	24.07	9.59	1.737	6	8.04	1.20E+01	3.23E-01	6.20E+00	9.54E+01	5.54E-01	2.75E+00	4.62E+01
blk8	-	16-May	16-May	0	6.37	2.47	30.19	10.35	1.9559	5	8.04	1.77E+01	2.25E-01	3.53E+00	5.55E+01	4.18E-01	2.68E+00	4.54E+01
blk5	-	16-May	16-May	0	5.59	1.89	13.44	5.99	0.8959	7	8.04	1.56E+01	4.44E-01	1.23E+01	1.03E+02	6.37E-01	6.06E+00	4.07E+01
blk14	-	16-May	16-May	0	3.92	1.83	7.63	3.08	0.452	7	8.04	4.26E+01	2.84E-01	7.50E+00	7.49E+01	9.53E-01	6.06E+00	6.91E+01
blk17	-	16-May	16-May	0	5.27	1.95	14.58	6.06	0.8485	7	8.04	1.46E+01	2.74E-01	6.34E+00	5.24E+01	8.43E-01	4.57E+00	9.84E+01
blk12	-	16-May	16-May	0	5.85	2.35	25.33	6.43	1.0062	6	8.04	3.09E+01	3.01E-01	6.66E+00	6.34E+01	5.97E-01	3.80E+00	8.60E+01
blk10	-	16-May	16-May	0	4.39	1.95	10.92	4.4	0.5886	7	8.04	1.40E+01	5.05E-01	1.46E+01	1.40E+02	1.03E+00	3.51E+00	6.61E+01
blk20	-	16-May	16-May	0	5.53	1.82	19.24	5.06	0.6855	7	8.04	3.34E+01	8.07E-01	6.55E+00	1.04E+02	1.16E+00	6.71E+00	1.19E+02
blk24	-	16-May	16-May	0	6.2	2.2	11.5	4.43	0.6086	7	8.04	8.45E+01	9.33E-01	7.67E+00	1.59E+02	1.46E+00	3.71E+00	9.95E+01
blk22	-	16-May	16-May	0	5.56	1.7	12.61	4.38	0.5481	8	8.04	4.00E+01	1.09E+00	5.41E+00	9.57E+01	1.46E+00	2.88E+00	6.01E+01
blk11	-	16-May	16-May	0	5.95	2.34	23.64	7.12	1.0452	7	8.04	3.40E+01	8.77E-01	4.57E+00	9.60E+01	1.10E+00	2.87E+00	7.87E+01
blk1	-	16-May	16-May	0	7.21	2.32	29.25	6.69	0.771	9	8.04	8.98E+00	1.04E+00	3.95E+00	6.60E+01	1.34E+00	3.40E+00	5.47E+01
blk7	-	16-May	16-May	0	7.35	2.54	27.98	6.31	0.7745	8	8.04	1.55E+01	1.03E+00	5.21E+00	6.54E+01	1.56E+00	3.51E+00	5.86E+01
blk16	-	16-May	16-May	0	5.86	1.85	15.92	5.59	0.6171	9	8.04	1.33E+01	1.31E+00	3.87E+00	7.23E+01	8.76E-01	3.49E+00	1.01E+02